# Conducting polymer materials for bioelectronics applications

**Isabel del Agua López**

Thesis Advisors:

Prof. David Mecerreyes

Dr. Ana Sanchez-Sanchez

University of the Basque Country UPV/EHU

Donostia-San Sebastian, Spain

2018

*To my dear family*

# Acknowledgments

In the first place, I would like to thank Professor David Mecerreyes for giving me the opportunity and the resources to do my PhD. His unconditional dedication and mentorship during these 3 years made this thesis possible with the help of Dr. Ana Sanchez-Sanchez as co-director. I would like to thank as well Professor George G. Malliaras for kindly welcoming me to his lab in France and for all my experiences over there. Thanks to my working period in Gardanne, I was able to broaden my knowledge in polymer science that I acquired in Polymat and implement it into the application point of view of a material. Together with them, I would like to thank the University of the Basque Country and the Ecole des Mines de Saint Etienne for providing me with the resources necessary for my research, particularly the trainings given by qualified staff, the laboratories and the equipment.

The knowledge I have acquired and the people I have met have made this PhD experience inevaluable and unforgettable. I would like to thank the members of BEL and Polymat:

In Bel: Roisin, Esma, Rod, Mary, Chris, Vincenzo, Donata, Paschalis, Ana S. Shaika, Alex, Marcel, Thomas, Jolien, Anna Maria, Gerwin, Usein, Magali, Ilke, Viviana, Mahmoudy, Babis, Shahab, Loig, Dimitrios, Eloise, Aimie, Yi, Adel, Clemence, and Simon.

In Polymat: Alex, Daniele, Ana S., Luca, Guiomar, Nerea, Haritz, Inaki, Leire, Sara, Naroa, Leire, Antonio, Asier, Sufi, Amaury, Anto, Maitane, Andere, Irma, Coralie, Esther, Ana M., Mehmet, Ana P, Alicia, Elodie, and Giulia.

Among helpful staff in Polymat, Ines and Monica deserve a special mention for their readiness to help.

Among all of you, I have found great colleagues always ready to help when needed, and most importantly friends who were my pillars when living in a new place. Looking backwards to the last 3 years, I realize now how lucky I was for pursuing my doctoral degree surrounded by passionate people. A PhD study is full of ups and downs where multiple challenges need to be overcome, and when surrounded by great teams, it is simply much easier to do.

I am also very thankful for my family for their love and support for every step of the journey in my life. Thanks to their support, any dreams can be accomplished and any challenges can be overcome.

# Table of contents

# Chapter 1.

# Introduction

# Chapter 1. Introduction

## 1.1. Conducting polymers and PEDOT:PSS

Since the discovery of the polyacetylene in the 70s, conducting polymers (CP) have been a hot topic under research due to their unusual properties and their huge potential applications. As a consequence of the importance of these materials, the Nobel prize in Chemistry in 2000 was awarded to A. J. Heeger, A. G. MacDiarmid, and H. Shirakawa for the *"for the discovery and development of electrically conductive polymers"*. The discovery of polyacetylene motivated the synthesis of many other conducting polymers. Although polymers are insulating by nature, CPs present conductivity due to their backbone which is formed by conjugated double bonds.

Figure 1.1 presents the chemical structure of the most common CPs such as polyacetylene (PA), polypyrrole (PPy), polyaniline (PANI), poly(p-phenylene-vinylene) (PPV), poly(3,4-ethylene dioxythiophene) (PEDOT), polyfuran (PF) and other polythiophene (PTh) derivatives.
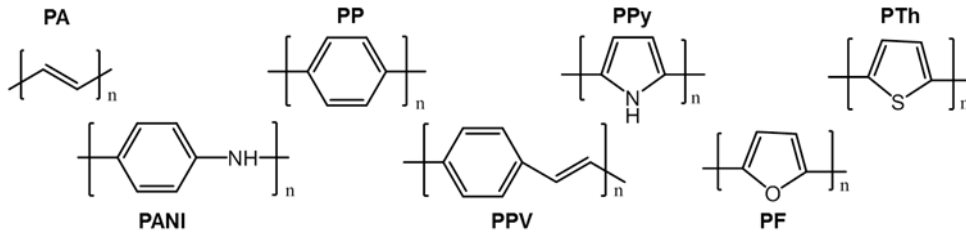
**Figure 1.1.** CPs structures.

Although CPs present low electrical conductivity in their pristine state, behaving as insulators, they became conductive when doped. The electrical conductivity of these polymers is explained as follows. A dopant agent removes or adds an electron from or to the polymer chain backbone, and a delocalized charge is created along the chain. This process is called doping and it occurs when the polymers are treated with a suitable oxidizing or reducing agents. The radical ion (charge) is surrounded by a distortion of the crystal lattice, what is known as a polaron. When the polaron travels along the polymer chains, conducts electricity. Doping processes enhance the conductivities of CPs to the metallic region and this process have an effect not only on the electronic properties of the polymers, but also on their electrical, optical, magnetic and structural properties. Nowadays CPs find numerous applications for energy storage like solar cells, batteries or fuel cells, sensors (gas), and biosensors. In addition, in biomedical engineering field, they fins applications like drug delivery, bioactuators, tissue engineering, neural interfaces, and electrodes.[1,2]

Among CPs, poly(3,4-ethylenedioxythiophene) (PEDOT) (structure in Figure 1.2) is considered the CP having the most current technological and commercial potential. This is due to its facile synthesis, high conductivity, redox and electrochromic properties, biocompatibility, and long-term air stability. PEDOT chains alone are not conducting, not soluble in any solvent and not processable. For this reason, charges must be introduced in the polymer backbone by

4

oxidation in order to impart conductivity to the polymer. The oxidative form of PEDOT needs counter ions to balance its positive charges. This counter ion is also called dopant and its role is to neutralize the PEDOT polymer backbone when it is in the oxidized form. The role of the oxidant is to introduce positive charges to the PEDOT backbone and balance them by the anionic counter-ions of the doping agent. PEDOT counterions can be monoatomic ions like chloride, polyatomic ions like sulfate, but also organic anions like tosylate (p-toluenesulfonic acid anion) or the polymer polystyrene sulfonate (PSS). The choice of the counterion affects the oxidation or doping level and moreover, the electronic properties and characteristics of the PEDOT complex.
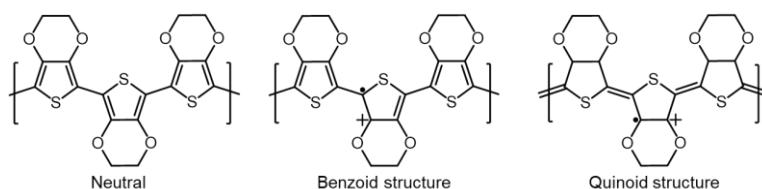


**Figure 1.2.** PEDOT neutral form, benzoid and quinoid structures.

As mentioned before, PEDOT is nowadays the most successful conducting polymer (Figure 1.3). PEDOT is Commercially available in the form of PEDOT:PSS aqueous dispersions which are synthetized by aqueous oxidative polymerization of EDOT in the presence of solubilized poly(styrene sulfonate) (PSS). By this method, the formed insoluble PEDOT particles are doped and stabilized simultaneously by PSS. Together PEDOT and PSS they form polymeric complex particles where PEDOT chains are surrounded by PSS shells which provide sufficient stability for PEDOT chains to be dispersed in the solvent (Figure 1.3). Although PEDOT:PSS can be dispersed in some polar organic solvents like alcohols,[3] it is most commonly used as a water dispersion. This solution typically contains a large excess of PSS with a weight ratio of PEDOT:PSS of 1:2.5.
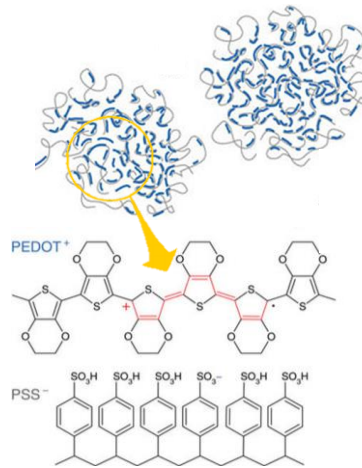
**Figure 1.3.** PEDOT:PSS conducting polymer.

PEDOT:PSS presents very advantageous characteristics in bioelectronics which makes the field rely and depend on it for numerous applications. As one example the PEDOT:PSS thin films have high transparency in the visible range, thermal stability, and mechanical flexibility. However, when an aqueous dispersion of PEDOT:PSS is casted, the film shows low conductivity, lower than 1 S cm$^{-1}$.[4,5] To increase the conductivity, enhancement agents that improve the conductivity of the dispersion are being intensively studied and applied. The so called secondary dopants are added to the PEDOT:PSS dispersion to enhance its conductivity. Many secondary dopants are known nowadays including organic solvents, ionic liquids, acids, salts, polyols, and surfactants.[6–9] Furthermore, other additives are needed to impart good film forming properties to the PEDOT:PSS dispersions. Those will be described in more detail in the next sub-section.

**1.1.2 Use of additives to improve the properties of PEDOT:PSS**

As mentioned before, PEDOT:PSS is commercialized in the form of an aqueous dispersion which can be processed in the form of thin films by spin-coating and solvent casting methods and generally applied in polymer electronics.[10,11] Finding applications as electrodes for electrophysiology, a variety of biosensors, organic electrochemical transistors (OECTs), small bioelectrode coatings.[12–21] However, PEDOT:PSS is rarely applied or employed as such. Many treatments and additives are included in the formulation modifying its characteristics to well suit its properties for each application. These additives very often added with the intention of increasing the electronic conductivity of the final film. They are organic solvents, ionic liquids, acids, salts, polyols, and surfactants.[6–8] (Figure 1.4) Furthermore, other types of additives like binders, crosslinkers, surfactants and solvents are added to PEDOT:PSS dispersions in order to improve the final film properties like film hardness and roughness, substrate attachment, coatability, film structure, etc.
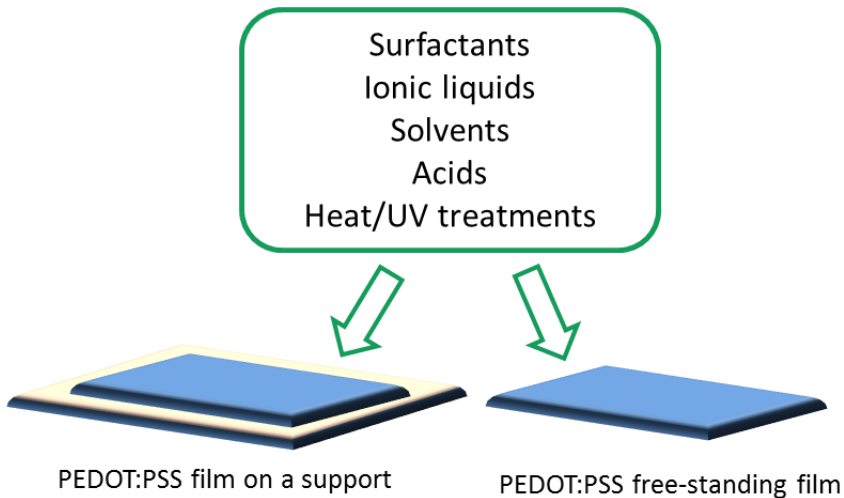


**Figure 1.4** Additives and treatments applied to PEDOT:PSS for film formation.

By the addition of the secondary dopants or influenced by thermal or UV post-treatments, PEDOT:PSS can exhibit a wide range of electrical conductivities from $10^{-2}$ to 4600 S cm$^{-1}$.[22–24] Post treatments can increase the conductivity as a direct consequence of conformational changes of PEDOT chains from benzoid to quinoid structure (Figure 1.2), phase separation between insulating PSS and conducting PEDOT chains, rearrangement of PEDOT, and excess PSS removal. Acid treatments like acetic acid, propionic acid, butyric acid, oxalic acid, sulfuric acid, hydrochloric acid,[25] boric acid,[26] and phosphoric acid[27] enhance the conductivity. As well, organic solvents are widely used with the same purpose like dimethyl formamide (DMF),[28] dimethyl sulfoxide (DMSO)[29,30] or tetrahydrofuran (THF).[31] The addition of solvents is normally accompanied by a high temperature post-deposition treatment. In this way, the solvent is evaporated and the morphological change in the film occurs. Other post-deposition treatment like the exposure to ultraviolet light enhances the conductivity as well.[32] The combination of concentrated sulfuric acid and heat treatments leads to the formation of highly conductive crystalline PEDOT.[33–36] In addition, ionic liquids (IL) were first used as dopants by Döbbelin et al.[37] Supporting the idea that the IL was inducing a phase separation between PSS and PEDOT grains. Imidazolium and pyrrolidonium IL types are found as conductivity enhancers.[38–40] Moreover, the surfactant dodecyl benzene sulfonic acid (DBSA) although it is an additive added to PEDOT dispersions because it facilitates film quality fabrication it has as well an influence on the conductivity.[41]

Once a PEDOT:PSS film is formed, there is a demand to keep its integrity, avoid delamination and redispersion of the polymer chains when in contact with water in an aqueous environment like cell media for *in vitro* studies or biological fluids for *in vivo* applications. In order to achieve this film stability, water soluble chemical compounds are being added to the PEDOT:PSS dispersion prior to the film formation. These chemicals are polymers like polyvinyl alcohol (PVA)[42,43] or polyethylene oxide (PEO).[44] The down side of the addition of these crosslinkers

is the drastic reduction in the conductivity up to several orders of magnitude with respect to pristine PEDOT:PSS. The silane based crosslinker, 3-glycidoxypropyltrimethoxysilane (GOPS)[45–47] showed to reduce the conductivity of PEDOT:PSS in a minor extend when used at low concentrations. Very recently, the most novel crosslinker divinyl sulfone (DVS) was presented. DVS has been shown to preserve the conductivity of the PEDOT:PSS without need of harsh heat treatments.[48]



**Figure 1.5.** Stretchable[49] and  flexible PEDOT films[50]

In the search to improve the properties of PEDOT:PSS, plenty of research effort has been dedicated to the developing of stretchable films (Figure 1.5). This will allow the fabrication of stretchable electronics with conducting polymers. Two ways have been investigated, the addition of elastic polymers like polydimethylsiloxane (PDMS)[51,52] into the dispersion or the deposition of the dispersion onto stretchable substrates. The first technique that includes an insulating elastomer in the dispersion has a detrimental effect on conductivity. Some surfactants have also a second effect; they increase the stretchability of PEDOT: PSS acting as plasticizers. For example, Zonyl[53] or Triton[54] increase the stretchability and ductility, allowing the material to withstand elastic deformation. The second technique is to make stretchable films on an elastic substrate, which increases the stretchability with less effect on the conductivity.  For that, elastic supports are used like PDMS,[55,56] polyvinyl alcohol (PVA),[57] or textiles.[58–60] But,

it is with the use of ionic liquids that researchers managed to achieve both mechanical stretchability along with high conductivity.[49,61]

## 1.2 Mixed conduction, OECT and electrolytes

CPs have mixed conduction. Both hole and ion transports are key properties for organic electronic device performance in many fields like electrochromic displays, energy harvesting, sensing devices, and mechanical actuators. In the field of bioelectronics, ion transport gets special important because biological systems communicate by ion fluxes. The different applications of PEDOT:PSS the in bioelectronics field are presented in Figure 1.6. PEDOT:PSS is currently applied in devices such as organic-electrochemical transistors (OECT), electrodes for electrophysiology, electronic textiles, electronic skin or organic-electronic ion-pumps. Those devices do several functions such as (bio)sensors of body signals as well as drug delivery.
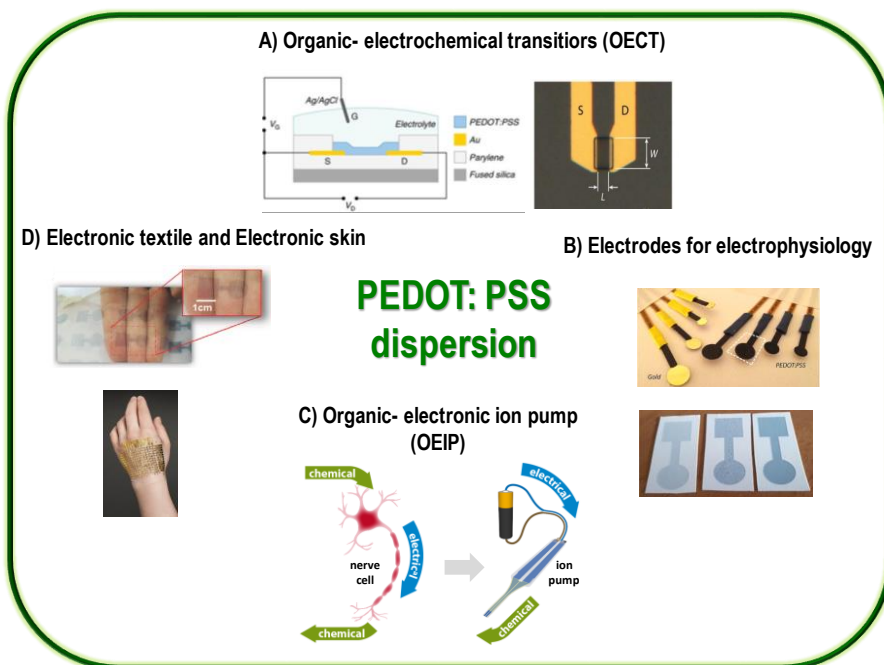
**Figure 1.6.** Different applications of PEDOT:PSS. a) organic-electrochemical transistor (OECT),[62] b) electrodes for electrophysiology,[63,64] c) organic-electronic ion pump (OEIP)[65] and d) electronic textile[66] and electronic skin.[67]

CPs which are mechanically and biologically compatible with biological tissues are able to communicate with them by their ability to conduct both electrons and ions. Several devices are based on CPs and their mixed conductivity in the bioelectronics field, like organic electrochemical transistors (OECTs) and organic electronic ion pumps (OEIPs). OEIPS are used for example in drug delivery[65] since ions are delivered when an electronic current is applied. OECTs are devices employed in this thesis work and thus, they deserve an extended introduction to their working principle. The active layer of an OECT is formed by a conducting polymer as can be observed in Figure 1.7.
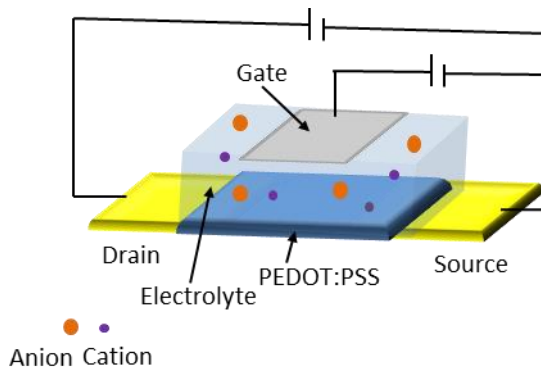
**Figure 1.7.** Schema of an OECT

The state-of-the-art CP is commonly PEDOT doped by PSS chains. In this case the OECT functioning is determined by hole transport (p-type). This CP active layer is in contact with an electrolyte and with the source and the drain; and, in contact with the electrolyte, there is a gate electrode. The gate can be planar or immersed in the electrolyte. Source and drain provide electrical contact to the active layer and when a voltage is applied to the drain ($V_D$) a current ($I_D$) flows through the active layer due to the presence of electron holes. This current is measured and determines the device ON state when this current is at the highest.[62,68] The gate is providing electrical contact to the electrolyte and when a positive voltage is applied at the gate ($V_G$), cations from the electrolyte are injected into the CP film. These cations couple negatively charged PSS chains reducing the number of PEDOT electron holes thus reducing the current that flows through the channel until the OECT reaches the OFF state. This process is ideally reversible and when a negative voltage is applied to the gate, cations exit the film increasing the PEDOT doping reaching again the OECT ON state. As the ionic current from the electrolyte to the channel is modulating the channel electronic current, we have an ion to electron conversion. The amplification capacity from the ionic to the electronic signals in the OECT is given by the

parameter called transconductance ($g_m$) which is quantifying the signal transduction. Transconductance is defined as $g_m=\Delta I_D/\Delta V_G$,[69] where $I_D$ is the drain current and $V_G$ is the gate voltage. $g_m$ depends on the volume of the channel.[70] Commonly, aqueous electrolytes are used to operate OECTs, for example NaCl solutions,[69,71] *phosphate-buffered saline* solution,[72,73] or cell media.[74–76] Proper operation of OECT is achieved when the ions of the electrolyte have high ionic mobility to allow for fast de-doping and doping of the OECT channel. As a possible alternative to aqueous electrolyte, coupling of OECTs and solid state electrolytes was demonstrated previously.[77,78] Solid state electrolytes display the interconnection properties of a solid network and the diffusive power of a liquid. The benefits of solid electrolytes over liquid ones are their chemical structure, mechanical stability and slower drying process maintaining the high ionic mobility during longer periods of time.[79] Their main drawback is that they normally show slower PEDOT:PSS switching response than when liquid electrolytes are employed. With high ionic mobility and high water retention, hydrogels are also good candidates for OECTs self-standing electrolytes.

## 1.3. PEDOT biopolymer aqueous dispersions

In most bioelectronics applications, the fine tuning of the interface of conducting polymers and biological molecules or tissues/organisms is a crucial parameter. As one illustrative example, the biotic/abiotic interface for interfacing with live cells can be improved by the incorporation of biological molecules such as nucleotides or proteins for functionality, e.g., for sensing. In this way, the biofunctionalized conductive polymer can enhance their ultimate properties such as biocompatibility and adhesion, and could help to reduce the inflammatory response of a device in living tissue. The two components of PEDOT:PSS are limited, due on the one hand to the lack of functionality of PEDOT and on the other hand to the low biocompatibility of PSS. To overcome these limitations,

much effort has been devoted to design innovative poly(dioxythiophene) polymer containing different functional groups for improved biocompatibility.

It is well known that EDOT monomer can be polymerized using different methods such as electrochemical polymerization, vapor phase polymerization (VPP) or chemical oxidative polymerization. Electrochemical and VPP polymerization methods usually give polymer films with very good properties such as surface quality, high conductivity and very stable redox chemistry. However, for large-scale applications, chemical polymerization is the preferred route due to its easy scale-up. For instance, this is the method used to produce industrially the PEDOT:PSS dispersions that are commercially available. PEDOT:PSS is currently being used in the area of bioelectronics due to its low toxicity with several cell types including endothelial, epithelial, fibroblast, macrophage, and most importantly human neuronal cell lines in vitro.[80–83] However, regardless of how promising this material has proven to be, the long-term effects such as PEDOT chains degradation and possible release of acidic PSS degradation products remains a potential issue.[84]

A demonstrated strategy to enhance the biocompatibility and reduce the cytotoxicity of conducting polymers like PEDOT is the use of biomolecules as dopants. Thus, the incorporation of biopolymers could be the way to overcome the limitations of PEDOT:PSS dispersions for specific applications. Although PEDOT:PSS has proven to be an appropriate material for cell culture,[81,85] the aim is to provide an environment that stimulates and persuades cell growth. The first attempts to synthetize PEDOT doped by biopolymers was pioneered by Inganäs et al. by the electropolymerization of EDOT in the presence of biomolecules (heparin, hyaluronic acid, fibrinogen, gellan gum, carboxymethyl cellulose, xanthan gum, and pectin)[86–88] showing their potential due to their non-toxicity[89] and finding applications as electrode interfaces for cell recordings.[85,87] Inspired by these polymer composites formed by PEDOT, different water-based

PEDOT:biopolymer dispersions have been more recently synthetized by different groups using chemical polymerization.

PEDOT:biopolymer aqueous dispersions synthesized by chemical polymerization have been reported using DNA,[90] sulfated cellulose,[91] dextran sulfonate,[92] hyaluronic acid , heparin, chondroitin sulfate,[93] pectin[94] and guar gum.[95] The synthesis of all of them is very similar and it can be exemplified in Figure 1.8 for the case of PEDOT:hyalunoric acid dispersions. A typical PEDOT:biopolymer dispersion is synthesized by chemical oxidative polymerization of the EDOT monomer using an oxidant in the presence of a biopolymer as a stabilizer and dopant. However, some parameters vary from one synthesis to another, and these include the PEDOT:biopolymer ratio, reaction temperature, concentration, time and oxidant used. In a typical experimental set-up, these biomolecules and EDOT are firstly dissolved in water; once dissolved, the oxidant is added to the solution. This oxidant can be ammonium persulfate $((NH_4)_2S_2O_8)$, potassium persulfate $(K_2S_2O_8)$, iron (III) chloride $(FeCl_3)$ or iron (III) p-toluenesulfonate $((CH_3C_6H_4SO_3)_3Fe)$. A catalyst is often employed such as iron (II) sulfate $(Fe_2(SO_4)_3)$ to accelerate the reaction kinetics. Once the reaction is complete, the dispersions are purified by ion exchange, filtered and/or dialyzed.
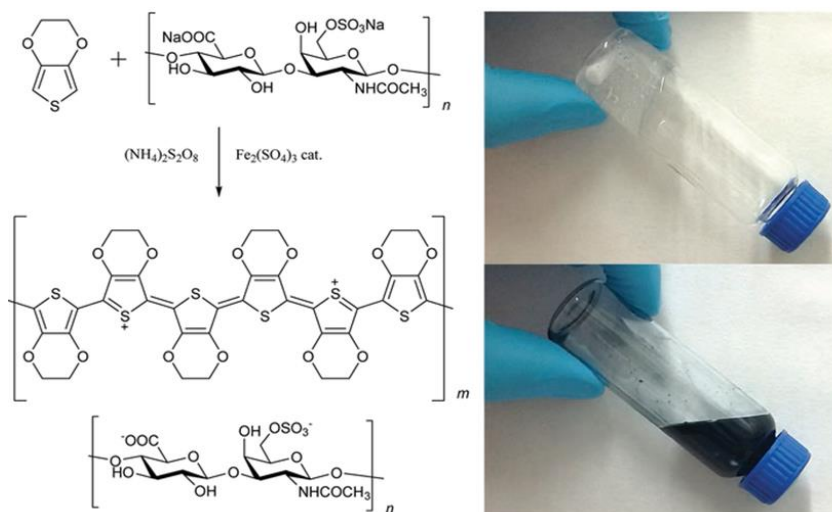
**Figure 1.8.** Synthetic route to PEDOT:hyaluronic acid aqueous dispersions.[93]

The PEDOT:biopolymer dispersions have a macroscopic aspect similar to PEDOT:PSS dispersions. As can be seen in the picture of Figure 1.8, dark blue dispersions are obtained. The dispersions are formed by PEDOT particles of sizes between 100–500 nm stabilized by the biopolymer. Particle size and morphology can be studied by UV-spectroscopy, light-scattering, scanning electron microscopy (SEM), and transmission electron microscopy (TEM). Similarly to PEDOT:PSS, the PEDOT:biopolymer dispersions can be processed in the form of thin films or the solution formulated to be inkjet printed, extrusion printed and spray coated. The electrochemical properties of the PEDOT:biopolymer films, for instance PEDOT:dextran sulfate or PEDOT:DNA present similar features to PEDOT:PSS. Furthermore, the electrical conductivity of drop-casted or spin-coated films presents similar values to pristine PEDOT:PSS without further treatments of between $10^{-1}$–10 S cm$^{-1}$.

Using this method, different PEDOT:biopolymer dispersions have been prepared as shown in Figure 1.9 and summarized in Table 1.1. The advantages of each

16

PEDOT:biopolymer material in comparison to PEDOT:PSS are discussed here. PEDOT:dextran sulfate presents two advantages. Firstly, it does not interfere with cell growth of L-929 cells in media in contrast with decreased cell numbers in culture when PEDOT:PSS is tested.[92] Secondly, PEDOT:dextran sulfate was absorbed into the PC12 cells while PEDOT:PSS was not. In the case of the PEDOT:DNA complex, the main advantages are its higher conductivity with respect to PEDOT:PSS and its non-acidic nature.[90] In the case of PEDOT:sulfate cellulose, it shows a higher conductivity than PEDOT:PSS which has been attributed to a higher proportion of PEDOT chains of quinoid structure than in PEDOT:PSS. In the case of PEDOT:glycosaminoglycans, they provide functional support in neuroregenerative processes and in the case of chondroitin sulfate, additional protection in oxidative milieu.[93]
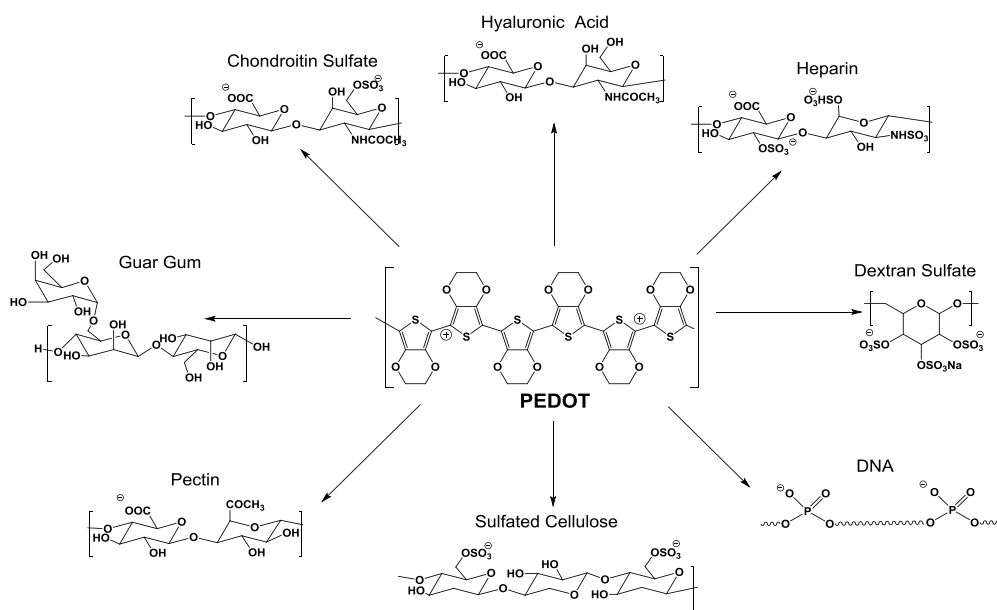


**Figure 1.9.** PEDOT:biopolymer dispersions employing hyaluronic acid, heparin, chondroitin sulfate,[93] dextran sulfate,[92] DNA,[90] sulfated cellulose,[91] pectin,[94] and guar gum[95].

In particular, PEDOT:biopolymers have been biologically tested by cell proliferation of a fibroblast cell line (L-929 cells) in the cases of dextran, heparin, hyaluronic acid and chondroitin sulfate. The biological study was more extended in the case of the glycosaminoglycans,[93] including cytotoxicity assays, SH-SY5Y differentiation studies and immunocytochemistry, and intracellular calcium measurements. In these studies, there are many biological findings. Hyaluronic acid, heparin and chondroitin sulfate do not interfere with physiological functions. They are more supportive for neuroregenerative processes compared to PEDOT:PSS and provide functional support. Moreover, chondroitin sulfate was found to have a neuroprotective effect against $H_2O_2$-induced cell death on SH-SY5Y cells. In the case of PEDOT:dextran sulfate, the studies showed higher L-929 cell line proliferation than PEDOT:PSS.

**Table 1.1.** Available PEDOT:biomolecule dispersions prepared by chemical oxidative polymerization. Achieved conductivities, biocompatibility test, particle size, morphology and applications.

| PEDOT:biomolec. | Conductivity (S·cm$^{-1}$) | Application | Biocompatibility test | Particle size and morph. |
|---|---|---|---|---|
| PEDOT:dextran sulfate [92] | 7 | Drug delivery, electrostimulation of cells | Cytotoxicity, L-929 cells | 394–691 nm |
| PEDOT:DNA [96] | 1 | biosensing, drug delivery | - | 50 nm fibers |
| PEDOT:heparin [93] | 0.05–0.001 | Recording/stimulating in vivo | Cytotoxicity, L-929 Cellular attachment, CCF-STTG1 cells Proliferation of SH-SY5Y cells | >1 µm spheres |
| PEDOT:chondroitin Sulfate [93] | 0.075–0.002 | Recording/stimulating in vivo | Cytotoxicity, L-929 Cellular attachment, CCF-STTG1 cells Proliferation of SH-SY5Y cells | 500 nm spheres |
| PEDOT:hyaluronic acid [93] | 0.071–0.003 | Recording/stimulating in vivo | Cytotoxicity, L-929 Cellular attachment, CCF-STTG1 cells Proliferation of SH-SY5Y cells | 200 nm spheres |

| | | | | |
|---|---|---|---|---|
| PEDOT:sulfated cellulose [91] | 0.576 | - | - | 250–350 nm |
| PEDOT:pectin [94] | <0.01 | - | - | - |
| PEDOT:guar gum [95] | 0.028–0.129 | Iongels | - | 100–300 nm spheres |

In Figure 1.10 we can find applications of PEDOT:biopolymer dispersions. Although there are thorough biocompatibility studies of these dispersions as mentioned above, little is known about their long-term effects when implanted.
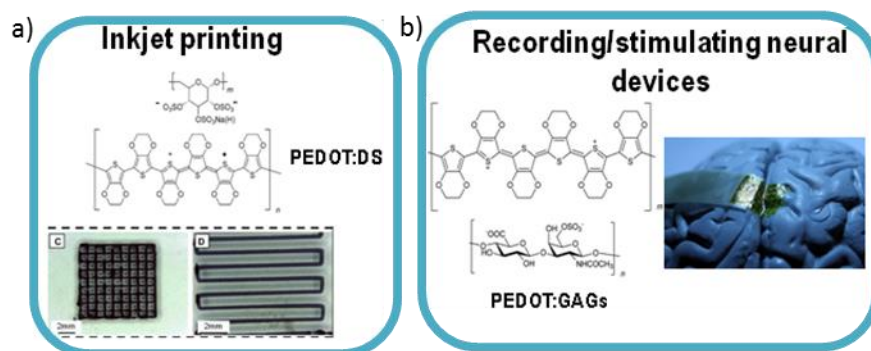


**Figure 1.10.** Different applications of PEDOT:biopolymer dispersions. (a) Inkjet printing. [92] (b) Recording/stimulating devices.[93]

The longest cytotoxic test performed so far had a duration of 96 h in the case of PEDOT:dextran sulfate. Although promising because of their satisfactory findings, these dispersions should undergo deeper study regarding their stability and possible long-term effects when in contact with living tissue.

PEDOT:biopolymer dispersions have great potential due to their improved biocompatibility, combined features and bio-based nature. The methods to increase the conductivity of these materials remains an unaddressed issue with

respect to the well-known methods used to increase the conductivity of PEDOT:PSS. This relatively low conductivity of PEDOT:biomolecules limits their applicability in some applications such as bioelectrodes.[84] The study of the effect of solvents or secondary dopants should be addressed. For instance, this effect was studied in the case of PEDOT:dextran sulfate, where ethylene glycol was added to the dispersion achieving higher conductivities (286% increase in conductivity reaching 20 $S \cdot cm^{-1}$). As polar organic compounds, ionic liquids and acids are able to induce phase separation in between PEDOT and PSS chains, PEDOT chains become more linearly oriented and more interconnected.[7,37,97] Treatments like these could be studied to induce the same consequences in PEDOT chains when biomolecules are used as dopants. Moreover, in order to extend their use, PEDOT:biomolecule dispersions should be applied and processed using different printing and coating techniques. For this reason, more applicability and synthesis studies should be performed to extend their use. If these limitations are encountered, PEDOT:biomolecule dispersions will find diverse applications in tissue engineering, drug delivery, biosensing, stimuli and neural recordings. Today, the advantages of PEDOT:biopolymer dispersions are mainly given in terms of biocompatibility and the available studies show their potential to offer functional support and protection in oxidative environments when implanted in vivo or applied in vitro.

## 1.4. Motivation, objectives and outline of the thesis

This thesis work is motivated by the fact that the expanding and developing bioelectronics field is demanding new materials that will play the interphase role in between biological tissues with electronics. In order to fulfill this task, these new materials need to be soft, biocompatible, and they should allow communication. For this reason, they need to present ionic and electronic conductivity to be able to translate the ion fluxes present in living tissue to electronic signals and vice-versa. If these materials present as well other

characteristics like flexibility, conformability, high conductivity and adhesive properties or being water based then they became even more suitable for diverse applications inside the field of bioelectronics.

Within this general objective, we have focused in developing new PEDOT type materials. As PEDOT:PSS is currently the most successful polymer in the field, we have attempted first to fabricate new materials that improved the performance of PEDOT:PSS. In this line we have developed new strategies to improve the performance of PEDOT:PSS in Organic Electrochemical Transistors (OECT), in electronic textiles as well as cutaneous electrodes by using new additives and cross-linking strategies for PEDOT:PSS. Furthermore, we targeted the preparation of a new hydrogel polymer electrolyte which showed excellent performance in PEDOT:PSS based devices like OECTs and cutaneous electrodes.

In the second part of this PhD thesis we have developed new PEDOT:polysaccharide dispersions as alternative materials to PEDOT:PSS. Two types of dispersions have been synthetized: one using the polysaccharide guar gum and a second one employing xanthan gum. First we investigated the synthesis of PEDOT:guar gum dispersion. This dispersion was then used to prepare new conductive iongels which combine the electronic conductive properties of PEDOT, the flexibility of the polysaccharide, and the ionic conductivity of the ionic liquids. This is a meaningful work since it is the first example in literature of a PEDOT iongel. Secondly, the PEDOT:xanthan gum dispersion was studied. Using this dispersion as the starting material, we fabricated conductive porous scaffolds for tissue engineering applications.
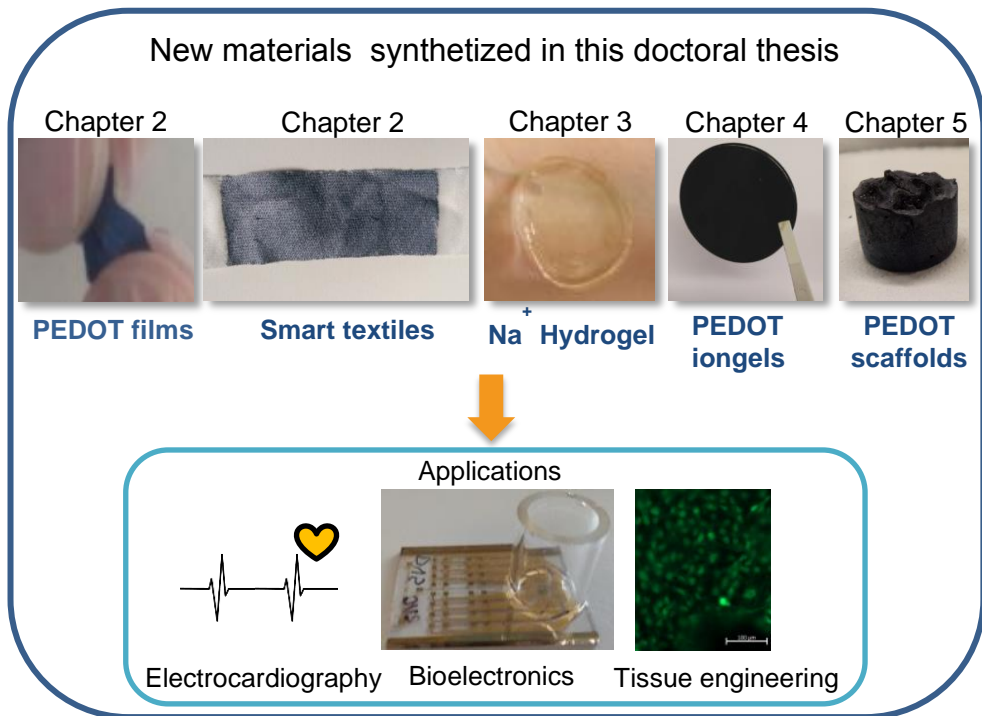
**Figure 1.11.** Work outline

This PhD thesis consists of six chapters. After the first introductory chapter, the second chapter deals with the investigation of a novel PEDOT:PSS crosslinker called divinyl sulfone (DVS) and the investigation of its use to synthetize PEDOT:PSS:DVS free-standing electrodes and smart textiles for cutaneous electrophysiology.

In the third chapter we find a newly synthetized single ion conductor hydrogel. Two applications of this hydrogel are studied: its use as a solid electrolyte in bioelectronics devices based on PEDOT:PSS like OECTs and as skin-electrode interphase in cutaneous electrodes for electrophysiology.

In the fourth chapter a PEDOT:polysaccharide water dispersion is synthetized through chemical oxidative polymerization as an alternative to the use of

PEDOT:PSS dispersion. Then the preparation and characterization of novel PEDOT iongel is presented.

Last, in chapter 5, PEDOT:polysaccharide porous scaffolds are introduced. These scaffolds are prepared by freeze-drying a PEDOT:polysaccharide dispersion. The material formed is porous and flexible and presents applications in the field of tissue engineering.

To conclude, chapter 6 shows the most relevant findings, future work, and conclusions obtained out of this three-year long work.

## 1.5. References

1  R. Ravichandran, S. Sundarrajan, J. R. Venugopal, S. Mukherjee and S. Ramakrishna, *J. R. Soc. Interface*, 2010, **7**, S559–S579.
2  Review on Conducting Polymers and Their Applications: Polymer-Plastics Technology and Engineering: Vol 51, No 14, http://www.tandfonline.com/doi/abs/10.1080/03602559.2012.710697?journalCode=lpte20, (accessed November 17, 2017).
3  S. Schumann, A. Elschner, D. Gaiser and W. Lövenich, *MRS Proc.*, 2015, **1771**, 207–212.
4  T. Stöcker, A. Köhler and R. Moos, *J. Polym. Sci. Part B Polym. Phys.*, 2012, **50**, 976–983.
5  D. Alemu, H.-Y. Wei, K.-C. Ho and C.-W. Chu, *Energy Environ. Sci.*, 2012, **5**, 9662.
6  J. Nevrela, M. Micjan, M. Novota, S. Kovacova, M. Pavuk, P. Juhasz, J. Kovac, J. Jakabovic and M. Weis, *J. Polym. Sci. Part B Polym. Phys.*, 2015, **53**, 1139–1146.
7  J. Ouyang, *Displays*, 2013, **34**, 423–436.
8  J. Saghaei, A. Fallahzadeh and M. H. Yousefi, *Org. Electron.*, 2015, **19**, 70–75.
9  A. Robert Hillman, S. J. Daisley and S. Bruckenstein, *Phys. Chem. Chem. Phys.*, 2007, **9**, 2379.
10 C. K. Chiang, C. R. Fincher, Y. W. Park, A. J. Heeger, H. Shirakawa, E. J. Louis, S. C. Gau and A. G. MacDiarmid, *Phys. Rev. Lett.*, 1977, **39**, 1098–1101.
11 Y. Wen and J. Xu, *J. Polym. Sci. Part Polym. Chem.*, 2017, **55**, 1121–1150.
12 D. Kumar and R. C. Sharma, *Eur. Polym. J.*, 1998, **34**, 1053–1060.

13 N. K. Guimard, N. Gomez and C. E. Schmidt, *Prog. Polym. Sci.*, 2007, **32**, 876–921.
14 J. Rivnay, R. M. Owens and G. G. Malliaras, *Chem. Mater.*, 2014, **26**, 679–685.
15 X. Strakosas, B. Wei, D. C. Martin, R. M. Owens, O. Nilsson, D. T. Simon, M. Berggren, C. Fischbach, G. G. Malliaras, D. Gourdon, V. F. Razumov, H. Sitter, S. Bauer and N. S. Sariciftci, *J Mater Chem B*, 2016, **4**, 4952–4968.
16 A. de Mel, G. Jell, M. M. Stevens and A. M. Seifalian, *Biomacromolecules*, 2008, **9**, 2969–2979.
17 J. Yang and D. C. Martin, *J. Mater. Res.*, 2006, **21**, 1124–1132.
18 L. K. Povlich, J. C. Cho, M. K. Leach, J. M. Corey, J. Kim and D. C. Martin, *Biochim. Biophys. Acta BBA - Gen. Subj.*, 2013, **1830**, 4288–4293.
19 X. Shen, L. Chen, J. Pan, Y. Hu, S. Li and J. Zhao, *Nanoscale Res. Lett.*, 2016, **11**, 532.
20 A. Herland, K. M. Persson, V. Lundin, M. Fahlman, M. Berggren, E. W. H. Jager and A. I. Teixeira, *Angew. Chem. Int. Ed.*, 2011, **50**, 12529–12533.
21 D. T. Simon, E. O. Gabrielsson, K. Tybrandt and M. Berggren, *Chem. Rev.*, 2016, **116**, 13009–13041.
22 J. Ouyang, *ACS Appl. Mater. Interfaces*, 2013, **5**, 13082–13088.
23 B. J. Worfolk, S. C. Andrews, S. Park, J. Reinspach, N. Liu, M. F. Toney, S. C. B. Mannsfeld and Z. Bao, *Proc. Natl. Acad. Sci.*, 2015, **112**, 14138–14143.
24 H. Shi, C. Liu, Q. Jiang and J. Xu, *Adv. Electron. Mater.*, 2015, **1**, 1500017.
25 Y. Xia and J. Ouyang, *ACS Appl. Mater. Interfaces*, 2010, **2**, 474–483.
26 Ö. Yagci, S. S. Yesilkaya, S. A. Yüksel, F. Ongül, N. M. Varal, M. Kus, S. Günes and O. Icelli, *Synth. Met.*, 2016, **212**, 12–18.
27 W. Meng, R. Ge, Z. Li, J. Tong, T. Liu, Q. Zhao, S. Xiong, F. Jiang, L. Mao and Y. Zhou, *ACS Appl. Mater. Interfaces*, 2015, **7**, 14089–14094.
28 Z. Fan, D. Du, Z. Yu, P. Li, Y. Xia and J. Ouyang, *ACS Appl. Mater. Interfaces*, 2016, **8**, 23204–23211.
29 D. Huang, T. Goh, J. Kong, Y. Zheng, S. Zhao, Z. Xu and A. D. Taylor, *Nanoscale*, 2017, **9**, 4236–4243.
30 I. Lee, G. W. Kim, M. Yang and T.-S. Kim, *ACS Appl. Mater. Interfaces*, 2016, **8**, 302–310.
31 Y. Xia and J. Ouyang, *J. Mater. Chem.*, 2011, **21**, 4927.
32 Y. Xing, M. Qian, G. Wang, G. Zhang, D. Guo and J. Wu, *Sci. China Technol. Sci.*, 2014, **57**, 44–48.
33 B. Cho, K. S. Park, J. Baek, H. S. Oh, Y.-E. Koo Lee and M. M. Sung, *Nano Lett.*, 2014, **14**, 3321–3327.
34 T. Takano, H. Masunaga, A. Fujiwara, H. Okuzaki and T. Sasaki, *Macromolecules*, 2012, **45**, 3859–3865.
35 Y. Xia, K. Sun and J. Ouyang, *Adv. Mater.*, 2012, **24**, 2436–2440.
36 N. Kim, S. Kee, S. H. Lee, B. H. Lee, Y. H. Kahng, Y.-R. Jo, B.-J. Kim and K. Lee, *Adv. Mater.*, 2014, **26**, 2268–2272.

37 M. Döbbelin, R. Marcilla, M. Salsamendi, C. Pozo-Gonzalo, P. M. Carrasco, J. A. Pomposo and D. Mecerreyes, *Chem. Mater.*, 2007, **19**, 2147–2149.

38 F. Atabaki, M. H. Yousefi, A. Abdolmaleki and M. Kalvandi, *Polym.-Plast. Technol. Eng.*, 2015, **54**, 1009–1016.

39 C. Badre, L. Marquant, A. M. Alsayed and L. A. Hough, *Adv. Funct. Mater.*, 2012, **22**, 2723–2727.

40 L. Zhao, J. Qiu, X. Cao, W. Dong, J. You and Y. Li, *Macromol. Res.*, 2013, **21**, 456–461.

41 S. Zhang, P. Kumar, A. S. Nouas, L. Fontaine, H. Tang and F. Cicoira, *APL Mater.*, 2015, **3**, 14911.

42 A. R. Hopkins and J. R. Reynolds, *Macromolecules*, 2000, **33**, 5221–5226.

43 C. Chen, J. C. LaRue, R. D. Nelson, L. Kulinsky and M. J. Madou, *J. Appl. Polym. Sci.*, 2012, **125**, 3134–3141.

44 T.-M. Huang, S. Batra, J. Hu, T. Miyoshi and M. Cakmak, *Polymer*, 2013, **54**, 6455–6462.

45 M. ElMahmoudy, S. Inal, A. Charrier, I. Uguz, G. G. Malliaras and S. Sanaur, *Macromol. Mater. Eng.*, 2017, **302**, n/a-n/a.

46 A. Williamson, J. Rivnay, L. Kergoat, A. Jonsson, S. Inal, I. Uguz, M. Ferro, A. Ivanov, T. A. Sjöström, D. T. Simon, M. Berggren, G. G. Malliaras and C. Bernard, *Adv. Mater.*, 2015, **27**, 3097–3097.

47 A. Håkansson, S. Han, S. Wang, J. Lu, S. Braun, M. Fahlman, M. Berggren, X. Crispin and S. Fabiano, *J. Polym. Sci. Part B Polym. Phys.*, 2017, **55**, 814–820.

48 D. Mantione, I. del Agua, W. Schaafsma, M. ElMahmoudy, I. Uguz, A. Sanchez-Sanchez, H. Sardon, B. Castro, G. G. Malliaras and D. Mecerreyes, *ACS Appl. Mater. Interfaces*, 2017, **9**, 18254–18262.

49 Y. Wang, C. Zhu, R. Pfattner, H. Yan, L. Jin, S. Chen, F. Molina-Lopez, F. Lissel, J. Liu, N. I. Rabiah, Z. Chen, J. W. Chung, C. Linder, M. F. Toney, B. Murmann and Z. Bao, *Sci. Adv.*, 2017, **3**, e1602076.

50 C. Yu, K. Choi, L. Yin and J. C. Grunlan, *ACS Nano*, 2011, **5**, 7885–7892.

51 K. Sun, S. Zhang, P. Li, Y. Xia, X. Zhang, D. Du, F. H. Isikgor and J. Ouyang, *J. Mater. Sci. Mater. Electron.*, 2015, **26**, 4438–4462.

52 T. S. Hansen, K. West, O. Hassager and N. B. Larsen, *Adv. Funct. Mater.*, 2007, **17**, 3069–3073.

53 S. Savagatrup, E. Chan, S. M. Renteria-Garcia, A. D. Printz, A. V. Zaretski, T. F. O'Connor, D. Rodriquez, E. Valle and D. J. Lipomi, *Adv. Funct. Mater.*, 2015, **25**, 427–436.

54 S.-S. Yoon and D.-Y. Khang, *J. Phys. Chem. C*, 2016, **120**, 29525–29532.

55 D. J. Lipomi, J. A. Lee, M. Vosgueritchian, B. C.-K. Tee, J. A. Bolander and Z. Bao, *Chem. Mater.*, 2012, **24**, 373–382.

56 M. Vosgueritchian, D. J. Lipomi and Z. Bao, *Adv. Funct. Mater.*, 2012, **22**, 421–428.

57 P. Li, K. Sun and J. Ouyang, *ACS Appl. Mater. Interfaces*, 2015, **7**, 18415–18423.

58 Y. Ding, M. A. Invernale and G. A. Sotzing, *ACS Appl. Mater. Interfaces*, 2010, **2**, 1588–1593.

59 X. Yu, X. Su, K. Yan, H. Hu, M. Peng, X. Cai and D. Zou, *Adv. Mater. Technol.*, 2016, **1**, 1600009.

60 C. Yeon, G. Kim, J. W. Lim and S. J. Yun, *RSC Adv*, 2017, **7**, 5888–5897.

61 M. Y. Teo, N. Kim, S. Kee, B. S. Kim, G. Kim, S. Hong, S. Jung and K. Lee, *ACS Appl. Mater. Interfaces*, 2017, **9**, 819–826.

62 D. Khodagholy, J. Rivnay, M. Sessolo, M. Gurfinkel, P. Leleux, L. H. Jimison, E. Stavrinidou, T. Herve, S. Sanaur, R. M. Owens and G. G. Malliaras, *Nat. Commun.*, 2013, **4**, ncomms3133.

63 P. Leleux, J.-M. Badier, J. Rivnay, C. Bénar, T. Hervé, P. Chauvel and G. G. Malliaras, *Adv. Healthc. Mater.*, 2014, **3**, 490–493.

64 E. Bihar, T. Roberts, M. Saadaoui, T. Hervé, J. B. De Graaf and G. G. Malliaras, *Adv. Healthc. Mater.*, 2017, **6**, n/a-n/a.

65 A. Williamson, J. Rivnay, L. Kergoat, A. Jonsson, S. Inal, I. Uguz, M. Ferro, A. Ivanov, T. A. Sjöström, D. T. Simon, M. Berggren, G. G. Malliaras and C. Bernard, *Adv. Mater.*, 2015, **27**, 3138–3144.

66 E. Bihar, T. Roberts, E. Ismailova, M. Saadaoui, M. Isik, A. Sanchez-Sanchez, D. Mecerreyes, T. Hervé, J. B. De Graaf and G. G. Malliaras, *Adv. Mater. Technol.*, 2017, **2**, n/a-n/a.

67 T. Someya, in *IEEE International Electron Devices Meeting 2003*, 2003, p. 8.4.1-8.4.4.

68 P. Andersson Ersman, D. Nilsson, J. Kawahara, G. Gustafsson and M. Berggren, *Org. Electron.*, 2013, **14**, 1276–1280.

69 A. Giovannitti, C. B. Nielsen, D.-T. Sbircea, S. Inal, M. Donahue, M. R. Niazi, D. A. Hanifi, A. Amassian, G. G. Malliaras, J. Rivnay and I. McCulloch, *Nat. Commun.*, 2016, **7**, 13066.

70 J. Rivnay, P. Leleux, M. Ferro, M. Sessolo, A. Williamson, D. A. Koutsouras, D. Khodagholy, M. Ramuz, X. Strakosas, R. M. Owens, C. Benar, J.-M. Badier, C. Bernard and G. G. Malliaras, *Sci. Adv.*, 2015, **1**, e1400251–e1400251.

71 A. Giovannitti, D.-T. Sbircea, S. Inal, C. B. Nielsen, E. Bandiello, D. A. Hanifi, M. Sessolo, G. G. Malliaras, I. McCulloch and J. Rivnay, *Proc. Natl. Acad. Sci.*, 2016, **113**, 12017–12022.

72 I. Gualandi, D. Tonelli, F. Mariani, E. Scavetta, M. Marzocchi and B. Fraboni, *Sci. Rep.*, , DOI:10.1038/srep35419.

73 L. Contat-Rodrigo, C. Pérez-Fuster, J. Lidón-Roger, A. Bonfiglio and E. García-Breijo, *Sensors*, 2016, **16**, 1599.

74 P. Lin, F. Yan, J. Yu, H. L. W. Chan and M. Yang, *Adv. Mater.*, 2010, **22**, 3655–3660.

75 J. Rivnay, P. Leleux, A. Hama, M. Ramuz, M. Huerta, G. G. Malliaras and R. M. Owens, *Sci. Rep.*, , DOI:10.1038/srep11613.

76 M. Ramuz, A. Hama, J. Rivnay, P. Leleux and R. M. Owens, *J Mater Chem B*, 2015, **3**, 5971–5977.

77 D. Khodagholy, V. F. Curto, K. J. Fraser, M. Gurfinkel, R. Byrne, D. Diamond, G. G. Malliaras, F. Benito-Lopez and R. M. Owens, *J. Mater. Chem.*, 2012, **22**, 4440.

78 Z. Yi, G. Natale, P. Kumar, E. Di Mauro, M.-C. Heuzey, F. Soavi, I. I. Perepichka, S. K. Varshney, C. Santato and F. Cicoira, *J Mater Chem C*, 2015, **3**, 6549–6553.

79 K. Nagamine, S. Chihara, H. Kai, H. Kaji and M. Nishizawa, *Sens. Actuators B Chem.*, 2016, **237**, 49–53.

80 F. Amorini, I. Zironi, M. Marzocchi, I. Gualandi, M. Calienni, T. Cramer, B. Fraboni and G. Castellani, *ACS Appl. Mater. Interfaces*, 2017, **9**, 6679–6689.

81 M. Marzocchi, I. Gualandi, M. Calienni, I. Zironi, E. Scavetta, G. Castellani and B. Fraboni, *ACS Appl. Mater. Interfaces*, 2015, **7**, 17993–18003.

82 S. Inal, A. Hama, M. Ferro, C. Pitsalidis, J. Oziat, D. Iandolo, A.-M. Pappa, M. Hadida, M. Huerta, D. Marchat, P. Mailley and R. M. Owens, *Adv. Biosyst.*, 2017, **1**, 1700052.

83 M. Ramuz, A. Hama, M. Huerta, J. Rivnay, P. Leleux and R. M. Owens, *Adv. Mater.*, 2014, **26**, 7083–7090.

84 M. Asplund, H. von Holst and O. Inganäs, *Biointerphases*, 2008, **3**, 83–93.

85 R. M. Miriani, M. R. Abidian and D. R. Kipke, IEEE, 2008, pp. 1841–1844.

86 E. M. Thaning, M. L. M. Asplund, T. A. Nyberg, O. W. Inganäs and H. von Holst, *J. Biomed. Mater. Res. B Appl. Biomater.*, 2010, **93B**, 407–415.

87 M. Suzuki, M. Nakayama, K. Tsuji, T. Adachi and K. Shimono, *Electrochemistry*, 2016, **84**, 354–357.

88 R. Lv, Y. Sun, F. Yu and H. Zhang, *J. Appl. Polym. Sci.*, 2012, **124**, 855–863.

89 M. Asplund, E. Thaning, J. Lundberg, A. C. Sandberg-Nordqvist, B. Kostyszyn, O. Inganäs and H. von Holst, *Biomed. Mater.*, 2009, **4**, 45009.

90 Y. Ner, M. A. Invernale, J. G. Grote, J. A. Stuart and G. A. Sotzing, *Synth. Met.*, 2010, **160**, 351–353.

91 M. Horikawa, T. Fujiki, T. Shirosaki, N. Ryu, H. Sakurai, S. Nagaoka and H. Ihara, *J Mater Chem C*, 2015, **3**, 8881–8887.

92 D. G. Harman, R. Gorkin, L. Stevens, B. Thompson, K. Wagner, B. Weng, J. H. Y. Chung, M. in het Panhuis and G. G. Wallace, *Acta Biomater.*, 2015, **14**, 33–42.

93 D. Mantione, I. del Agua, W. Schaafsma, J. Diez-Garcia, B. Castro, H. Sardon and D. Mecerreyes, *Macromol. Biosci.*, 2016, **16**, 1227–1238.

94 A. I. Hofmann, D. Katsigiannopoulos, M. Mumtaz, I. Petsagkourakis, G. Pecastaings, G. Fleury, C. Schatz, E. Pavlopoulou, C. Brochon, G. Hadziioannou and E. Cloutet, *Macromolecules*, 2017, **50**, 1959–1969.

95 I. del Agua, D. Mantione, N. Casado, A. Sanchez-Sanchez, G. G. Malliaras and D. Mecerreyes, *ACS Macro Lett.*, 2017, **6**, 473–478.

96 Y. Ner, M. A. Invernale, J. G. Grote, J. A. Stuart and G. A. Sotzing, *Synth. Met.*, 2010, **160**, 351–353.

97 H. Yan, T. Jo and H. Okuzaki, *Polym. J.*, 2009, **41**, 1028–1029.

# Chapter 2.

# DVS-crosslinked PEDOT:PSS free-standing and textile electrodes
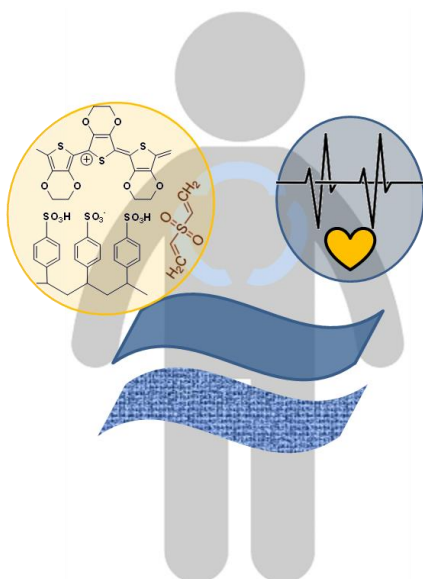
# Chapter 2. DVS-crosslinked PEDOT:PSS free-standing and textile electrodes

## 2.1. Introduction

Health monitoring using wearable devices are great technological improvements that allows to record human physiological signals in a continuous way.[1] This helps patients with heart pathologies to benefit from continuous monitoring of their vital signals while being at home. This is also useful for healthy patients and athletes that can profit from it as preventive medicine while continuing their ordinary life routine. Among a variety of physiological signals, brain activity by electroencephalography (EEG), cardiac activity by electrocardiography (ECG) and muscle activity by electromyography (EMG) can be recorded with cutaneous electrodes in a non-invasive way. The main specifications for cutaneous electrodes rely on the need to be comfortable and to provide good contact with the body. They should not present any toxicity or allergic reactions to the skin and furthermore, they should be easy to wear and can be produced at low cost.

In the field of bioelectronics, traditional metal electrodes are actually being replaced by conducting polymer electrodes based on poly(3,4-ethylenedioxythiophene) derivatives which have many benefits in recording electrophysiological signals.[2–5] When PEDOT:PSS is used in cutaneous electrodes, these electrodes show low impedance in contact with skin improving the signal to noise ratio. Due to their organic nature conducting polymers have many advantages in the development of flexible, conformable, stretchable, and importantly wearable electronics. The development of electronics that can be embedded in our clothing or body is of extreme interest for the development of next generation medical devices that can continuously monitor our health. For instance, it is possible to make conformable tattoo electrodes with PEDOT:PSS that conformably adhere to the skin,[6,7] providing seamless communication channel with the human body. Recently, electronic textiles using PEDOT electrodes are appeared as another type of technology facilitating the interface with the skin. They are formed by coating PEDOT:PSS water dispersion on textile fibers.[8] In this way, these PEDOT fiber-based electrodes combine the stretchability and breathability of textiles with organic electronic properties.[9,10] In general in PEDOT coatings, a (3-Glycidyloxypropyl)trimethoxysilane (GOPS) crosslinker is commonly used,[11,12] which provides polymer adhesion to the substrate avoiding its redispersion when in contact with water. However, this crosslinker is not ideal as it reduces the overall conductivity of PEDOT:PSS, hereby lowering electrode performance.

In this work we propose to use a novel type of additive such as divinyl sulfone (DVS) crosslinker to alter PEDOT:PSS' properties towards water stable, mechanically robust and electronically conductive material. Here we present the fabrication of two types of PEDOT:PSS:DVS electrodes: free-standing films and textile electrodes. Following electrochemical and mechanical evaluations the ECG recordings were successfully obtained with these electrodes as proof of their applicability in cutaneous electrophysiology. The free-standing films can be

used in wearable devices attaching to the body as second skin while textile electrodes are more suitable for long-term applications. By introducing the DVS crosslinker, the PEDOT electrodes show remarkable stability in water, and it does not reduce PEDOT:PSS' conductivity. PEDOT:PSS:DVS electrodes are more elastic and therefore their resistivity is little affected when stretched in water.

## 2.2. Results and discussion

### 2.2.1. Fabrication and characterization of PEDOT:PSS free-standing films

Free-standing films were fabricated by crosslinking PEDOT:PSS with divinyl sulfone and simply detaching it by peeling. The crosslinking mechanisms of PEDOT:PSS by DVS has been studied recently[13] and here we use the same procedure. This formulation has the advantage of being easily detached from the substrate compared to conventional GOPS containing formulation which strongly adheres to any surface. Our fabrication process is shown in Figure 2.1a. First, the PEDOT:PSS aqueous dispersion is well-mixed with DVS and then drop-casted onto a glass slide. It has been demonstrated that crosslinking reaction of DVS is based on the reaction of vinyl groups with nucleophiles like alcohol groups available in the PEDOT:PSS formulation.[13,14] Water is evaporated by applying moderate temperature (60 $^{o}$C), and the formed film can be directly peeled-off from the substrate. In this way, a flexible and elastic in water PEDOT freestanding film is formed.
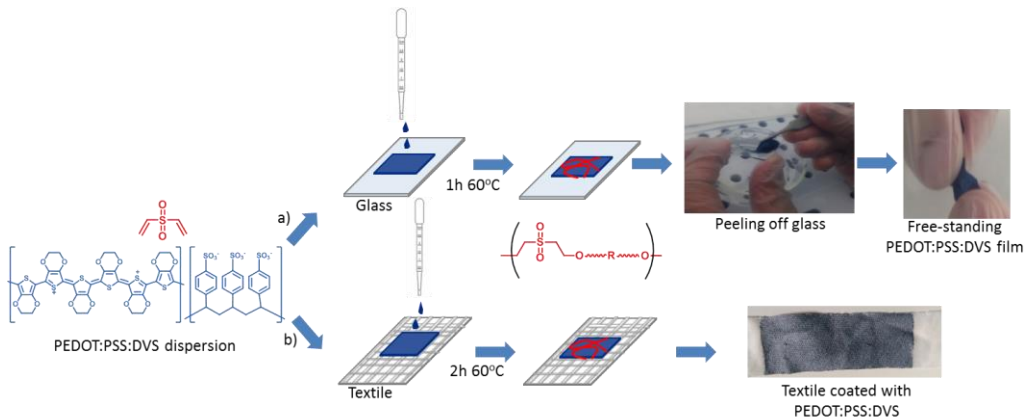
**Figure 2.1.** Synthetic route: a) the way of fabrication of PEDOT:PSS:DVS free-standing films and b) PEDOT:PSS:DVS-coated textile. A blend on PEDOT:PSS with DVS is made, then it is dropcasted on the substrate. After a heat treatment at 60 $^o$C DVS crosslinks and water is evaporated resulting in the final material.

Mechanical tests have been performed and Young's modulus of the film is 19.3 ± 0.7 MPa with a strain at break of 15 ± 0.4 % (tested sample dimensions and graphs are available in Figure 2.2) were measured. It is well know that mechanical properties of PEDOT can be easily affected by any type of additives and even by the type of dopants.[15] We observe that the effect of the DVS results in increase of the strain at break value and reduction of the Young's modulus of the film when compared with pristine PEDOT:PSS (550 MPa and 5 % elongation at break, published elsewhere).[16] The 10 % gain in stretchability of the PEDOT:PSS film should in addition better tolerate skin stretching and movement without the electrode being damaged in wearable conditions.
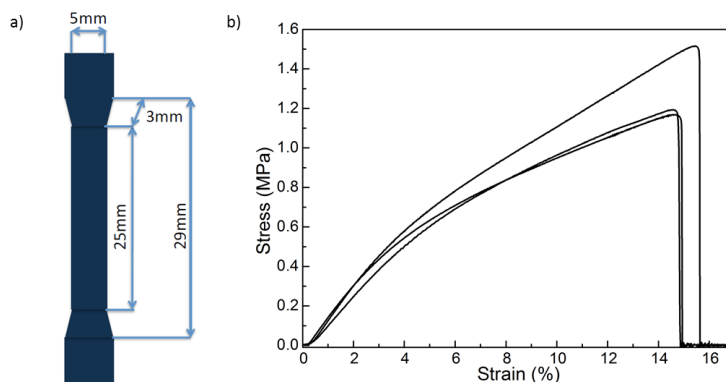
**Figure 2.2**. Free-standing PEDOT:PSS:DVS film stretchability study. a) Sample dimensions for stretching studies (thickness 0.5 mm), b) Stress-strain curves for strain at break and Young's modulus calculations.

Interestingly, the electrical conductivity measured with four point probe (4PP) of the DVS crosslinked PEDOT:PSS film shows a value of 605.9 ± 28.4 S cm$^{-1}$, when compared with other crosslinkers which induce a drop in conductivity.[15] The electroactive properties of the PEDOT:PSS film were measured using cyclic voltammetry. Typical cyclic voltammograms were recorded from -0.8 V to +0.8 V at various scan rates (5, 10, 20, 50, 100 mV s$^{-1}$) and they show the reduction and oxidation broad anodic and cathodic peaks of PEDOT:PSS (Figure 2.3a). The current peaks are similar to the previously reported ones for PEDOT:PSS on top of a platinum electrode.[17] In Figure 2.3b, it can be observed that anodic and cathodic currents are proportional to the square root of the scan rate indicating that the redox process is not controlled by diffusion and providing evidence of the enhanced electroactivity of the crosslinked PEDOT:PSS film. Figure 2.3c shows a schematic representation of the experimental setup of cyclic voltammetry of the free-standing film in 0.1 M NaCl solution.
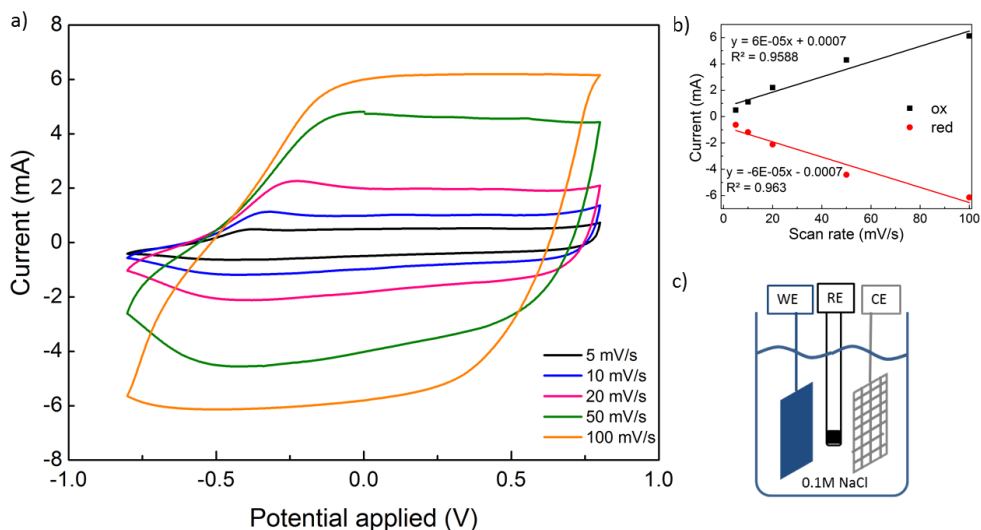
**Figure 2.3.** a) PEDOT:PSS:DVS free-standing film electrochemical characterization by cyclic voltammetry at different scan rates, b) evaluation of the anodic and cathodic peak currents over scan rate and c) schematic illustration of an electrochemical cell setup including PEDOT:PSS:DVS working, Ag/AgCl reference and Pt counter electrodes in 0.1M NaCl electrolyte solution.

## 2.2.2. Fabrication of electronic textiles by coating polyester textiles with PEDOT:PSS:DVS

Although we have demonstrated the wearability of PEDOT free-standing electrodes and their flexibility. It is still possible to augment its flexibility and reduce its fragility by combining this material within a textile support. This will make the electrode wearable for long periods of time, facilitating the connection with an acquisition system. Textile PEDOT electrodes have been fabricated in the past[9,12,18] using stamping or deep coating techniques. In most of the cases, the crosslinkers that promote the adhesion of the PEDOT:PSS are used to achieve stable coatings. However, the conductivity drop and textile stiffening are usually observed when crosslinkers are added to PEDOT:PSS formulation. The

impact of the DVS crosslinker was evaluated on a stretchable substrate where we coated textile fibers using the procedure shown in Figure 1, route b. The process is similar to the previously described free-standing but in this case the conducting polymer remains attached to the polyester fibers. The CV of textile electrodes demonstrate the electroactivity of the PEDOT:PSS:DVS coating with a scan rate dependent capacitive behavior similar to that observed in the free-standing film and is shown in Figure 2.4.
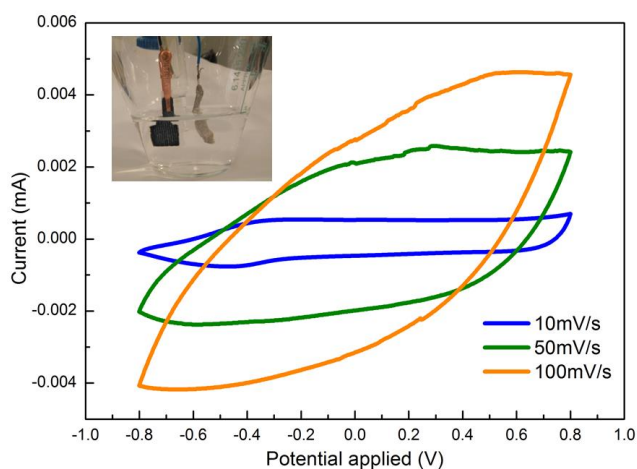


**Figure 2.4.** Cyclic voltammograms of textile coated with PEDOT:PSS:DVS at different scan rates in 0.1 M NaCl solution. In left top corner, the picture of the experimental set up.

In order to evaluate the mechanical robustness of the conducting textiles, we have compared the electrical resistance of coated polyester without crosslinker, using DVS and with the commonly used GOPS crosslinkers. In the first study (Figure 2.6a), the textile was progressively stretched from 0 to 100 % and in the second study (Figure 2.6c) the same stretching was performed at 20 % for 100 times and the resistance was measured every 10 stretches. The same studies

were performed in dry and wet conditions (Figure 2.6b and Figure 2.6d) and considerable difference in resistance was observed. First of all, the initial electrical resistance of the textiles can be seen in Figure 2.6a and the sample with GOPS crosslinker shows a higher value. This is not surprising since it is well known that the addition of GOPS to the PEDOT:PSS dispersion reduces its conductivity.[19] When using DVS as a crosslinker the results are similar with those obtained without crosslinker proving that DVS does not decrease the PEDOT:PSS' electrical properties. We also observe a general increase of resistance with the degree of stretching and with the number of stretches. When in dry conditions, this increase is more pronounced in the case of GOPS than when using DVS. On the other hand, under wet conditions, the resistance of PEDOT:PSS with GOPS and with DVS shows similar behavior at the beginning although in this case as well, the resistance increases with stretching and with the number of stretches of the GOPS samples (Figure 2.6b,d). We found that PEDOT:PSS:GOPS-coated textiles in wet condition is more reliable than dry condition. This is due to the reduced stiffness of the film when swelling thus preserving better the resistance.[19] The largest difference is observed for only PEDOT:PSS-coated textile electrode whose initial resistance is slightly higher since the samples were immersed in MilliQ water overnight before the starting of the experiment. With the increase of stretching and with the number of stretches, PEDOT:PSS samples show a higher increase in resistance (Figure 2.5b) with a rapid progression after 80% stretching. This observation highlights the need for a crosslinker that fixes the polymer chains to the textile avoiding its redispersion when in contact with water. Among crosslinkers, DVS is clearly more suitable than GOPS as it preserves the initial low resistance of the coated textile.
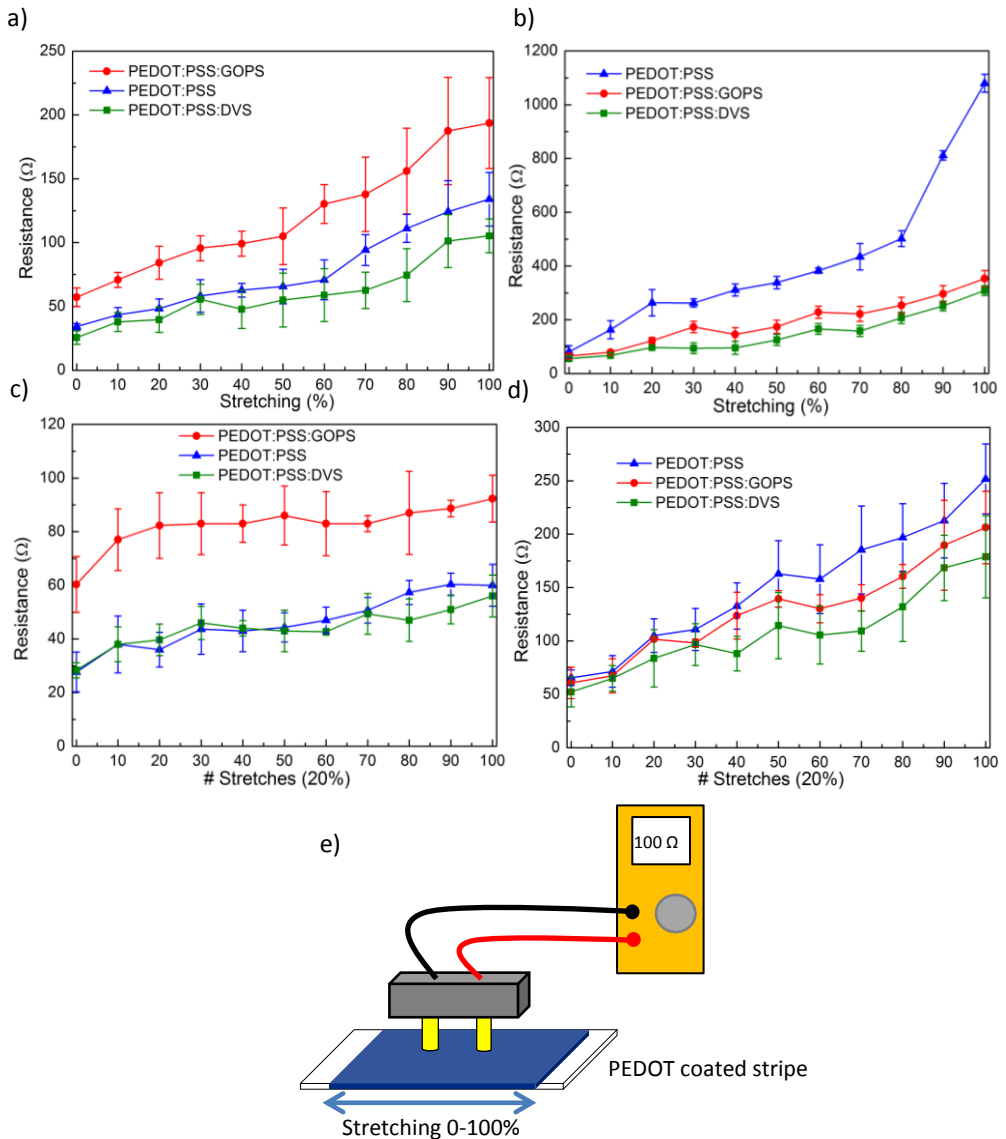
**Figure 2.5.** PEDOT:PSS-coated textile stretching and electrical resistance studies in dry and wet conditions. a) Resistance vs stretching percentage in dry conditions, b) resistance vs stretching percentage in wet conditions, c) resistance vs number of stretches at 20 % stretching in dry conditions, d) resistance vs

number of stretches at 20 % stretching in wet conditions, and e) measurement set-up.

In order to confirm the stability of PEDOT:PSS in water and compare both crosslinkers, we have included an experiment in water (Figure 2.6) where it is demonstrated the lower variation of the resistance in wet conditions when a crosslinker is used during 31 days. Electrode stability in water is important because we are looking for wearable electrodes that are in contact with moisture and sweat of the user. Moreover, we want to be able to wash or clean the electrode with water for hygiene before users use.
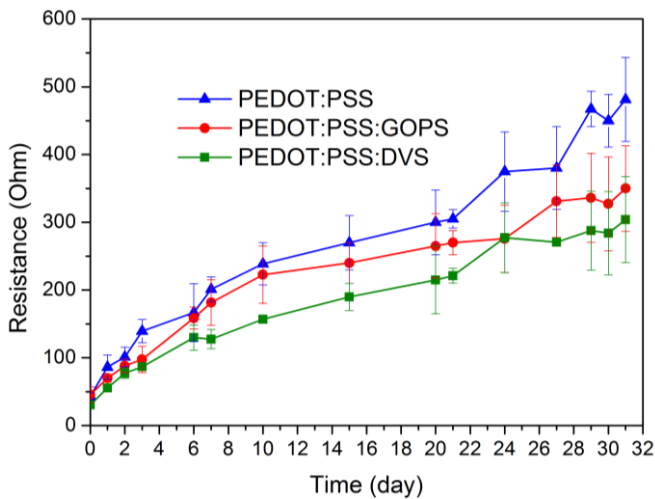


**Figure 2.6**.Textile resistance study in DI water over 31 days for textile coated with PEDOT:PSS, PEDOT:PSS:GOPS, and PEDOT:PSS:DVS (No stretching has been performed). Data at day 0 corresponds with the initial resistance before starting the wet experiment.

The reason for the different increase in electrical resistance during the stretching studies can be correlated to the stiffness of the fibers. This is supported by other

studies that correlate higher electrical conductivity with an improvement in stretchability.[16,20,21] The increase of the stiffness when the textile is coated with and without a PEDOT:PSS crosslinker was via the Young's modulus and shown in Figure 2.7a, b. The smallest value corresponds to the non-coated textile. When the textile is coated with PEDOT:PSS, its Young's modulus increases, and this increase is more noticeable when the PEDOT:PSS is crosslinked. Coating increases the stiffness to the textile because the presence of polymers are restricting the mobility of the fibres. The impact of the crosslinkers results in an increase of the Young's modulus, with the GOPS being higher than the DVS, and the textile becomes stiffer. In Figure 2.7 SEM images of the coated polyester fibers with PEDOT:PSS:GOPS, PEDOT:PSS:DVS, and PEDOT:PSS are also provided. These images illustrate a very homogeneous PEDOT:PSS coating due to the good penetration of PEDOT:PSS inside of the textile. This is observed in the three cases and no differences are identified among crosslinkers. SEM pictures were also taken at the end of the complete stretching study. We observe a delamination of the polymer coating from the fibers that causes the decrease in their conductive performances. Although there are not clear visual polymer delamination differences among the three samples, the conductivity lost is higher in the GOPS crosslinker. Together, these results underline the beneficial effect of using a DVS crosslinker for the development of mechanically stable PEDOT:PSS-based electronic textiles. We could observe that PEDOT:PSS:DVS formulation can be homogeneously deposited on polyesters, showing improved electronic and mechanical properties in dry and wet environments.
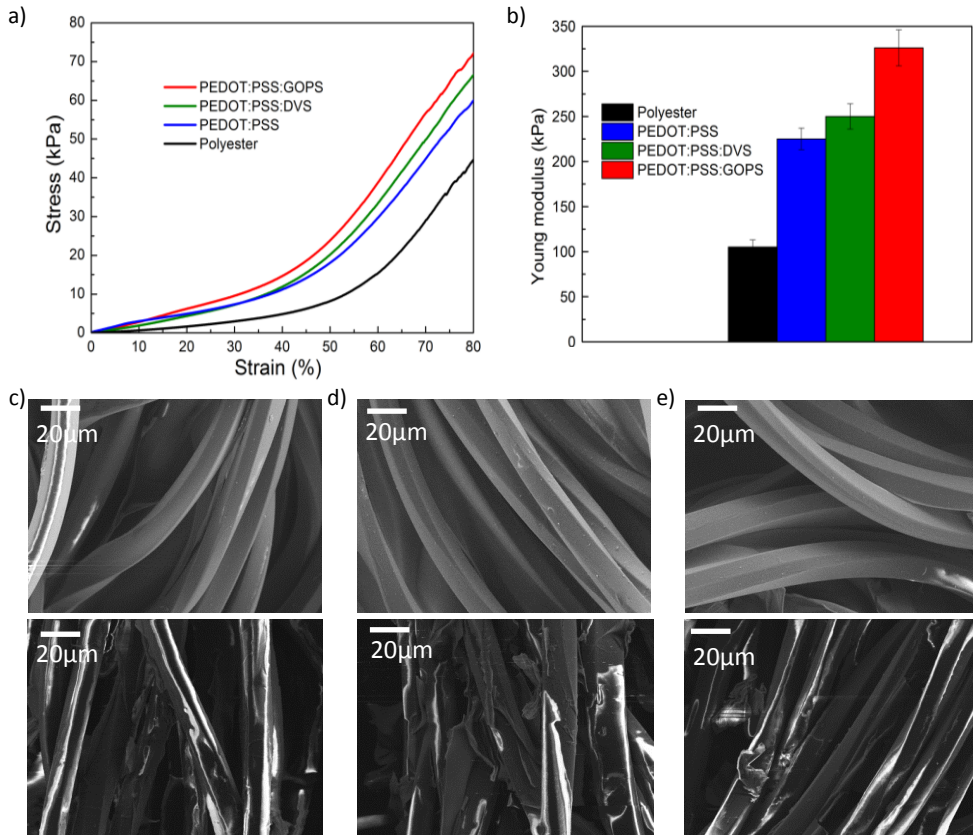
**Figure 2.7.** Textile characterization. a) Stress-strain test on textile coated with PEDOT:PSS:GOPS, PEDOT:PSS:DVS, PEDOT:PSS and not coated textile, b) Young's modulus of textile coated with PEDOT:PSS:GOPS, PEDOT:PSS:DVS, PEDOT:PSS and not coated textile, c) SEM images of textile coated with PEDOT:PSS:DVS before (on top) and after stretching (bottom) d) SEM image of textile covered with PEDOT:PSS:GOPS before (on top) and after stretching (bottom) e) SEM image of PEDOT:PSS-coated textile before (on top) and after 60% stretching (bottom).

### 2.2.3. Electrocardiographic recordings using wearable PEDOT:PSS:DVS textile electrodes

The reported formulation of PEDOT:PSS:DVS finds applications in cutaneous monitoring both as a free-standing film or embedded onto a textile. In our study we have chosen to perform ECG recordings since this is a standard and widespread human health evaluation technique. Wearable ECG systems enable the detection of diseases like arrhythmia and tachycardia. The continuous ECG monitoring can be used in preventive medicine but also to provide general health feedback to healthy patients. In order to test the applicability of these electrodes in health monitoring, we first evaluated the impedance on skin of the textile and free-standing electrodes and we then performed electrocardiographic recordings. Experimental setups are schematically shown in Figure 2.8a, c.

Impedance spectroscopy performed with these electrodes exhibit frequency dependent behavior with a similar shape over a large range of frequencies. When PEDOT:PSS freestanding and textiles electrodes are compared to commercially available Ag/AgCl medical electrodes, we observe a general reduction of the measured impedance at lower frequencies, usually observed in PEDOT-coated electrodes, and an inversed behavior at high frequencies. At lower frequencies a plateau is observed when the maximum impedance is reached. This is in the range of 1 MOhm for the medical electrode, and one order of magnitude lower for the textile electrodes. This reduction is even larger (25 times lower) in the case of the PEDOT:PSS:DVS free-standing film electrode since it better conforms to skin. The frequency at which the plateau behavior is reached differs among electrodes. For PEDOT:PSS-based electrodes this is observed from 0.1 up to 200 Hz, while for the medical electrode, this occurs from 0.1 to 10 Hz. In fact, the shape of the impedance curves is consistent with those measured on skin and reported in the literature. Mainly it is attributed to the low pass filter comportment with Cut-off frequency of 10 Hz for medical electrode, 50Hz for textile electrode and 200 Hz for free-standing film electrode. It should be

43

noted that the observed increase of the impedance in the free-standing and textile electrodes beyond cut-off frequency could be explained by the absence of an ionic gel which is usually employed during such measurements.
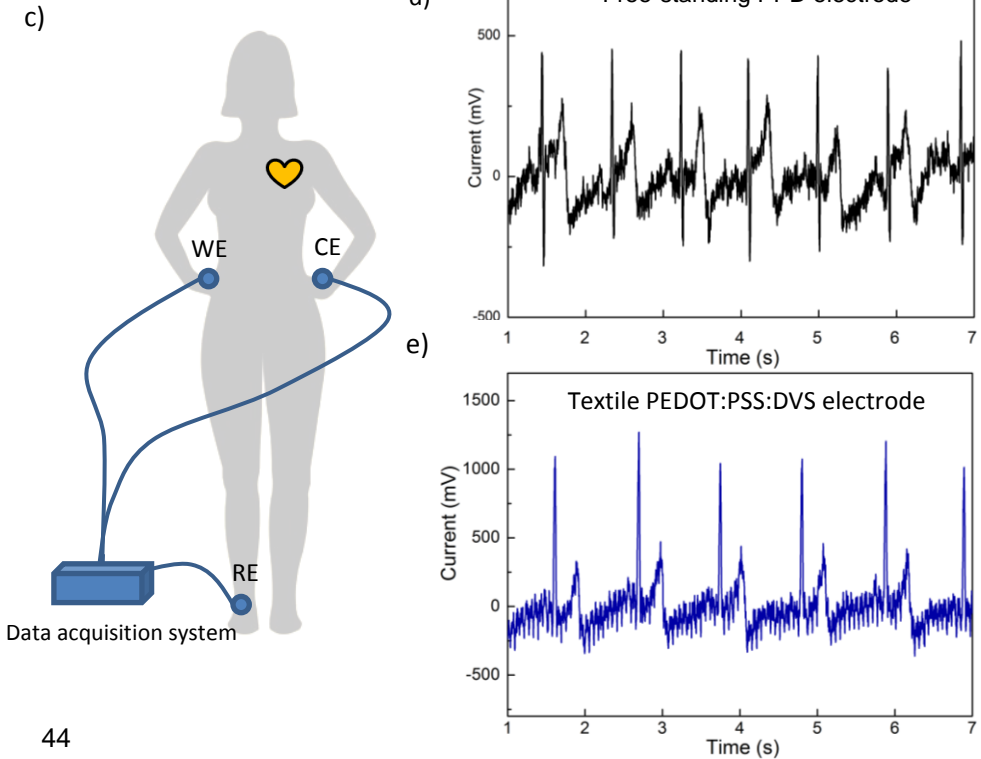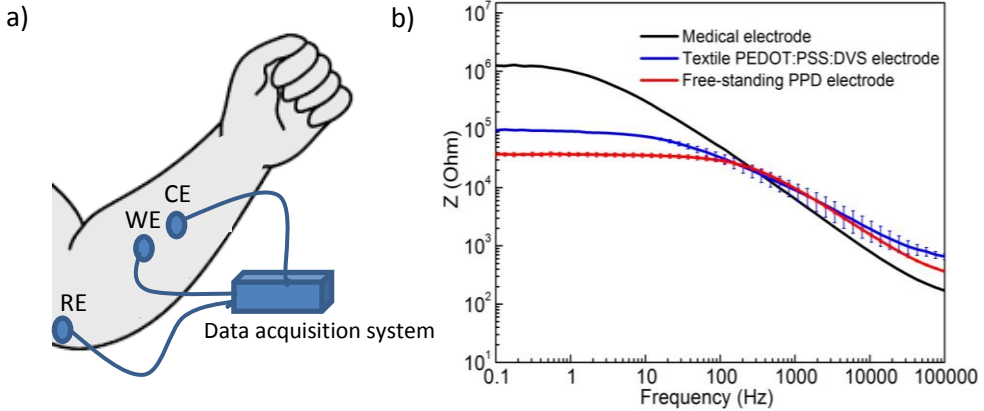
**Figure 2.8.** Measurements of the electrical impedance on skin and ECG recordings. a) Schematic presentation of 3 electrode configuration set-up for impedance measurements, RE on the elbow and WE and CE on the forearm. A drop of DI water (0.05 mL) was added at the interface in between WE and CE electrodes and the skin.  b) Comparison of the impedance on skin for medical, free-standing film and textile PEDOT:PSS:DVS electrodes. c) 3 electrode configuration set-up, RE on the ankle and WE and CE on wrists for ECG recordings. d) ECG recorded with PEDOT:PSS:DVS film electrodes e) ECG recorded with PEDOT:PSS:DVS textile electrodes.

ECG measurements with both types of electrodes, with similar electrode surface areas of 1 $cm^2$, were successfully done on a healthy subject. The electrodes were able to detect distinctly the typical waveform of the heart activity with comparable amplitudes, as shown in Figure 2.8d, e. Previously reported by our group knitted polyester electrodes have demonstrated capability to better tolerate friction or skin movements by reducing motion artefacts. This is also reflected on the ECG data in Figure 2.8e obtained with textile electrodes, which show a remarkably stable signal baseline compare to those obtained with free-standing films (Figure 2.8d). The resolution and signal quality of the raw ECG recorded with textile electrodes are remarkably good without any particular signal filtering or noise canceling treatment. The presence in both cases of the low frequency baseline noise can be reduced by mean of introduction of ionic gels promoting better electrode/skin contact. The ability to record high quality ECG signal with textile electrodes makes them great candidates in wearable electrode fabrication that are also comfortable to wearers for longer periods of time.

## 2.2.4 Electromyography recordings using wearable PEDOT:PSS:DVS free-standing film electrodes

PEDOT:PSS:DVS electrodes find applications in cutaneous health monitoring. In this case, the objective is to achieve electrical activity recordings with the use of free-standing film electrodes. The experimental set-up for recordings is shown in Figure 2.9a. A 3 electrode configuration is used, the RE is an Ag/AgCl electrode on the elbow and CE and WE are our free-standing PEDOT:PSS:DVS film located on top of the muscle which electrical activity is of our interest. In Figure 2.9b we can see an image of a film on top of the skin similar to the ones used as electrodes.
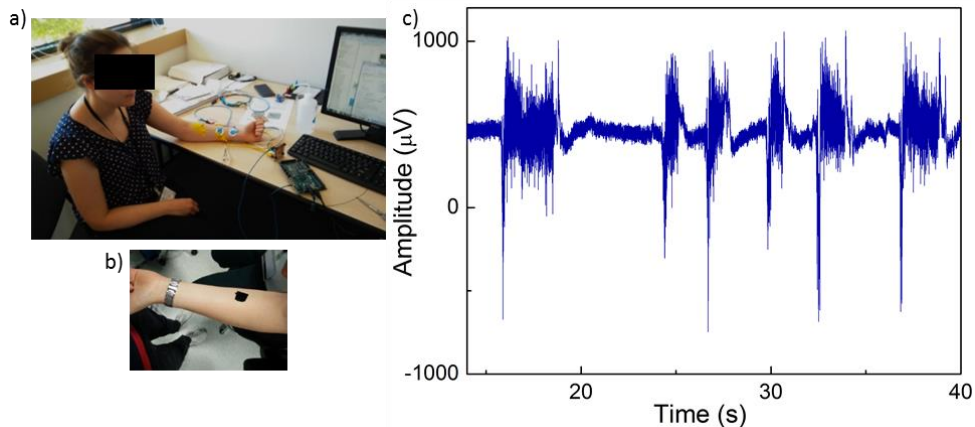


**Figure 2.9.** Electromyography recordings. a) recording set-up on the arm of a volunteer, b) conformable PEDOT:PSS:DVS film on the skin, and c) muscle contraction peaks during 27 seconds recording corresponding to the electrical activity of the Flexor Carpi Radialis muscle of the volunteer.

In Figure 2.9c the graph is showing the muscle contractions. A base line is observed when the muscle is relaxed, and when the volunteer contracts it, activity spikes are observed. We observe first the activity of the muscle corresponding to a long contraction followed by shorter contractions that are

closer in time. Thanks to their conformability to the skin, ECG and EMG recordings are successfully obtained with PEDOT:PSS:DVS electrodes showing their versatility.

## 2.3. Conclusions

In this chapter, we present a new chemical formulation of conducting PEDOT:PSS crosslinked with DVS. The electrodes made using this new material demonstrate a great performance for cutaneous electrophysiology, EMG and ECG. We were able to measure distinguishable ECG with both the free- standing films and electronic textile electrodes. In both cases we observe lower impedance with respect to traditional medical electrodes and a typical capacitive behavior revealed by cyclic voltammetry. Interestingly, PEDOT:PSS:DVS has been shown to form free-standing films in a very straightforward manner without the need of sacrificial layers or difficult synthetic steps. Moreover, the use of DVS increases the stretchability of the material reaching 15% elongation at break. When this dispersion is applied to textile, the textile become conductive and it maintains better its conductivity after stretching stress in dry and wet conditions. These durable and stretchable electronic textiles allow precise electrophysiological recordings in a comfortable way. Together with stretch evaluations, the ECG recordings obtained with PEDOT:PSS:DVS textile electrodes pave the way towards the development of mechanically robust wearable electronic clothing finding an application in health monitoring.

## 2.4. Experimental section

**Free-standing films fabrication:** The films were formed as follow. First, a mixture of 10 mL of PEDOT:PSS (Clevios PH1000) from Heraeous, with 5% v/v ethylene glycol from Sigma, and 1% v/v divinyl sulfone from Sigma was made. This solution was drop-casted on a glass slide and heated up until complete dryness at 60 $^{o}$C. The film formed was peeled-off and used as such. For

47

characterization, the films were tested electrochemically and mechanically. Mechanical tests were performed in an INSTRON 5900 using Blue Hill software, for mechanical testing the films were cut Protolaser S (LPKF) and the dimensions can be found in the Figure 2.2a. Cyclic voltammetry tests were performed in a potentiostat Autolab PGSTAT302N on a 2 cm$^2$ film 0.5 mm thickness where only 1 cm$^2$ was submerged in the electrolyte for testing.

**Textile electrode fabrication:** The deposition of PEDOT:PSS formulation is based on a direct patterning technique published elsewhere.[12] PDMS from Dow corning was deposited on the textile creating a hydrophobic layer when cured. The remaining areas were coated with PEDOT dispersion by drop-casting. The different PEDOT dispersions coated on textile where made according to the following formulation: PEDOT:PSS dispersion was made with Clevios PH1000 containing 5 % v/v EG, and 50 μL of DBSA for each 10 mL of dispersion. PEDOT:PSS:DVS dispersion was made with Clevios PH1000 containing 5 % v/v EG, 1 % v/v DVS, and 50 μL of DBSA for each 10 mL of dispersion. PEDOT:PSS:GOPS dispersion was made with Clevios PH1000 containing 5 % v/v EG, 1 % v/v GOPS, and 50 μL of DBSA each 10 mL of dispersion. 450 μL of these dispersions were coated on textiles of 2x5 cm2 for stretching and electrical measurements. Textile stripes were dried at 60 oC for 2 h and prior to be tested in wet conditions, they were submerged in DI water overnight for conditioning. For the stretching studies, the textile was stretched and the resistance was measured. In wet conditions, the textile was submerged in DI water for 1 h prior stretching. The stretching was performed and then dried for 2-3 h for resistance measurement. SEM images were taken before and after the stretching study with a Zeiss Sigma FESEM equipment.

**PEDOT:PSS:DVS electrodes configuration:** A PEDOT:PSS:DVS film was fabricated in the same way as the film for stretching studies. The film was cut in a

48

rectangular shape 1x2 cm$^2$.1 cm$^2$ of the electrode was used for connection and 1 cm$^2$ was used for contact with skin.

**PEDOT:PSS:DVS textile electrodes fabrication:** 50 μL of the same PEDOT:PSS:DVS dispersion made for stretching studies was added to the surface of the textile electrode of 1.5 cm$^2$. 0.5 cm$^2$ was used for connection and 1cm$^2$ was in the contact with skin.

**Impedance on skin measurements:** A 3 electrode configuration was chosen for measurements. The reference electrode was placed on the elbow (Medical electrodes from Ambu sensor N medical Ag/AgCl), WE and CE were placed on the forearm separated by 2 cm. The RE and CE were Ag/AgCl electrodes and the WE was the studied electrode. Impedance was measured at the range of frequencies from 0.1 to 10$^5$ Hz. A drop of DI water (0.05 mL) was added at the interface in between WE and the skin.

**ECG recordings:** A 3 electrode configuration was used. On the ankle the reference electrode (RE) was placed, the working (WE) and counter electrodes (CE) were on the left and right wrists, respectively. A drop of DI water (0.05 mL) was added at the interface in between WE and the skin and CE electrode and the skin. The reference was an Ag/AgCl electrode. ECG was recorded with an INTAN equipped with a RHD2216 amplifier, a RHD2000 evaluation board, and a RHD2000 electrode adapter board. The RHD2000 interface and Matlab software were used for data processing.

**EMG recordings:** A 3 electrode configuration was used. On the elbow the reference electrode (RE) was placed, the working (WE) and counter electrodes (CE) were located on top of the Flexor Carpi Radialis muscle (inner lower part of the arm). A drop of DI water (0.05 mL) was added at the interface in between WE

and the skin and CE electrode and the skin. The reference was an Ag/AgCl electrode. EMG was recorded with an INTAN equipped with a RHD2216 amplifier, a RHD2000 evaluation board, and a RHD2000 electrode adapter board. The RHD2000 interface and Matlab software were used for data processing.

## 2.5 References

1  S. Majumder, T. Mondal and M. Deen, *Sensors*, 2017, **17**, 130.
2  E. Castagnola, A. Ansaldo, E. Maggiolini, T. Ius, M. Skrap, D. Ricci and L. Fadiga, *Front. Neuroengineering*, , DOI:10.3389/fneng.2014.00008.
3  K. A. Ludwig, N. B. Langhals, M. D. Joseph, S. M. Richardson-Burns, J. L. Hendricks and D. R. Kipke, *J. Neural Eng.*, 2011, **8**, 14001.
4  A. Karimullah, D. R.S. Cumming, M. Riehle and N. Gadegaard, *Sens. Actuators B Chem.*, 2013, **176**, 667–674.
5  X. Cui and D. C. Martin, *Sens. Actuators B Chem.*, 2003, **89**, 92–102.
6  T. Vuorinen, J. Niittynen, T. Kankkunen, T. M. Kraft and M. Mäntysalo, *Sci. Rep.*, , DOI:10.1038/srep35289.
7  A. Zucca, C. Cipriani, Sudha, S. Tarantino, D. Ricci, V. Mattoli and F. Greco, *Adv. Healthc. Mater.*, 2015, **4**, 983–990.
8  M. Getnet Tadesse, C. Loghin, Y. Chen, L. Wang, D. Catalin and V. Nierstrasz, *Smart Mater. Struct.*, 2017, **26**, 65016.
9  D. Pani, A. Dessì, J. F. Saenz-Cogollo, G. Barabino, B. Fraboni and A. Bonfiglio, *IEEE Trans. Biomed. Eng.*, 2016, **63**, 540–549.
10 I. Gualandi, M. Marzocchi, A. Achilli, D. Cavedale, A. Bonfiglio and B. Fraboni, *Sci. Rep.*, , DOI:10.1038/srep33637.
11 S. Takamatsu, T. Lonjaret, E. Ismailova, A. Masuda, T. Itoh and G. G. Malliaras, *Adv. Mater.*, 2016, **28**, 4485–4488.
12 S. Takamatsu, T. Lonjaret, D. Crisp, J.-M. Badier, G. G. Malliaras and E. Ismailova, *Sci. Rep.*, 2015, **5**, 15003.
13 D. Mantione, I. del Agua, W. Schaafsma, M. ElMahmoudy, I. Uguz, A. Sanchez-Sanchez, H. Sardon, B. Castro, G. G. Malliaras and D. Mecerreyes, *ACS Appl. Mater. Interfaces*, 2017, **9**, 18254–18262.
14 C. Wang and C. Qi, *Tetrahedron*, 2013, **69**, 5348–5354.
15 S. Baek, R. A. Green and L. A. Poole-Warren, *J. Biomed. Mater. Res. A*, 2014, **102**, 2743–2754.
16 M. Y. Teo, N. Kim, S. Kee, B. S. Kim, G. Kim, S. Hong, S. Jung and K. Lee, *ACS Appl. Mater. Interfaces*, 2017, **9**, 819–826.

17 P. R. Das, L. Komsiyska, O. Osters and G. Wittstock, *J. Electrochem. Soc.*, 2015, **162**, A674–A678.

18 E. Bihar, T. Roberts, M. Saadaoui, T. Hervé, J. B. De Graaf and G. G. Malliaras, *Adv. Healthc. Mater.*, 2017, **6**, 1601167.

19 M. ElMahmoudy, S. Inal, A. Charrier, I. Uguz, G. G. Malliaras and S. Sanaur, *Macromol. Mater. Eng.*, 2017, **302**, n/a-n/a.

20 D. J. Lipomi, J. A. Lee, M. Vosgueritchian, B. C.-K. Tee, J. A. Bolander and Z. Bao, *Chem. Mater.*, 2012, **24**, 373–382.

21 M. Vosgueritchian, D. J. Lipomi and Z. Bao, *Adv. Funct. Mater.*, 2012, **22**, 421–428.

# Chapter 3.

# Universal hydrogel electrolyte for bioelectronics devices based on PEDOT:PSS
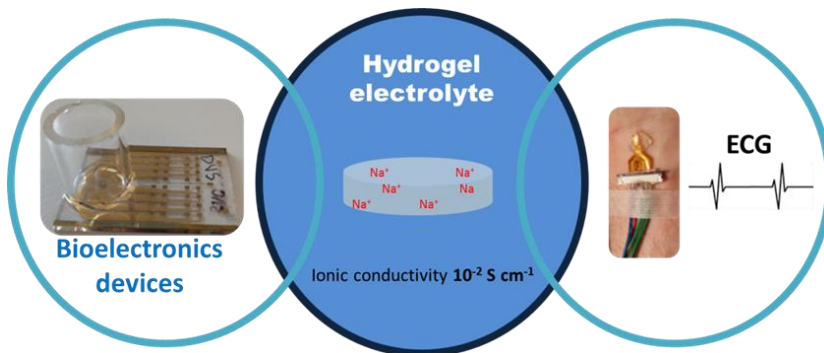
# Chapter 3. Universal hydrogel electrolyte for bioelectronics devices based on PEDOT:PSS

## 3.1. Introduction

The development of novel bioelectronics devices relies on the accessibility of innovative materials for interfacing rigid recording devices with soft biological tissues. These materials should exhibit high ionic/electronic conductivity, tuneable mechanical properties such as strength/softness as well as good adhesion to tissues. Hydrogels are 3D polymer networks with hydrophilic and soft nature that are able to absorb and retain large amounts of water in their structure. Currently, hydrogels have been used for several applications in drug delivery, tissue engineering, electrode functionalisation, biosensors or advanced bioelectronics devices.[1,2] Hydrogels are clinically used to interface medical metallic electrodes with

the patient skin in order to perform electrophysiological studies and measure vital functions, such as Electroencephalography (EEG), Electromyography (EMG).[3] Due to the inherent ionic conductive properties, hydrogels reduce the impedance in between the electrode and the skin[4] and, as a result, the electrical activity of the heart and the brain can be accurately recorded. In addition, hydrogels used in clinical settings should not cause skin irritations and provide good contact and conformability with the body contourns.[5]

Electrically conductive polymers are of great interest in the field of bioelectronics as materials that can improve the interface between electronics and biology due to their soft nature and their mixed conduction. Among many conducting polymers, poly(3,4-ethylenedioxythiophene):poly(styrene sulfonate) (PEDOT:PSS) has been widely used in bioelectronics applications such as electrodes for electrophysiology, biosensors,[6] organic electrochemical transistors (OECTs)[7] and bioelectrode coatings.[8] Organic Electrochemical Transistors (OECTs) are a novel class of devices that have been used as transducers of biological signals, both in vitro,[9–12] and in vivo.[13]

OECTs are transistors operating at low voltage (typically <1 V) that are able to transduce biological ionic signals to an output current with an excellent amplification capacity.[15,16] PEDOT:PSS is commonly used as the active material for OECTs operating in depletion mode. When a positive bias is applied to the gate, cations from the electrolyte enter in the PEDOT:PSS film. A decrease in the hole density of the PEDOT chains results to a reduced number of carriers, thus decreasing the drain current.[10] Commonly, aqueous electrolytes are used to operate OECTs, for example NaCl solutions,[13,17] phosphate-buffered saline solution,[6,18] or cell media.[19–21] Proper operation of OECT is achieved when the ions of the electrolyte have high ionic mobility to allow for fast de-doping/doping of the

OECT channel. On the other hand, the use of a liquid electrolyte with OECTs can limit its application for the development of novel sensing architectures such as wearable bioelectronics devices. The use of solid state electrolytes to operate OECTs has been shown to be a valid alternative to aqueous electrolyte.[22,23] However, these devices showed slow performance.[24]

In this work, a universal hydrogel is presented which shows a high ionic mobility and interaction with PEDOT:PSS. This hydrogel was synthesized by cost-effective in-situ (photo)polymerization of acrylate-PEG monomers in a clean and fast way with high degree of control over the final hydrogel structure and shape. PEG based hydrogels are known to present high water content retention[25] and biocompatible[26] nature. In this study we report the synthesis and characterization of a new sodium conducting hydrogel formed by copolymerization of sodium acrylate ionic monomer with neutral ones containing PEG. This hydrogel is stable, ionic conductive and adhesive to substrates including skin. These characteristics altogether make it a successful interface material for cutaneous electrodes and a gel electrolyte with high ionic mobility to provide fast ON and OFF switching in OECTs.

## 3.2. Results and discussion

### 3.2.1. Na$^+$ PEG Hydrogel synthesis and characterization

The acrylic poly(ethylene glycol) or poly(ethylene oxide) Na$^+$ PEG based hydrogel containing sodium mobile ions was synthesized by photo-polymerization according to the reaction shown in Scheme 3.1. In a typical reaction a poly(ethylene glycol) acrylate (PEGA) monomer was copolymerized with sodium acrylate (NaA) and crosslinked with an small amount of poly(ethylene glycol) diacrylate (PEGDA) by UV (254 nm)

curing during 20 minutes in the presence of a given amount of water and a photoinitiator. PEG acrylate macromonomer (11 % w/w) was used to enhance water retention of the hydrogel, while PEGDA was chosen to obtain a water insoluble network, as it contains two reactive groups capable of cross-linking the hydrogel acrylate backbone. PEGDA is present in 2 % w/w to ensure stability without stiffen the material. As sodium acrylate was added in the monomer mixture, the resulting hydrogel presents a negative charge on the polymeric backbone (anionic polyelectrolyte network) and sodium cations are free to move within the hydrogel network. Sodium acrylate is present in 4 % w/w, providing sodium mobile cations and obtaining ionic conductivities of $10^{-2}$ S cm$^{-1}$ at RT.
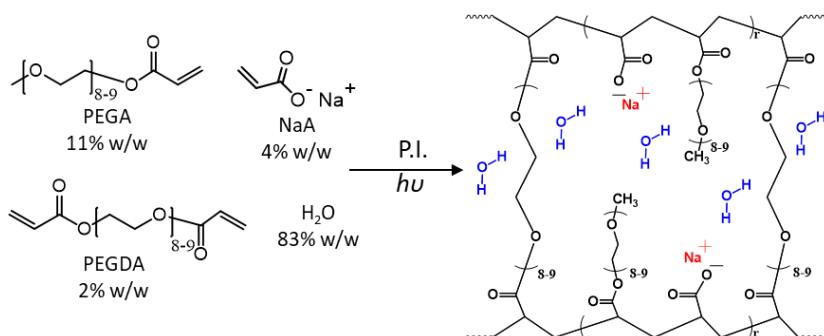


**Scheme 3.1.** Na$^{+}$ PEG-hydrogel synthesis. Photopolymerization reaction of PEGA, PEGDA, and NaA in the presence of water.

The ionic conductivity of the hydrogel can be varied accordingly to the composition of the hydrogel, as shown in Figure 3.1a As expected, the maximum conductivity is achieved when the water content is the highest and it decreases when the water content is lower as the presence of a higher amount of water favors the mobility of ions. In Figure 3.1a, the conductivities of the hydrogels synthetized with different water contents were plotted. The highest ionic conductivity value was observed for the

hydrogel containing 83% w/w of water which showed a value of $3.6 \cdot 10^{-2}$ S cm$^{-1}$ at RT. When the water content of the hydrogel was 63 % w/w the conductivity was $1.1 \cdot 10^{-2}$ S cm$^{-1}$ and when the water content was 43 % w/w the conductivity decreased to $1.6 \cdot 10^{-3}$ S cm$^{-1}$. The lowest conductivity measured was $6.9 \cdot 10^{-5}$ S cm$^{-1}$ when the hydrogel water content was 3 % w/w. Due to the obtained results, we selected the 83% w/w hydrogel to continue with the studies with the highest ionic conductivity possible.
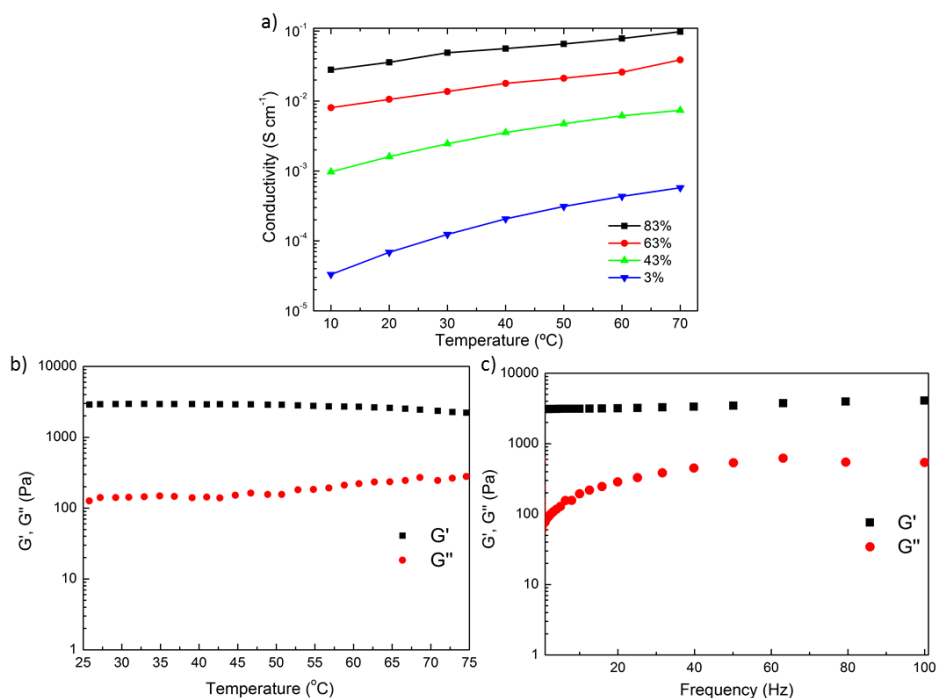


**Figure 3.1.** Na$^+$ PEG-hydrogel characterization. a) Ionic conductivity of hydrogels at different water contents at 83, 63, 43, and 3% w/w, b) and c) rheological behavior, G' and G" evolution with temperature and frequency for hydrogel 83% w/w.

Rheological properties of the 83% w/w hydrogel were analysed by frequency sweep measurements. The evolution of elastic (G') and viscous (G'') moduli of the hydrogel as a function of the frequency and temperature (Figure 3.1b and 3.1c) was studied. G' modulus is higher than G'' on the whole frequency range and independent of frequency, which is typical of a solid-like behaviour. Interestingly, the hydrogel shows high temperature stability in the temperature range from 25 to 75 $^{\circ}$C.
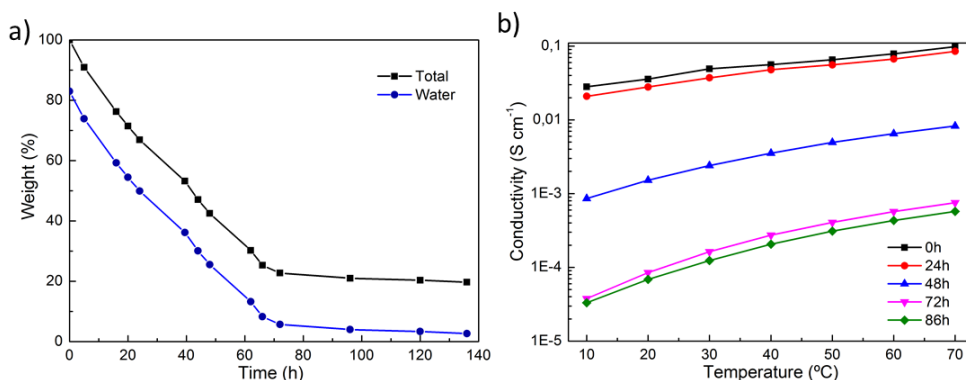


**Figure 3.2.** Hydrogel drying process, total weight and water loss over time at controlled conditions, 55 % humidity and 22 $^{\circ}$C (a), and evolution of the ionic conductivity during the drying process, at 0, 24, 48, 72, and 86 h (b).

One of the main limitations of clinically used hydrogels is the continuous loss of water overtime while operating. This can result on a completely dry hydrogel and failure of the sensors. The water loss of the hydrogel (83% w/w) by evaporation was quantified gravimetrically over a period of 140 h (Figure 3.2a). As expected, the drying process of the hydrogel resulted in the loss of ionic conductivity which was studied as well. For this experiment, the hydrogel was weighted continuously every couple of hours until a stable weight was reached, followed by conductivity measurements

of the hydrogel. Figure 3.2b. shows the plot of conductivity as a function of the temperature in the range between 10 and 70 °C. The loss of water comes together with a reduction in ionic conductivity. As expected the conductivity of the hydrogel is very high when synthetized due to the presence of $Na^+$ ions together with the high content of water in the system ($10^{-2}$-$10^{-1}$ S cm$^{-1}$). After 24 h, 33 % of water was lost through water evaporation but the conductivity did not change substantially (2.7 $10^{-2}$ S cm$^{-1}$). After 48 h, 69 % of the water content was lost and the conductivity started decreasing to reach 1.5 $10^{-3}$ S cm$^{-1}$. At 72 h, the complete hydrogel dryness was nearly reached; only 7 % of the initial water weight remained in the hydrogel structure and the conductivity dropped further to 8.5 $10^{-5}$ S cm$^{-1}$. It is important to notice that the loss of water does not reduce substantially the ionic mobility until 72 h, which gives a timeframe of several days to employ this hydrogel when high ionic mobilities are required.

To study if there is unpolymerized monomer in the crosslinked gel, the gel was immersed for 24h in deuterated water. The soluble fraction was measured by ^{1}H-NMR spectroscopy. If there is unreacted monomer, it will be dissolved in the aqueous face and the signals associated with the monomers will be present on the spectra. As it can be seen in the hydrogel spectra (Figure 3.3) the signal from the acrylate groups has disappeared confirming complete hydrogel polymerization.
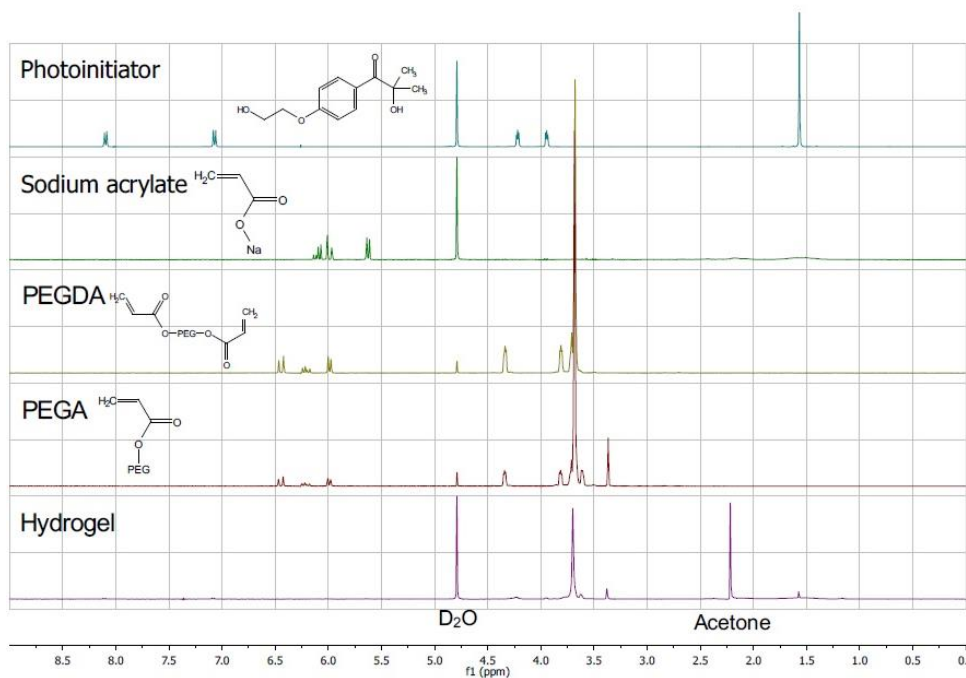
**Figure 3.3.** $^1$H-NMR spectra in D$_2$O of 2-hydroxy-4'-(2-hydroxyethoxy)-2-methylpropiophenone (photoiniciator), sodium acrylate, poly(ethylene glycol) diacrylate, poly(ethylene glycol) acrylate, and the NMR of the remaining solvent after submersion of the hydrogel during 24 h in D$_2$0.

In this work we were looking for a hydrogel able to interact with PEDOT:PSS and to facilitate its electrochemical response. For this reason, the hydrogel was employed in a simple test as a solid electrolyte onto PEDOT:PSS to investigate if it is able to dope and de-dope PEDOT:PSS films (Figure 3.4), as this phenomenon is caused by ions moving in and out of the conducting polymer film. Na$^+$ ions should move throughout the hydrogel and penetrate/leave the film ideally at fast velocity in a reversible way. The speed of the process depends on the hydrated radius of the ions (the smaller the faster)[16] in the electrolyte media, and the swelling of the

PEDOT:PSS film when in contact with the electrolyte. In this context, a hydrogel with high water content (with low viscosity) and the presence of mobile and small Na$^+$ as single ion conductor should be an appropriate gel electrolyte for PEDOT:PSS hole density manipulation.
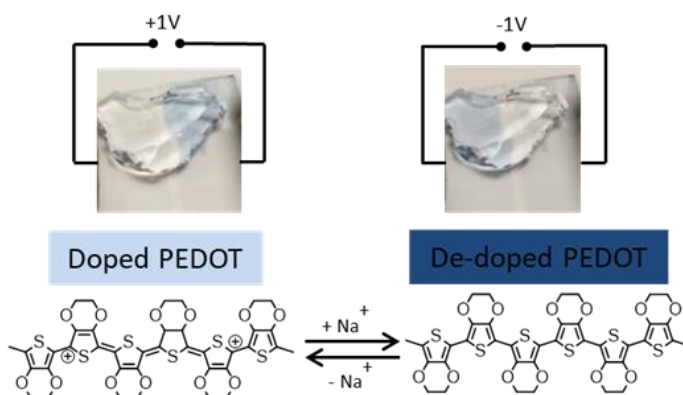


**Figure 3.4.** PEDOT switching test. Two spin-coated PEDOT:PSS electrodes on a glass slide connected by a solid electrolyte.

Thus, by applying a potential in between the two contacts (+1V, -1V), Na$^+$ ions should penetrate/exit the PEDOT:PSS film. The results are visible as PEDOT is an electrochromic polymer and it changes its colour depending on its oxidation state. When a potential difference was applied in between the two electrodes (Figure 3.4), Na$^+$ ions penetrate the negative biased PEDOT:PSS electrode inducing PEDOT de-doping turning dark blue. When Na$^+$ ions exit the film at the reversed potential, the PEDOT chains get doped turning light blue. This simple test was fully reversible; it could turn for the 100 cycles that the experiment lasted indicating that the Na$^+$ PEG-hydrogel provides enough cations to the doping process without degradation of the film. It is worth to note that the fully swollen hydrogel and the content of Na$^+$ included in the polyelectrolyte network are key factors in this experiment as these two together contribute to the reversible

doping/de-doping process.[17,27] This initial characterization study showed good interaction between PEDOT:PSS and the polyelectrolyte hydrogel in the same way as when liquid electrolyte are used. These satisfactory results enable us to test the performance of this hydrogel for cutaneous electrophysiology and for an OECT operation.

### 3.2.2. Na$^+$ PEG-Hydrogel for cutaneous electrophysiology

PEDOT:PSS has recently been used for the fabrication of cutaneous electrodes to measure electrophysiological body signals, using inkjet printed PEDOT:PSS electrodes on paper,[7] PEDOT:PSS electrodes on textile,[28] or PEDOT:PSS on gold electrodes.[29] PEDOT:PSS electrodes can directly be in contact with the skin or to have an ion conducting gel on top of it to decrease the impedance with the skin and improve the adhesion. So far, iongels were developed for this purpose due to the stability of its ionic conductivity over time. However, a hydrogel will offer some advantages like higher ionic conductivity and lower toxicity than the iongels. Thanks to PEG biologically inert nature and good adhesion to the skin, the Na$^+$ PEG-hydrogel is a good candidate for improving the performance of PEDOT in cutaneous electrodes. In general, hydrogels for electrophysiological recordings must withstand friction with the skin of the patient and with the recording electrodes. Our hydrogel showed good adhesion to the skin (Figure 3.5) and it was also able to stand mechanical constraints caused by the movements of the patient when the electrode was left on the patient skin for several hours.
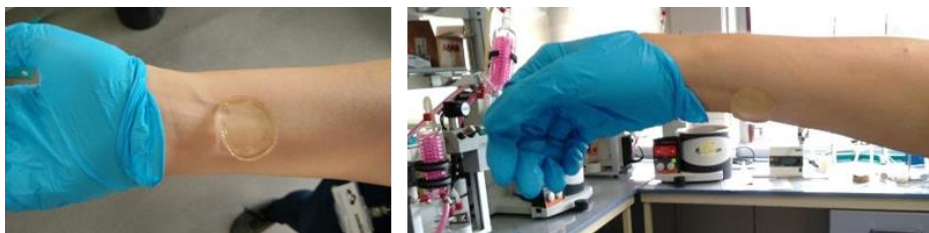
**Figure 3.5.** Hydrogel adhesion to the skin of a volunteer. The hydrogel has adhesive and conformable properties.

To test this hydrogel in cutaneous electrophysiology, ECG signals were recorded on a healthy patient (Figure 3.6).
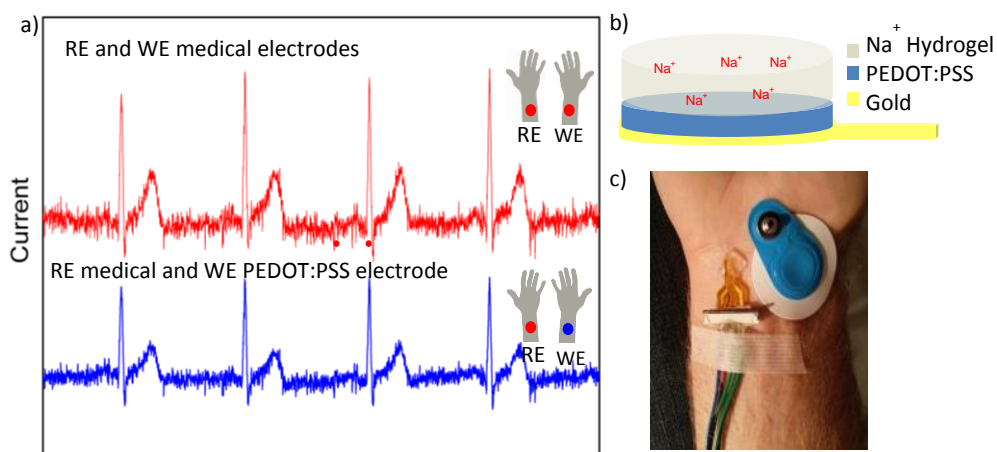


**Figure 3.6.** Electrophysiological recordings. a) ECG recordings with two medical electrodes (in red) and one medical electrode as a reference and PEDOT electrode with hydrogel as a working electrode (in blue). On the right, both electrode set-ups representation on grey wrists, b) electrode and hydrogel schema, and c) PEDOT:PSS-hydrogel electrode and medical electrode on the wrist of the patient.

The ECG signal recorded with electrodes containing the Na$^+$ PEG-hydrogel showed similar quality as the one recorded with medical electrodes. This result confirmed that our hydrogel is a good interface between the electrodes and the skin providing successful transcutaneous signal transduction. The flexibility, adhesion and conformability characteristics of the hydrogel also ensure good wearability of the electrode and minimum discomfort for the person. The electrode together with the hydrogel allow recording during motion and in the long-term. Moreover, the integrity of the hydrogel is not at risk when affected by sweeting or water splashes as the crosslinked structure does not dissolve in water and it has sufficient mechanical stability. In Figure 3.6b there is a schema of the electrode used. The first gold layer provides electronic conductivity and the PEDOT:PSS layer on top reduces the skin-electrode impedance.[30,31] The soft and polymeric nature of both the PEDOT:PSS film and the hydrogel, ensures quality signal transduction. As can be seen in Figure 3.6a, we recorded a distinguishable ECG. These ECG signals are analysed by cardiologists to diagnose cardiac affections and are useful for preventive medicine.

This hydrogel provides good quality signal recording without the problems encountered when medical Ag/AgCl electrodes are employed. Electrode delamination problems are avoided without the need of extra glue that medical electrodes require and on top of it, this hydrogel did not cause skin irritation or pain when the electrode together with the gel is removed.

### 3.2.3. Na$^+$ PEG-Hydrogel as solid electrolyte for OECTs

The benefits of solid electrolytes over liquid ones are their chemical structure, mechanical stability and slower drying process maintaining the high ionic mobility during longer periods of time. So the use of the Na$^+$ PEG-hydrogel in OECTs with PEDOT:PSS channels will lead to a fully

solid device which will lead to a time-stable OECT device. In order to characterize the performance of this hydrogel as solid electrolyte on an OECT, several studies were carried out. Thus, IV curves, bandwidth measurements (transconductance vs frequency), and lastly a cycle test showed the performance of an OECT in the long term under stressful conditions (Figure 3.7). For comparison, the same tests were carried out on an OECT with equal characteristics but using a liquid electrolyte, based on the standard 0.1M NaCl aqueous solution (Figure 3.8). The OECT schematic drawing in Figure 3.7a shows the cross-section of the device architecture and the electrical system for device operation. In this planar configuration, a planar PEDOT:PSS gate, source and drain are covered by the hydrogel as solid electrolyte on top. The IV curves in Figure 3.7b show the performance of the device with channel dimensions of 100*100 $\mu m^2$. It has a maximum current of -2.3 mA (at $V_G$=−0.2 V) and a maximum transconductance of 4.5 mS (at $V_G$=0 V).

The bandwidth measurement in Figure 3.7d shows the dependency of the transconductance with frequency. The device was biased with $V_D$=−0.5 V and, at the gate, a sinusoidal bias was applied (ΔVgs = 25 mV). It is observable that transconductance values of 3.3-3.2 mS are maintained until slightly above 100 Hz, having a cut-off frequency of 525 Hz. These results are very similar to the ones obtained with NaCl 0.1M in Figure 3.7b. In the case of the NaCl solution, transconductance values of 3.6-3.5 mS are maintained until slightly above 100 Hz, having a cut-off frequency of 429 Hz.
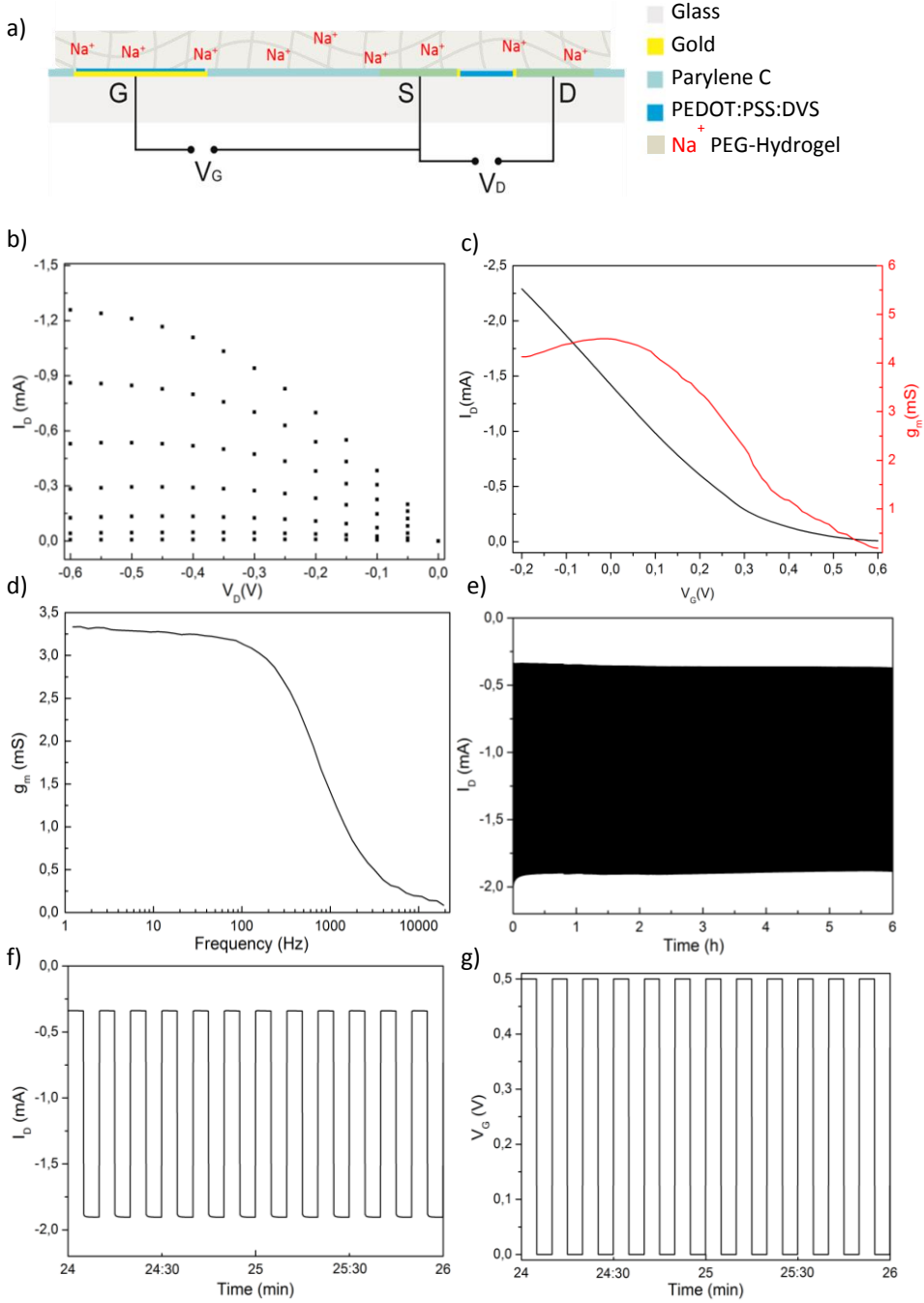
**Figure 3.7.** OECT performance and long-term measurements with the hydrogel as solid electrolyte. (a) Planar OECT schema and solid electrolyte on top, (b) IV output characteristics over the range of $V_G$=0 V to 0.6 V, with a $V_G$ step size of 0.05 V, (c) IV transfer curve (black) and transconductance (red) in the range of $V_G$= −0.2V to 0.6 V, (d) bandwidth measurements (transconductance vs frequency), (e) cycle test 6 h operation, and (f,g) drain current and applied gate voltage pulses during 2 min of a 6 h operation.

For OECT recordings of biological processes, stable operation without PEDOT:PSS:DVS degradation is crucial. In order to check the long-term performance of the device, a stress-study of the OECT under high duty conditions was carried out for 6 h. The results are very satisfactory as the OECT transistor channel is extremely stable and comparable with the results obtained using 0.1M NaCl solution (Figure 3.8c). The maximum and minimum current are −1.91 and −0.34 mA respectively at the start of the test and −1.85 and −0.2 mA at the end. There is only a small variation in the maximum current of 3.14 % during the 6 h of operation. In Figure 3.7f we observe 2 random min of the cycle test where we observe how fast the device is able to switch from the dope to the de-doped state of the OECT channel and the reverse. The voltage at the gate is varied from 0.5 V to 0 V every 5 seconds (Figure 3.7g) having response times of <100 ms. Comparing these results with the ones obtained with 0.1M NaCl solution. In Figure 3.8b we observe the bandwidth measurements where there is a maximum transconductance of 3.6 mS with a cut-off frequency of 429 Hz. The 6 h cycling test shows the stability of the device in Figure 3.8c.

All in all, it can be concluded from the OECT measurements that the hydrogel is an appropriate electrolyte for high device performance. It shows high stability and high transconductance values. The success of the

69

studied solid electrolyte can be explained by its high ionic conductivity in the same order of magnitude as NaCl 0.1M solution which has a conductivity of $10^{-2}$ S cm$^{-1}$.[32] Furthermore, the high content of water within the structure of the hydrogel (83% w/w) is up taken by the PEDOT:PSS:DVS film, swelling and improving the ionic mobility within the PEDOT channel.[33,34] This is the reason why, on the whole, it is a fast device able to switch on and off in <100 ms, similar rates as obtained when liquid aqueous electrolytes are used.[35]
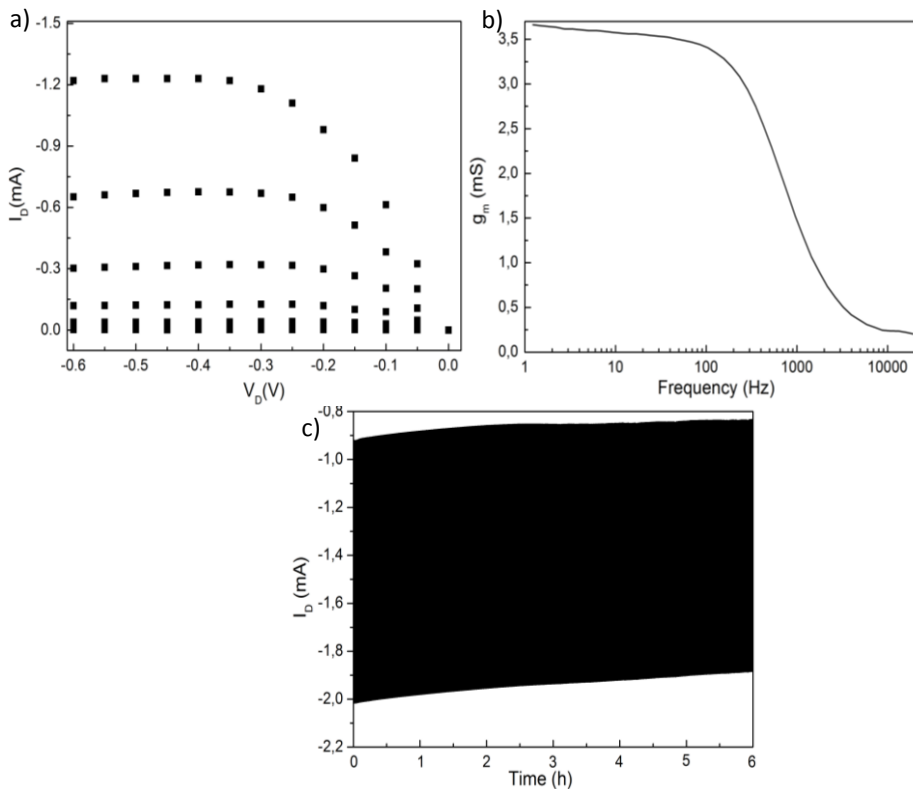


**Figure 3.8.** OECT performance and long-term measurements with aqueous NaCl 0.1M as electrolyte. (a) IV output characteristics over the range of $V_G$=0 V to 0.6 V, with a $V_G$ step size of 0.05 V, (b) bandwidth measurements (transconductance vs frequency), (c) cycle test 6 h operation.

### 3.3. Conclusions

In this chapter, we presented PEG-based Na$^+$ conducting hydrogels with universal applications to different devices in the field of bioelectronics. Hydrogels were synthesized using fast photopolymerization of commercially available monomers such as poly(ethylene glycol)-dimethacrylate and sodium acrylate. The hydrogel showed high ionic conductivity values at room temperature ($10^{-2}$ S cm$^{-1}$) as characterized by electrochemical impedance spectroscopy. Due to their high ionic mobilities and durability, hydrogels were successfully employed as a self-standing electrolyte to provide contact in between skin and PEDOT electrodes for ECG recordings. The recorded ECG signals had the characteristic PQRST peaks analysed by doctors, proving the capacity of the hydrogel to provide good transcutaneous signal transduction. In addition, hydrogels were used to operate OECTs. The OECT showed a very stable operation during 6 h high duty cycle test and fast switching performance similar to the performance when liquid electrolytes are employed. As an added advantage, the synthesis of the hydrogel can be included during the photolithography device fabrication. Overall, this study shows that Na$^+$ PEG-hydrogels are effective for bioelectronics devices based on PEDOT:PSS. Whereas previous studies show that OECTs with liquid electrolytes exhibit faster switching response than OECTs with solid electrolytes,[24] this is not the case in the study we present. Interestingly, using this hydrogel as electrolyte, the switching response is similar than when aqueous NaCl 0.1M solution is used.

## 3.4. Experimental part

### Na$^+$ PEG-Hydrogel synthesis and characterization

A chemically cross-linked Na$^+$ PEG-hydrogel was synthetized by UV-polymerization. For 1 g of hydrogel solution, 0.11 g of poly(ethylene glycol) acrylate (Mw = 375 g mol$^{-1}$), 0.02 g of poly(ethylene glycol) diacrylate (Mw = 575 g mol$^{-1}$), 0.04g of sodium acrylate, and 0.0051 g of the photoiniciator 2-hydroxy-4′-(2-hydroxyethoxy)-2-methylpropiophenone were dissolved in in 0.83 g of DI water (Milli Q). Solution was purged with N$_2$ and irradiated with UV light during 20 min for polymerization. A UV chamber from Boekel scientific was used for hydrogel crosslinking, model 234100. All reagents come from Sigma-Aldrich. Hydrogels with other water contents (63, 43, and 3 %w/w) were synthetized using the same procedure and maintaining the same monomer ratios.

Hydrogels were characterized rheologically, by impedance spectroscopy, and by NMR. For Rheological measurements an AR-1500EX instrument was employed for experiments from TA instruments equipped with a Peltier system for temperature control. Two types of measurements with a 40mm steel plate were performed. A frequency sweep step experiment (frequency 100-0.1Hz, strain 0.4%, at 25 $^o$C), and a temperature ramp step experiment (temperature 25-75 $^o$C, ramp 3 $^o$C min$^{-1}$, frequency 1Hz, strain 0.4%). For Impedance measurements an Autolab PGSTAT302N equipment with a Microcell HC from Metrohm was used. Hydrogel discs with a diameter of 12 mm and thickness of 1.5 mm were placed in between two blocking electrodes. Impedance was measured at range of temperatures from 10 to 70 $^o$C. The ionic conductivity of each sample was calculated from to the real part of the impedance (Z'). Finally, $^1$H-NMR has been performed on a Bruker Advance 400 MHz, using D$_2$O from Deutero GmbH.

**Electrode fabrication and operation**

A flexible electrode was fabricated by covering a kapton foil (25µm thickness) with a Cr layer (10 nm thick) and a layer gold (80 nm thick), both by thermal evaporation and, on top, a thin film (~150 nm) of PEDOT:PSS (Clevios PH 1000 from Heraeous) was spin-coated.

ECG measurements were recorded in a low noise room shielded from external magnetic signals. Ambu sensor N medical Ag/AgCl electrodes were used as standard ECG electrodes. A battery was used for the supply voltage to avoid the noise coming from the ground. A Braintronics voltage recording system was used to measure the output voltage and recorded using a Brainbox EEG-1166. 2 ECG signals were recorded on the same healthy patient using a two electrode configuration. First signal was measured with two medical electrodes placed on both wrists of the patient as reference and working electrodes. A second ECG signal was measured using a medical electrode on one wrist as reference electrode and a PEDOT:PSS electrode as working electrode on the other wrist including the hydrogel as interphase between patient's skin and the electrode.

**OECT fabrication and operation**

Microscope glass slides were cleaned in an ultrasonic bath for 15 min in a 2 %v/v soap (micro-90) aqueous solution, rinsed in DI water and followed by sonication for another 15 min in isopropanol:acetone 1:1 v/v. After rinsing the glass substrates with DI water and activate them with $O_2$ plasma, gold interconnects were patterned via a lift-off process by spin-coating S1813 photoresist (Shipley) and exposing it with UV light using a SUSS MJB4 contact aligner and developing it in MF-26 developer. First, an adhesion enhancer layer of chrome (10 nm thick) followed by a second layer of gold (100 nm thick) were thermally evaporated onto the glass

substrate followed by lift-off process in acetone. Second, an insulation layer of parylene-C (1.7 µm thick) was deposited using A-174 silane as an adhesion promoter. This was followed by spin coating of a layer of soap (2% v/v soap (micro-90)) to avoid the adhesion of a second sacrificial layer of parylene-C (2 µm) which was deposited on top. Reactive ion etching (RIE) was used to define the OECT channel geometry (100x100 µm²), gate electrode (5x5 mm²) and contact pads of the device. A PEDOT:PSS dispersion containing 1% v/v of the crosslinker divinyl sulfone,[35] 5%  v/v of the solvent ethylene glycol and 0.05 % v/v of the surfactant dodecylbenzenesulphonic acid (all from Sigma-Aldrich) was spin-coated at 1500 rpm to obtain a thickness of ~100 nm. OECT channels and gate geometries were obtained by peeling-off the last layer of parylene-C.

The OCET was operated according to the following. Cycle test were executed with a Keithley instrument 2602A. Data were collected by pulsing the gate bias from 0 to 0.5 V (t pulse 5 s, high duty cycle) whilst applying a drain bias of -0.5 V.  For frequency dependent an IV measurements, a National Instruments PXIe-1062Q was employed. A source-measurement device NI PXIe-4145 was employed to put the transistor channel bias and gate potential was applied with a NI PXI-6289 device. To execute frequency-dependent measurements, gate and output drain currents were registered using two NI-PXI-4071 digital multimeters (DMM). Bandwidth measurements were conducted by applying a sinusoidal bias at the gate ($\Delta V_{gs}$ = 25 mV and 1 Hz < f <20 kHz) whilst maintaining a constant bias at the drain ($V_{Ds}$ = −0.5 V). A customized LabVIEW program was employed to control measurement parameters.

## 3.5 References

1   E. M. Ahmed, *J. Adv. Res.*, 2015, **6**, 105–121.
2   E. Caló and V. V. Khutoryanskiy, *Eur. Polym. J.*, 2015, **65**, 252–267.
3   K. Nagamine, S. Chihara, H. Kai, H. Kaji and M. Nishizawa, *Sens. Actuators B Chem.*, 2016, **237**, 49–53.
4   A. Searle and L. Kirkup, *Physiol. Meas.*, 2000, **21**, 271–283.
5   P. Leleux, C. Johnson, X. Strakosas, J. Rivnay, T. Hervé, R. M. Owens and G. G. Malliaras, *Adv. Healthc. Mater.*, 2014, **3**, 1377–1380.
6   I. Gualandi, D. Tonelli, F. Mariani, E. Scavetta, M. Marzocchi and B. Fraboni, *Sci. Rep.*, , DOI:10.1038/srep35419.
7   E. Bihar, T. Roberts, M. Saadaoui, T. Hervé, J. B. De Graaf and G. G. Malliaras, *Adv. Healthc. Mater.*, 2017, **6**, 1601167.
8   U. A. Aregueta-Robles, A. J. Woolley, L. A. Poole-Warren, N. H. Lovell and R. A. Green, *Front. Neuroengineering*, , DOI:10.3389/fneng.2014.00015.
9   X. Strakosas, M. Bongo and R. M. Owens, *J. Appl. Polym. Sci.*, 2015, **132**, n/a-n/a.
10  X. Gu, C. Yao, Y. Liu and I.-M. Hsing, *Adv. Healthc. Mater.*, 2016, **5**, 2345–2351.
11  A. Spanu, *Organic Transistor Devices for In Vitro Electrophysiological Applications*, Springer, 2016.
12  V. F. Curto, B. Marchiori, A. Hama, A.-M. Pappa, M. P. Ferro, M. Braendlein, J. Rivnay, M. Fiocchi, G. G. Malliaras, M. Ramuz and R. M. Owens, *Microsyst. Nanoeng.*, 2017, **3**, 17028.
13  A. Giovannitti, D.-T. Sbircea, S. Inal, C. B. Nielsen, E. Bandiello, D. A. Hanifi, M. Sessolo, G. G. Malliaras, I. McCulloch and J. Rivnay, *Proc. Natl. Acad. Sci.*, 2016, **113**, 12017–12022.
14  D. Khodagholy, T. Doublet, P. Quilichini, M. Gurfinkel, P. Leleux, A. Ghestem, E. Ismailova, T. Hervé, S. Sanaur, C. Bernard and G. G. Malliaras, *Nat. Commun.*, 2013, **4**, 1575.
15  J. Rivnay, P. Leleux, M. Ferro, M. Sessolo, A. Williamson, D. A. Koutsouras, D. Khodagholy, M. Ramuz, X. Strakosas, R. M. Owens, C. Benar, J.-M. Badier, C. Bernard and G. G. Malliaras, *Sci. Adv.*, 2015, **1**, e1400251–e1400251.
16  D. Khodagholy, J. Rivnay, M. Sessolo, M. Gurfinkel, P. Leleux, L. H. Jimison, E. Stavrinidou, T. Herve, S. Sanaur, R. M. Owens and G. G. Malliaras, *Nat. Commun.*, , DOI:10.1038/ncomms3133.
17  A. Giovannitti, C. B. Nielsen, D.-T. Sbircea, S. Inal, M. Donahue, M. R. Niazi, D. A. Hanifi, A. Amassian, G. G. Malliaras, J. Rivnay and I. McCulloch, *Nat. Commun.*, 2016, **7**, 13066.
18  L. Contat-Rodrigo, C. Pérez-Fuster, J. Lidón-Roger, A. Bonfiglio and E. García-Breijo, *Sensors*, 2016, **16**, 1599.

19 P. Lin, F. Yan, J. Yu, H. L. W. Chan and M. Yang, *Adv. Mater.*, 2010, **22**, 3655–3660.
20 J. Rivnay, P. Leleux, A. Hama, M. Ramuz, M. Huerta, G. G. Malliaras and R. M. Owens, *Sci. Rep.*, , DOI:10.1038/srep11613.
21 M. Ramuz, A. Hama, J. Rivnay, P. Leleux and R. M. Owens, *J Mater Chem B*, 2015, **3**, 5971–5977.
22 D. Khodagholy, V. F. Curto, K. J. Fraser, M. Gurfinkel, R. Byrne, D. Diamond, G. G. Malliaras, F. Benito-Lopez and R. M. Owens, *J. Mater. Chem.*, 2012, **22**, 4440.
23 Z. Yi, G. Natale, P. Kumar, E. D. Mauro, M.-C. Heuzey, F. Soavi, I. I. Perepichka, S. K. Varshney, C. Santato and F. Cicoira, *J Mater Chem C*, 2015, **3**, 6549–6553.
24 L. Mracek, T. Syrovy, S. Pretl, S. Nespurek and A. Hamacek, in *2016 39th International Spring Seminar on Electronics Technology (ISSE)*, 2016, pp. 66–70.
25 J. W. Hwang, S. M. Noh, B. Kim and H. W. Jung, *J. Appl. Polym. Sci.*, 2015, **132**, n/a-n/a.
26 M. Hahn, L. Taite, J. Moon, M. Rowland, K. Ruffino and J. West, *Biomaterials*, 2006, **27**, 2519–2524.
27 C. Karunakaran, K. Bhargava and R. Benjamin, *Biosensors and Bioelectronics*, Elsevier, 2015.
28 S. Takamatsu, T. Lonjaret, D. Crisp, J.-M. Badier, G. G. Malliaras and E. Ismailova, *Sci. Rep.*, 2015, **5**, 15003.
29 M. Isik, T. Lonjaret, H. Sardon, R. Marcilla, T. Herve, G. G. Malliaras, E. Ismailova and D. Mecerreyes, *J Mater Chem C*, 2015, **3**, 8942–8948.
30 A. R. Harris, P. J. Molino, R. M. I. Kapsa, G. M. Clark, A. G. Paolini and G. G. Wallace, *The Analyst*, 2015, **140**, 3164–3174.
31 C. Nick, C. Thielemann and H. F. Schlaak, IEEE, 2014, pp. 160–165.
32 G. Xie, F. He, X. Liu, L. Si and D. Guo, *Sci. Rep.*, , DOI:10.1038/srep25002.
33 E. Stavrinidou, P. Leleux, H. Rajaona, D. Khodagholy, J. Rivnay, M. Lindau, S. Sanaur and G. G. Malliaras, *Adv. Mater.*, 2013, **25**, 4488–4493.
34 T. Darmanin and F. Guittard, *Mater. Chem. Phys.*, 2014, **146**, 6–11.
35 D. Mantione, I. del Agua, W. Schaafsma, M. ElMahmoudy, I. Uguz, A. Sanchez-Sanchez, H. Sardon, B. Castro, G. G. Malliaras and D. Mecerreyes, *ACS Appl. Mater. Interfaces*, 2017, **9**, 18254–18262.

# Chapter 4.

# Conducting polymer iongels based on PEDOT and guar gum



Electro conductive

Ionic conductive

Flexible

# Chapter 4. Conducting polymer iongels based on PEDOT and guar gum

## 4.1. Introduction

Conducting polymer hydrogels are attracting much interest in biomedical and energy-storage devices due to their unique electrochemical properties including their ability to conduct both electrons and ions. They suffer, however, from poor environmental stability due to water evaporation which causes the loss of mechanical and ion conduction properties. Here we show for the first time an environmentally stable conducting polymer gel where the continuous phase is a non-volatile ionic liquid. The novel conducting iongel is formed by a natural polysaccharide (guar gum), a conductive poly-mer poly(3,4-ethylenedioxythiophene) (PEDOT) and an ionic liquid (IL) 1-butyl-3-methylimidazolium chloride (BMIMCl). Firstly, an aqueous dispersion of PEDOT:guar gum is synthesized by an oxidative polymerization process of EDOT in the presence of the polysaccharide as stabilizer. The resulting PEDOT:guar gum was isolated as a powder by removing the water via freeze drying process. In the final step, conducting iongels were prepared by the

PEDOT:guar gum mixed with the ionic liquid by a heating-cooling process. The rheological properties show that the material exhibits gel type behavior between 20 and 80 °C. Interestingly, the conducting polymer iongel presents redox properties as well as high ionic conductivities ($10^{-2}$ S cm$^{-1}$). This material presents a unique combination of properties by mixing the electronic conductivity of PEDOT, the ionic conductivity and negligible vapor pressure of the ionic liquid and the support and flexibility given by guar gum.

Conducting polymer hydrogels represent a unique class of materials that offer synergies between the advantageous features of hydrogels and conducting polymers. Conducting polymer hydrogels are gels, which are swollen with water and contain a conducting polymer along with a supporting polymer as constituents. Nowadays, these conducting hydrogels have been demonstrated on a variety of polymers such as polypyrrole, polyaniline, PEDOT and supporting polymers such as polyacrylamide, poly(acrylic acid) or several biopolymers such as alginates, cellulose, gelatin, etc.[1,2] The most intrinsic characteristic of conducting polymer hydrogels is the combination in the same material of the electroactivity given by the conducting polymer and the ionic conductivity given by the aqueous media. For this reason, these polymers present very interesting applications in energy and bioelectronics[3] through several devices such as supercapacitors, electrochemical sensors, drug delivery systems and organic transistors (OFETs and OECTs).   Among the different type of conducting hydrogels, PEDOT based ones are preferred nowadays due to its high conductivity and performance in bioelectronics devices.[4,5]

One drawback of conducting polymer hydrogels is that, at the end of the day, they dry due to water evaporation losing their mechanical and electrical properties. For this reason, conducting gels which are environmentally stable are researched. Iongels are a relatively new type of gels where the liquid phase, percolating throughout the solid phase, is an ionic liquid (IL).[6,7] The properties given by the ionic liquids such as the high ionic conductivity and low volatility are

preserved in the iongels, making them suitable and very attractive soft solid materials for several applications. Although the field of iongels is rapidly expanding, to the best of our knowledge, there has been no report yet on the synthesis of conducting polymer iongels. In this work, we present for the first time a conducting polymer iongel. The conducting iongel is formed by a natural polysaccharide (guar gum), a conductive polymer (PEDOT) and an ionic liquid (IL): 1-butyl-3-methylimidazolium chloride (BMIMCl).

## 4.2. Results and discussion

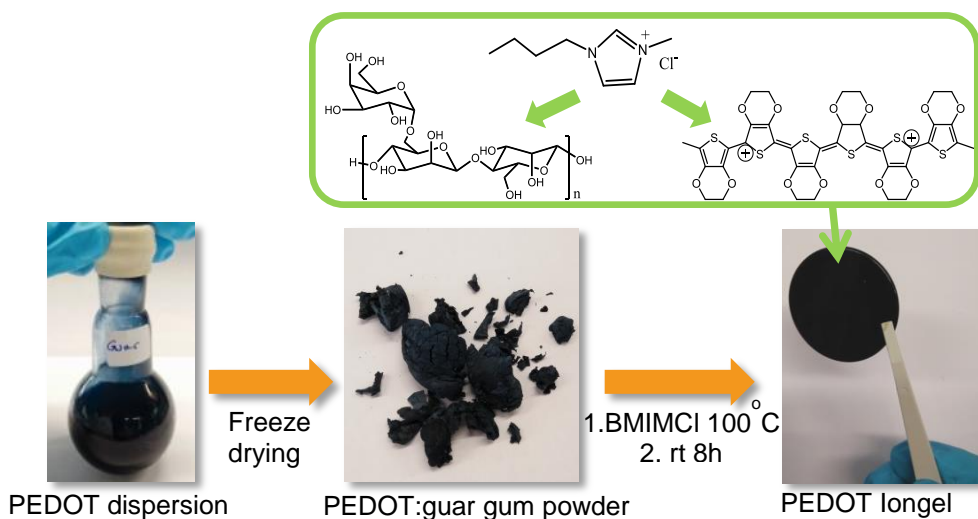### 4.2.1. Synthetic route towards PEDOT Iongels



**Figure 4.1**. Synthetic route for conducting polymer Iongels based on PEDOT, guar gum and ionic liquid BMIMCl.

Iongels can be prepared using different synthetic methods which can be classified by the chemical nature of the gelators, such as low molecular weight

81

compounds, organosilane agents,[8] (meth)acrylic resins,[9] epoxy resins,[10] poly(ionic liquid)s,[11] polysacharides[12] or triblock copoly-mers.[13–16] One interesting gelator for ionic liquids is a high molecular weight polysaccharide such as guar gum. Guar gum iongels have been recently reported simply by mixing through a heating-cooling cycle with various imidazolium type ionic liquids such as BMIMCl, 1-ethyl-3-methylimidazolium methylphosphonate (EMIMMP), and 1-allyl-3-methylimidazolium (AMIMCl).[17–19] In this work we complement the excellent ionic conductivity and good mechanical properties of guar gum iongels with the electronic properties of PEDOT.

The synthetic route towards PEDOT:guar gum:BMIMCl iongels is depicted in Figure 4.1. In a first step a PEDOT:guar gum composite is prepared by oxidative polymerization of EDOT in the presence of the guar gum as stabilizer. The PEDOT:guar gum composite was obtained by freeze-drying of the water solvent. In the second step, conducting polymer iongels were prepared by mixing the PEDOT:guar gum composite with the ionic liquid 1-ethyl-3-methylimidazolium chloride (BMIMCl) by a simple hot-cooling process. PEDOT iongels were obtained as soft, self-standing and flexible films as shown in the image of Figure 4.1.

### 4.2.2 Dispersions synthesis and characterization

The use of polysaccharides as stabilizers for the synthesis of PEDOT dispersions is a popular strategy[20,21] due to the increased biocompatibility of the obtained materials versus the commercially available poly(3,4-ethylenedioxythiophene) polystyrene sulfonate (PEDOT:PSS). However, guar gum was not investigated yet. Figure 4.2 shows the chemical oxidative polymerization of EDOT in the presence of guar gum as stabilizer. As it can be seen in the images of the reaction (Figure 4.2b), at the beginning the mixture is a white viscous dispersion. After 24 h of reaction, the dispersion acquires the characteristic bright blue color of PEDOT. The chemical oxidative polymerization was followed by HPLC,

measuring the 3,4-ethylenedioxythiophene (EDOT) monomer consumption over time (Figure 4.3a). As it can be observed, the reaction reaches completion (99% polymerization) within 96 h. It is worth noting that this reaction is slow when compared with other PEDOT:polysaccharides or PEDOT:PSS reactions which take less than 24 h. This may be due to the high viscosity 485±9 (mPas) which is characteristic of the guar gum aqueous dispersions. This might be the factor that slows down the reaction kinetics.[22] As it is well known, this increase in the viscosity could reduce the diffusion of reacting species such as monomer and oxidant necessary to promote the polymerization, increasing the reaction time. Interestingly, a decrease in viscosity of the dispersion is observed during the reaction (381±13 mPa). A similar viscosity decrease was observed before in the case of other polysaccharides and it is associated with the ability of the forming PEDOT chains to break the intramolecular hydrogen bonding between polysaccharide chains.[20]

a)



b)



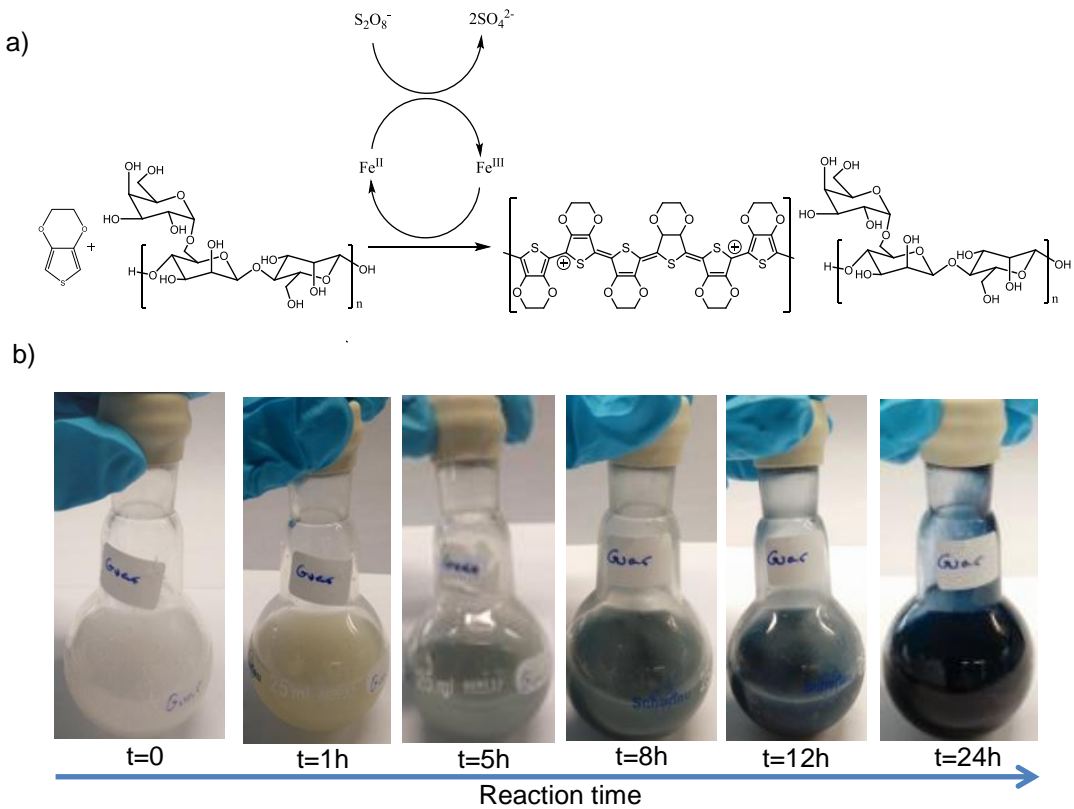| t=0 | t=1h | t=5h | t=8h | t=12h | t=24h |

Reaction time

**Figure 4.2.** (a) Chemical oxidative polymerization of EDOT in the presence of guar gum. (b) UV-Vis-NIR absorbance spectra of the PEDOT:guar gum dispersions. (c) Color changes during the first 24 h of polymerization of PEDOT:guar gum (0.25:0.75).
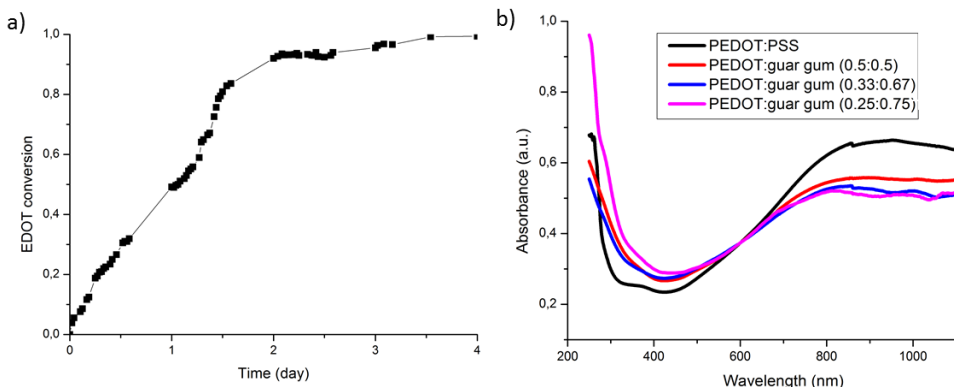
**Figure 4.3.** (a) Kinetic reaction profile (monomer conversion over reaction time) measured by HPLC for chemically oxidative polymerization of PEDOT:guar gum (0.25:0.75), b) UV-Vis-NIR absorbance spectroscopy of PEDOT:guar gum (0.5:0.5, 0.33:0.67, 0.25:0.75) and PEDOT:PSS.

The PEDOT: guar gum dispersions were further characterized by UV-Vis-NIR absorbance spectroscopy and com-pared to commercially available PEDOT:PSS (Figure 4.3b). Two characteristic absorption bands of PEDOT:PSS were observed, the absorption band of PEDOT π - π* centered at 800-900 nm[23] and a broad polaron band that extends in the NIR region, centered at 1150 nm. This broad polaron band in the NIR is generally attributed to the doped material and it is related to the conductivity of the material confirming the conducting nature of the PEDOT:guar gum. Using this synthetic method, we prepared several PEDOT:guar gum dispersions by varying the weight ratio between the conducting polymer and the stabilizer (PEDOT:guar gum: 0.25:0.75; 0,33:0.67, 0.5:0.5; 0.67:0.33). After drop-casting on a glass slide, the electrical conductivity of these PEDOT:guar gum dry powders was measured by 4-point probe (4PP) method. The electrical conductivity showed values between 2.8 $10^{-2}$ S cm$^{-1}$ and 1.29 $10^{-1}$ S cm$^{-1}$ (Table 4.1). The conductivity values show a clear trend, conductivity increases when increasing the amount of PEDOT by reason of the

higher content of conductive polymer chains. It is worth noting that the $10^{-1}$ S cm$^{-1}$ conductivity value is similar to the one of PEDOT:PSS commercial dispersions without any additional post-treatment.[24,25]

**Table 4.1.** Formulation and conductivity values of PEDOT:guar gum dispersions.

| PEDOT:guar gum ratio | PEDOT content (g) | Guar gum content (g) | $(NH_4)_2S_2O_8$ (g) | Conductivity (S cm$^{-1}$) |
|---|---|---|---|---|
| 0.25:0.75 | 0.1 | 0.3 | 0.24 | $2.8 \ 10^{-2}$ |
| 0.33:0.67 | 0.13 | 0.27 | 0.38 | $7.0 \ 10^{-2}$ |
| 0.5:0.5 | 0.2 | 0.2 | 0.47 | $1.29 \ 10^{-1}$ |
| 0.67:0.33 | 0.27 | 0.13 | 0.64 | $10^{-1}$ |

PEDOT chains due to the π-conjugated thiophene rings, present conductivity when in their oxidized state. Depending on the doping state, they have more or less charge transport sites. The changes in doping state are accompanied by a change in color from light to dark blue, because PEDOT presents electrochromism. Depending on its oxidation state, it absorbs in the Vis or NIR range. The oxidation level of PEDOT:guar gum dispersions and commercial PEDOT:PSS was determined by UV-Vis-NIR spectrometry using two reducing agents: Sodium sulfite ($Na_2SO_3$) and sodium borohydride ($NaBH_4$) (Figure 4.4) According to the literature,[26] the reduction level of the PEDOT:PSS increases with the redox potential of the reducing agent. As it is observed, the reduction of PEDOT:guar gum dispersions with a moderate reducing agent ($Na_2SO_3$) (in blue) lead to a decrease in the absorption band related to the dication chains contribution (above 1250 nm) indicating the reduction of PEDOT chains into neutral chains. On top of that, the formation of a new absorption band at around 600 nm is observed. This band is attributed to the presence of PEDOT neutral chains.[27] It is important to remark that this new band is not present the case of PEDOT:PSS dispersions when treated with $Na_2SO_3$, which indicates that PEDOT neutral chains are not formed for this reducing agent.[28] Further reduction (in orange), obtained with strong reducing agent ($NaBH_4$), led to a further decrease

86

of absorbance at 1250 nm and in the case of PEDOT:PSS a new band around 660 nm is created, corresponding to neutral PEDOT chains. The fact that a moderate reducing agent has a stronger reducing effect on PEDOT:guar gum dispersions than in PEDOT:PSS dispersions shows that although PEDOT chains are doped when stabilized by guar gum, PEDOT is doped to a lesser extent than when stabilized by PSS chains. These results are in agreement with 4-point probe conductivity measurements which show that PEDOT:guar gum dispersions present slightly lower conductivity than PEDOT:PSS dispersions.
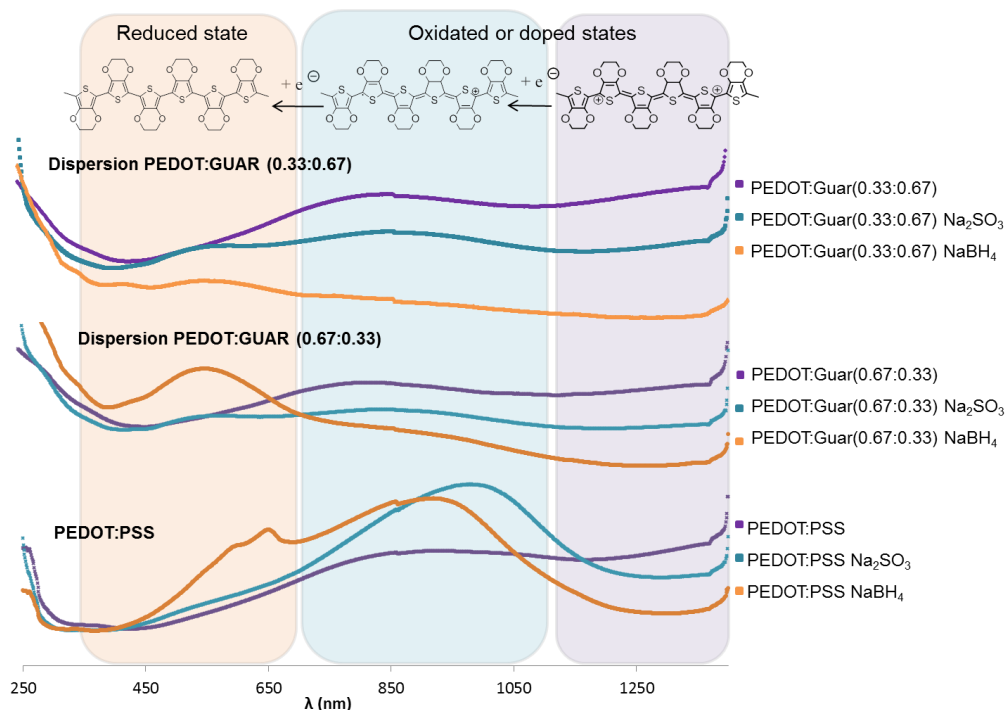


**Figure 4.4.** UV-Vis NIR determination of PEDOT doping state for 3 dispersions: PEDOT:guar (0.33:0.67) PEDOT:guar (0.67:0.33) and PEDOT:PSS. In purple dispersions without treatment, in blue dispersions treated with $Na_2SO_3$ and in orange dispersions treated with $NaBH_4$.

Next, the PEDOT:guar gum powders were obtained by freeze-drying the obtained aqueous dispersions. In order to verify the intimate mixing of the PEDOT and guar gum, the obtained powders were characterized by transmission electronic microscopy (TEM) and scanning electron microscope (SEM). Figure 4.5 shows the TEM and SEM  images of PEDOT and guar gum diluted dispersions evaporated onto the TEM grid and the SEM support, respectively. In every case, the PEDOT:guar gum form spherical agglomerates with particle sizes in between 100 and 300 nm. Particle size and morphology do not show differences in between dispersions. In addition, a conducting PEDOT core is observed surrounded by a non-conducting guar gum corona.  Same particle size and spherical powdery morphology were determined by both techniques. Altogether, the images confirm the intimate mixing of the PEDOT and guar gum composites, obtained by the dispersion polymerization and drying method.

**Figure 4.5.** Transmission electron microscope (TEM) and scanning electron microscope (SEM) images. (a) TEM images of PEDOT:guar gum dispersion (0.67:0.33). (b) TEM images of PEDOT:guar gum dispersion (0.33:0.67). (c) SEM images of PEDOT:guar gum dispersion (0.33:0.67).

### 4.2.3 Iongels synthesis and characterization

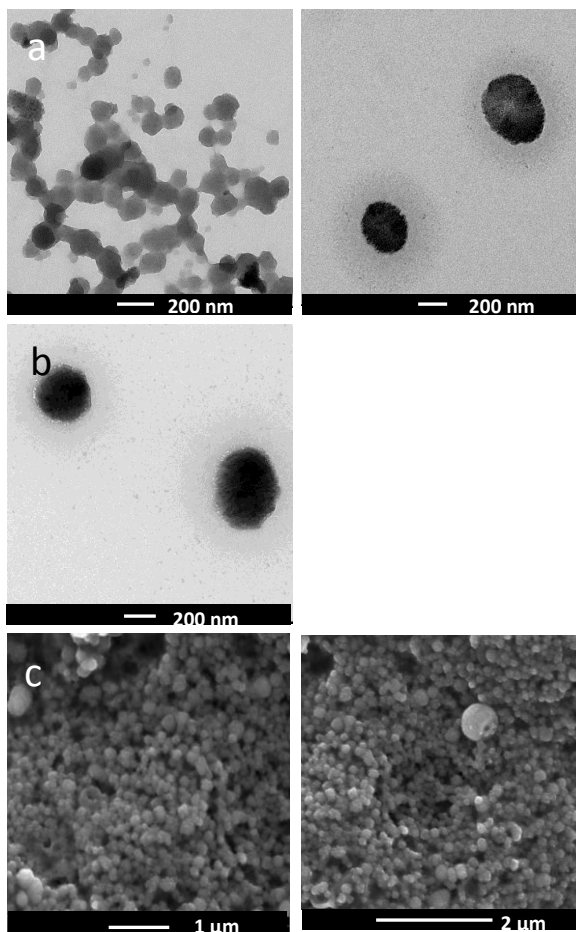In the last step, PEDOT:guar gum iongels were prepared in a similar way to previously reported guar gum iongels.[17] Briefly, the iongels were formed by mixing of the PEDOT:guar gum dry composite with the ionic liquid (IL): 1-butyl-3-methylimidazolium chloride (BMIMCl). When heating at 100 $^{o}$C for 3 h under mechanical stirring, the IL was able to solubilize the blend and form a viscous solution. Upon cooling, this solution solidifies and jellifies forming a self-standing iongel film. PEDOT:guar gum iongels with different IL content (between 65% and 90%) were synthetized but 75% wt was found to be optimal in order to have an homogenous blend for all the different PEDOT:guar gum ratios, avoiding leakages of the IL in excess.

The rheological properties of iongels are one of the most important properties for their practical application as gel network of rubbery nature. Because of that, rheological properties of the iongels were analyzed by frequency sweep measurements. The evolution of elastic (G') and viscous (G'') moduli of the iongels as a function of frequency and temperature was studied (Figure 4.6). In all PEDOT:guar gum ratios studied (0.5:0.5, 0.33:0.67, and 0.25:0.75), G' modulus is higher than G'' on the whole frequency range and independent of frequency, which is typical of a solid-like behavior.[29] In fact, ideal gels display almost purely elastic response where the elastic modulus is higher than the viscous modulus. Higher modulus is observed when decreasing the amount of PEDOT in the gel structure, indicating that PEDOT chains weaken the gel structure, which is in accordance to another study of hydrogels containing PEDOT and polysaccharide.[30] As it can be observed in Figure 4.6b, the iongels show high temperature stability in the temperature range of 25 to 80 $^{o}$C. The drop in both moduli due to the softening of the gels was observed at higher temperatures than 80 $^{o}$C. It is known that guar gum form iongels due to the physical crosslinking of ionic liquids owing to the strong hydrogen bonding interactions between the polysaccharide chains.[17] At high temperatures, the

90

mobility of PEDOT, guar chains, and IL increases, because of to the disruption of their physical interactions and the gel properties of the material are lost. In any case, the rheological properties confirm that be-tween room temperature and 80 °C, these materials are iongels formed by a non-volatile ionic liquid percolating through a solid phase composed of guar gum and the con-ducting polymer PEDOT. Regarding the influence of PEDOT content in the stability of the gels with temperature. PEDOT content does not found to have any effect showing that PEDOT chains at these concentrations do not weaken the gel in terms of temperature stability.
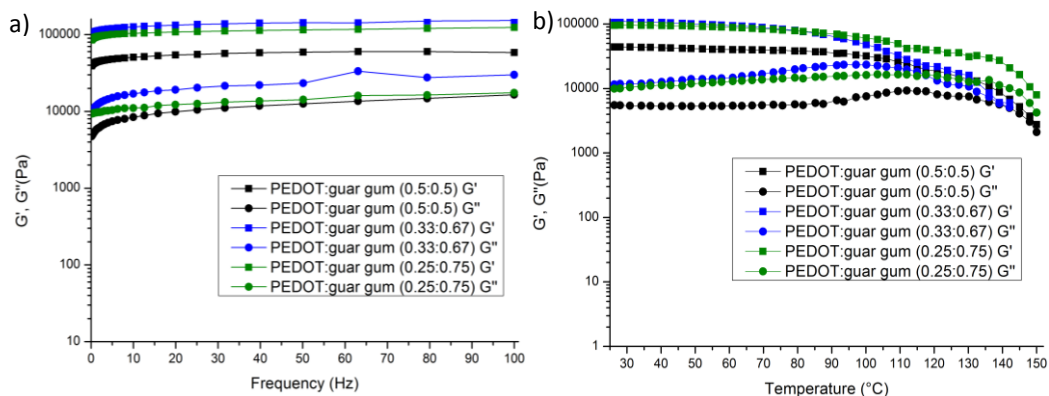


**Figure 4.6.** Rheological behavior. (a) Evolution of G' (squares) G'' (circles) as function of frequency for PEDOT:guar gum films. (b) Evolution of G' (squares) G'' (circles) as function of temperature.

Finally it was investigated whether PEDOT:guar gum: BMIMCL iongel combines in the same material the electroactivity given by the conducting polymer and the ionic conductivity given by the ionic liquid. Cyclic voltammetry experiments (CV) of these iongels were carried out in order to confirm the redox activity. The cyclic voltammogram of a PEDOT:guar gum iongel (0.5:0.5) film in 0.1 M LiTFSi in

MeTHF (Figure 4.7a) is characterized by a capacitive shape, typical of conducting polymers and very similar to that of the PEDOT:PSS.[31] Due to the presence of the free ionic liquid confined in the polymer matrix, PEDOT:guar gum iongels are solid electrolytes with high ionic conductivities. In this case, the presence of the ionic liquid constitutes 75% of the total gel weight. For this reason, the ionic conductivities of electroconductive iongels were determined by impedance spectroscopy from -10 $^{\circ}$C to 60 $^{\circ}$C as shown in Figure 4.7b. Spectroscopy impedance measurements show ionic conductivities of $10^{-2}$ S cm$^{-1}$. As expected, the ionic conductivity increases with temperature due to the increase in carrier mobility. Ionic conductivity also increases with the amount of PEDOT. The best conductivity values were obtained for the iongel with the highest PEDOT content, PEDOT:guar gum (0.5:0.5) iongel. This shows the positive contribution of oxidized PEDOT chains in the average ionic conductivity.



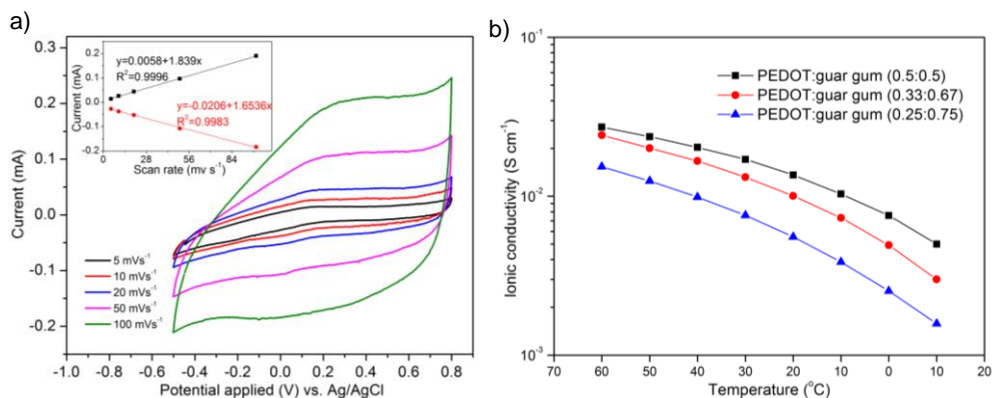**Figure 4.7**. (a) Cyclic voltammogram for PEDOT:guar gum iongel (0.5:0.5) containing 75% BMIMCl in Methyl Tetrahydrofuran 0.1M LiTFSi solution at a potential scan rate of 5 mV s$^{-1}$. (b) Temperature dependence of the ionic conductivity for 3 different PEDOT:guar gum iongel ratios: 0.5:0.5, 0.33:0.67, and 0.25:0.75.

## 4.3. Conclusion

In conclusion, we have presented a new type of iongel which combines the properties of a flexible polysaccharide (guar gum), a conducting polymer (PEDOT) and an ionic liquid (BMIMCl) which acts as a crosslinker. These materials serve as a proof of concept and first example of conducting polymer iongel. This simple synthetic approach can be applied to polypyrrole and polyaniline expanding the potential of these conducting iongels. The best iongel formulation in terms of ionic conductivity was found to be the PEDOT:guar gum (0.5:0.5) with 75% wt BMIMCl due to the contribution of PEDOT chains in the overall iongel conductivity. All in all, these polymeric soft materials combine the redox properties of conducting polymers and the ionic conductivity of ionic liquids together with their negligible vapor pressure. This unique combination of properties may bring advantages to some applications of conducting gels in the area of energy and bioelectronics.

## 4.4 Experimental part

**Materials:** 3,4-Ethylenedioxythiophene (EDOT), 1-butyl-3-methylimidazolium chloride (BMIMCl), 2-methyltetrahydrofuran (MeTHF), sodium sulfite ($Na_2SO_3$), Sodium borohydride ($NaBH_4$) and acetonitrile were purchased from Acros Organic. Guar gum, ammonium persulfate, benzyl alcohol, iron sulfate, dulbecco's phosphate buffer saline, sodium sulfate, and sodium borohydrate were purchased from Sigma Aldrich. Lithium bis-trifluoromethanesulfonimide was provided by Solvionic and high conducing PEDOT:PSS (Clevios PH 1000) by Heraeus. Regenerated Cellulose dialysis membrane (12-14 kD) was purchased from Spectrumlabs. Quartz cuvettes came from Agilent and 40 mm diameter and 12 mm height glass petri-dishes from Brand.

**Syntheses:**

**Synthesis of PEDOT:guar gum dispersions:** PEDOT:guar gum dispersions with 2% solids content were synthetized by oxidative polymerization according to the following procedure. In a 25 mL round bottom flask containing 19.6 mL of MilliQ water 0.3 g, 0.27 g, 0.2 g or 0.13 g of guar gum were dissolved and purged with N2. Afterwards, 0.1 g, 0.13 g, 0.2 g, or 0.27 g of EDOT monomer, together with the 1.5 eq of ammonium persulfate $((NH_4)_2S_2O_8)$ and a catalytic amount (5 mg) of iron (III) sulfate $(Fe_2(SO_4)_3)$ was added respectively. Reaction was kept at 0 $^o$C until completion (4 days). The dispersions were purified by dialysis with MilliQ water. Finally, dispersions containing different PEDOT:guar gum ratios were obtaining varying he initial amount of grams (Table 4.1) (0.25:0.75, 0.33:0.67, 0.5:0.5, and 0.67:0.33).

**Synthesis of PEDOT:guar gum:** BMIMCL Iongels: PEDOT:guar gum iongels with different IL content (between 65% and 90% wt of IL) were synthesized. It was found that above > 80% wt of IL content, the IL leaks out from the gel and below < 70% wt of IL content, IL does not able to dissolve all the PEDOT:guar gum powder. The homogeneous blend was observed when the mixture of powder and the IL was heated up with 75% wt of IL content. For the synthesis of iongels, PEDOT:guar gum dispersions were lyophilized and a dry polymer blend was obtained. 0.5 g of dry polymer blend together with 1.5 g of IL were mechanically mixed and left in the oven for 3h at 100 $^o$C. The viscous blend was poured into a glass petri dish and left standing at r.t. overnight. The material jellifies obtaining a crosslinked solid gel.

**Characterization Techniques:**

**Kinetic studies:** The polymerization reaction was followed until completion by High Pressure Liquid Chromatography (HPLC) using a Hewlett-Packard HPLC series 1100 apparatus with a Lichrosphere 100 CN (5 µm) column from Agilent

Technologies. The eluent was water:acetonitrile 1:1 0.8 mL min$^{-1}$ at room temperature (r.t.). The reaction was sampled every 30 min according to the following, 10 µL of reactor mixture were put in 5 mL of acetonitrile containing 1 µL of benzyl alcohol as internal standard. 20 µL of this solution were injected directly into the HPLC. EDOT concentration was calculated by plotting EDOT peak areas (5.2 min retention time) in a calibration line.

**Viscosity:** Measurements were performed with a SV-10 Vibro-viscometer from Malvern. Dispersions were analyzed without modification.

**Conductivity:** The measurements of conductivity were performed on a four-point probe Veeco/Miller FPP5000 using layer resistivity function.

-UV-Vis-NIR measurements: A UV/Vis/NIR Spectrometer PerkinElmer Lambda 950 was used. In quartz cuvettes, a solution 2% v/v in water of each PEDOT:guar gum dispersion was analyzed. All spectra were normalized.

**TEM measurements:** The dispersed particles as well as the morphology of the films casted from the dispersions were analyzed by Transmission Electron Microscopy (TEM), TECNAI G2 20 TWIN (FEI), operating at an accelerating voltage of 200 kV in a bright-field image mode.

**SEM measurements:** SEM images were taken with an Hitachi Analytical TableTop Microscope/Benchtop SEM TM3030. For measurements, the dispersion was diluted in Milli Q water 5%v/v and dropcasted.

**Rheological measurements:** Rheological experiments were performed with an AR-1500EX from TA instruments and temperature was controlled by a Peltier system. Two type of measurements were performed using a 40 mm steel plate: 1) Frequency sweep step; frequency 100-0.1 Hz, strain 0.4%, gap 500 µm, temperature 25$^{o}$C.  2) Temperature ramp step; temperature 25-150 $^{o}$C, ramp 3$^{o}$C min$^{-1}$, frequency 1 Hz, strain 0.4%, gap 500 µm.

**Cyclic voltammetry measurements:** An Autolab PGSTAT302N equipment from Metrohm was used. Recorded in a three electrode arrangement, using a Pt counter electrode and an Ag/AgCl reference electrode. The iongel (0.024 g, area

1 cm$^2$) was deposited on a Pt electrode at 100 $^o$C and let it cool down for solidification/jellification. The solvent and electrolyte used were acetonitrile and 0.1 M LiClO$_4$ respectively. The voltage range was set from -0.5 V to 0.8 V at 5, 10, 20, 50, 100 mV s$^{-1}$ scan rates.

**Impedance measurements:** An Autolab PGSTAT302N equipment with a Microcell HC from Metrohm was used. Iongel discs with a diameter of 12 mm and thickness of 1.5 mm were placed in between two electrodes one made of steel and the other made of gold. Impedance was measured at range of temperatures from -10 to 60 $^o$C. The ionic conductivity of each sample was calculated according to the real part of the resistance (Z') while the imaginary part of resistance (Z'') was assumed to be zero.

## 4.5 References

1 J. Stejskal, *Chem. Pap.*, , DOI:10.1007/s11696-016-0072-9.
2 D. Mawad, A. Lauto and G. G. Wallace, in *Polymeric Hydrogels as Smart Biomaterials*, ed. S. Kalia, Springer International Publishing, Cham, 2016, pp. 19–44.
3 Y. Ido, D. Takahashi, M. Sasaki, K. Nagamine, T. Miyake, P. Jasinski and M. Nishizawa, *ACS Macro Lett.*, 2012, **1**, 400–403.
4 M. Isik, T. Lonjaret, H. Sardon, R. Marcilla, T. Herve, G. G. Malliaras, E. Ismailova and D. Mecerreyes, *J Mater Chem C*, 2015, **3**, 8942–8948.
5 E. Bihar, Y. Deng, T. Miyake, M. Saadaoui, G. G. Malliaras and M. Rolandi, *Sci. Rep.*, 2016, **6**, 27582.
6 J. Le Bideau, L. Viau and A. Vioux, *Chem Soc Rev*, 2011, **40**, 907–925.
7 D. Mecerreyes, *Applications of Ionic Liquids in Polymer Science and Technology*, Springer, 2015.
8 S. Thiemann, S. J. Sachnov, M. Gruber, F. Gannott, S. Spallek, M. Schweiger, J. Krückel, J. Kaschta, E. Spiecker, P. Wasserscheid and J. Zaumseil, *J Mater Chem C*, 2014, **2**, 2423–2430.
9 X. Zhang, S.-J. Wang, J. Peng, J.-Q. Li, L. Xu and M.-L. Zhai, *Nucl. Sci. Tech.*, , DOI:10.1007/s41365-016-0039-0.
10 T. K. L. Nguyen, S. Livi, B. G. Soares, S. Pruvost, J. Duchet-Rumeau and J.-F. Gérard, *ACS Sustain. Chem. Eng.*, 2016, **4**, 481–490.
11 M. G. Cowan, D. L. Gin and R. D. Noble, *Acc. Chem. Res.*, 2016, **49**, 724–732.

12 A. Takada and J. Kadokawa, *Biomolecules*, 2015, **5**, 244–262.

13 C. R. López-Barrón, D. Li, N. J. Wagner and J. L. Caplan, *Macromolecules*, 2014, **47**, 7484–7495.

14 M. A. B. H. Susan, T. Kaneko, A. Noda and M. Watanabe, *J. Am. Chem. Soc.*, 2005, **127**, 4976–4983.

15 C. C. Hall, C. Zhou, S. P. O. Danielsen and T. P. Lodge, *Macromolecules*, 2016, **49**, 2298–2306.

16 C. R. López-Barrón, R. Chen and N. J. Wagner, *ACS Macro Lett.*, 2016, **5**, 1332–1338.

17 L. Verger, S. Corre, R. Poirot, G. Quintard, E. Fleury and A. Charlot, *Carbohydr. Polym.*, 2014, **102**, 932–940.

18 K. Prasad, H. Izawa, Y. Kaneko and J. Kadokawa, *J. Mater. Chem.*, 2009, **19**, 4088.

19 J.-I. Kadokawa, in *Ionic Liquids: Applications and Perspectives*, ed. A. Kokorin, InTech, 2011.

20 D. Mantione, I. del Agua, W. Schaafsma, J. Diez-Garcia, B. Castro, H. Sardon and D. Mecerreyes, *Macromol. Biosci.*, 2016, **16**, 1227–1238.

21 D. G. Harman, R. Gorkin, L. Stevens, B. Thompson, K. Wagner, B. Weng, J. H. Y. Chung, M. in het Panhuis and G. G. Wallace, *Acta Biomater.*, 2015, **14**, 33–42.

22 J. Casas, A. Mohedano and F. Garcia-Ochoa, *J. Sci. Food Agric.*, 2000, **80**, 1722–1727.

23 M. Łapkowski and A. Proń, *Synth. Met.*, 2000, **110**, 79–83.

24 I. Cruz-Cruz, M. Reyes-Reyes, M. A. Aguilar-Frutis, A. G. Rodriguez and R. López-Sandoval, *Synth. Met.*, 2010, **160**, 1501–1506.

25 I. Cruz-Cruz, M. Reyes-Reyes and R. López-Sandoval, *Thin Solid Films*, 2013, **531**, 385–390.

26 N. Massonnet, A. Carella, O. Jaudouin, P. Rannou, G. Laval, C. Celle and J.-P. Simonato, *J Mater Chem C*, 2014, **2**, 1278–1283.

27 I. Cruz-Cruz, M. Reyes-Reyes, I. A. Rosales-Gallegos, A. Y. Gorbatchev, J. M. Flores-Camacho and R. López-Sandoval, *J. Phys. Chem. C*, 2015, **119**, 19305–19311.

28 J. C. Carlberg, *J. Electrochem. Soc.*, 1998, **145**, 3810.

29 *Gels: Structures, Properties, and Functions*, Springer Berlin Heidelberg, Berlin, Heidelberg, 2009.

30 H. Warren and M. in het Panhuis, *MRS Proc.*, , DOI:10.1557/opl.2013.1101.

31 P. R. Das, L. Komsiyska, O. Osters and G. Wittstock, *J. Electrochem. Soc.*, 2015, **162**, A674–A678.

# Chapter 5.

# Conducting Polymer Scaffolds based on PEDOT and Xanthan Gum for live-cell Monitoring



PEDOT:Xanthan Gum:DVS     Freeze drying     Porous Scaffold     Cell seeding     Cell growth
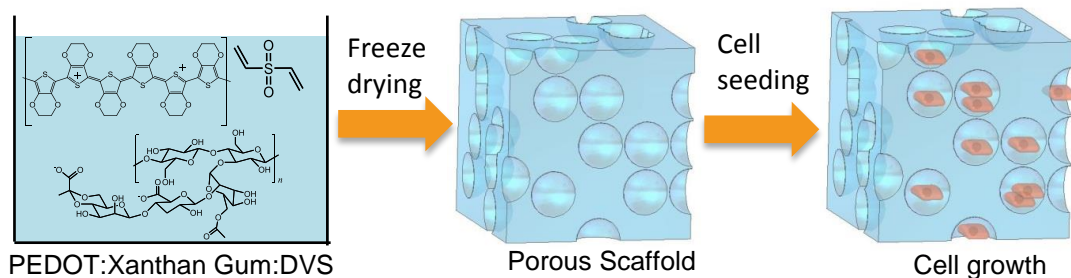
# Chapter 5. Conducting Polymer Scaffolds based on PEDOT and Xanthan Gum for live-cell Monitoring

## 5.1. Introduction

3D cell culture in artificial environments finds numerous applications. It is currently used for cancer research, drug discovery, and regenerative medicine among many other research areas. In order to culture cells *in vitro*, 3D structures that support cell attachment and guide cells for tissue development are needed.[1] These structures are normally made of polymeric materials; polymers which allow to design scaffolds with certain structural and mechanical properties.[2] Among these scaffold properties, their porosity and stiffness are of crucial importance. Their void structure is a key factor as interconnected pores create pore networks, which aid diffusion of nutrients and oxygen and removal of waste,[3] and facilitate scaffold colonization.[4] The mechanical behavior of the

scaffold should mimic the extracellular matrix (ECM),[2] providing an environment as similar as possible to cell natural environment.

Due to the immense possibilities of scaffold design, even electrical properties have been induced by the use of conducting polymers (CP). These are polymers with alternating single and double bonds backbones which, by the process of doping (adding or removing electrons), delocalize charges are induced thus behaving as electronic conductors. Conducting polymers used in tissue engineering are polypyrrole,[5,6] polyaniline[7] and poly(3,4-ethylenedioxythiophene).[9–11] The advantages of conducting scaffolds are that they can deliver electrical stimulus to the cells, stimulating cell growth.[12] They have been used to enhance bone, muscle and nerve tissue regeneration.[6] Moreover, they are also used in drug delivery, with drugs bound in the scaffolds released through an electrical signal.[12] Conductive scaffolds can be synthesized by many techniques and, in particular, PEDOT scaffolds have been synthesized by chemical oxidative polymerization,[13] by  polymerization of EDOT monomer around a previously synthesized scaffold,[14] by vapor phase polymerization (VPP) on the scaffold,[15] or by electrochemical polymerization.[16,17] Another alternative is to use the freeze-drying method  to fabricate PEDOT:PSS three dimensional (3D) scaffolds.[18,19] Additives are added prior to the freeze-drying method like crosslinkers and surfactants (3-glycidoxypropyltrimethoxysilane (GOPS) or/and sodium dodecylbenzenesulfonate (DBSA)) to improve mechanical robustness and stability in water, or even proteins like collagen to improve cell growth.

For their success in tissue engineering applications, the scaffolds should act as an artificial extracellular matrix (ECM). ECM in the human body is composed of proteins and polysaccharides.[20] and these materials are normally used for scaffold synthesis.[21,22] Polysaccharides form hydrogels in water reducing the stiffness of the scaffolds to values more relevant in biological tissues. Among

polysaccharides employed, xanthan gum scaffolds present special interest due to their processability and biocompatibility.[19,20] They have been used to improve osteoblast growth,[25] and fibroblast proliferation.[5]

Recently, PEDOT:biopolymer water dispersions combining the characteristics of polysaccharides together with the conductivity given by PEDOT chains have been synthesized by chemical oxidative polymerization.[26,27] These works inspired us to combine the use of these dispersions and the freeze-drying method to synthesize new PEDOT:polysaccharide scaffolds. By including polysaccharides in a conducting scaffold, the natural ECM can be better mimicked positively influencing cell growth.

We present in this work a new synthetic route to elaborate PEDOT scaffolds which include polysaccharides embedded in the structure since they are included in the initial PEDOT particle structure. Thanks to the polysaccharide content, these scaffolds mimic better the ECM than PEDOT:PSS scaffolds with high degree of porosity and surface roughness attributed to the polysaccharide content. The synthetic strategy consists of three steps: first an aqueous blend of PEDOT:polysaccharide is formed by oxidative polymerization of 3,4-ethylenedioxythiophene (EDOT) in the presence of xanthan gum as stabilizer. Second a crosslinker divinyl sulfone is added to the aqueous dispersion and third, a freeze-drying step. PEDOT:polysaccharide dispersions have been characterized by UV and HPLC and the 3D scaffolds formed are used to grow MDCK type cells.

## 5.2. Results and Discussion

### 5.2.1. General synthetic route towards scaffold fabrication

PEDOT scaffolds for tissue engineering and cell monitoring are prepared through the freeze-drying method. The process requires certain key steps. First of all, a water dispersion has been synthesized by chemical polymerization in a similar

manner to other PEDOT:polysaccharide water dispersions present in literature.[26,27] The polymerization reaction can be found in Figure 5.1.
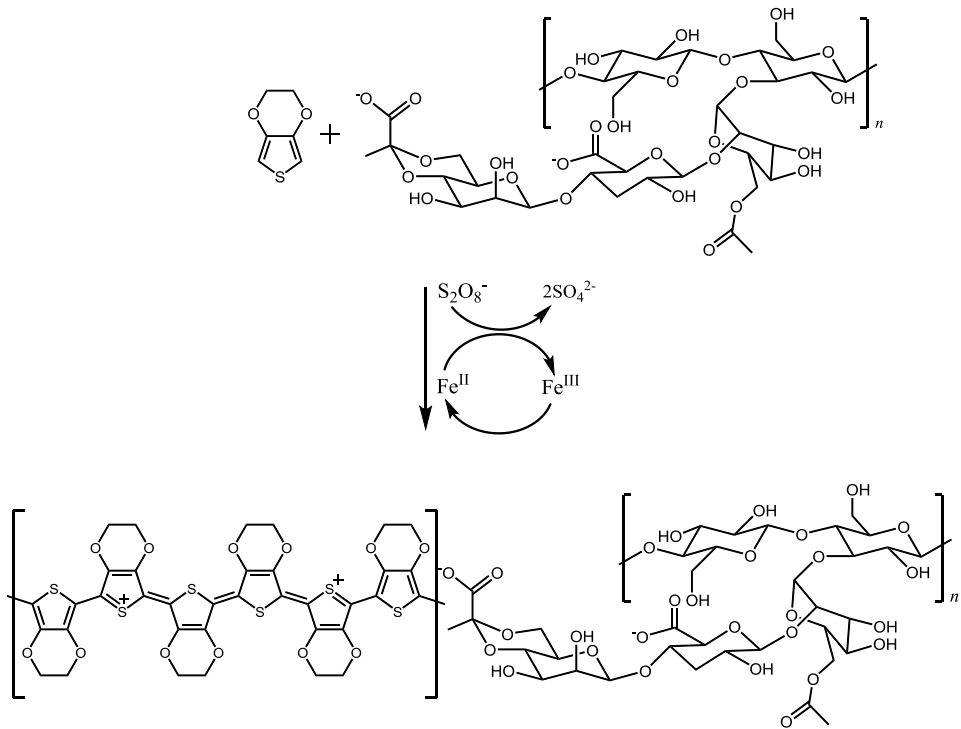


**Figure 5.1**. PEDOT:xanthan gum synthetic reaction.

EDOT monomer is polymerized in water in the presence of the polysaccharide xanthan gum by oxidative polymerization with the oxidant ammonium persulfate $((NH_4)_2S_2O_8)$ in the presence of a catalyst iron (III) sulfate $(Fe_2(SO_4)_3)$. In this way, a dispersion of PEDOT and xanthan gum is formed. In a second step, the crosslinker divinyl sulfone (DVS) is added together with a small amount of PEDOT:PSS to aid the crosslinking reaction. This formulation is mixed well and poured into a container with the desired shape to perform the free-drying step and thus obtain PEDOT scaffolds with porous structure.

In this work, divinyl sulfone is the crosslinker used to stabilize the scaffold structure and avoid its redispersion when in contact with aqueous media. The use of this crosslinker is a novelty in the production of  PEDOT scaffolds synthesized by the freeze drying method, because (3-glycidyloxypropyl)trimethoxysilane (GOPS) is generally used for the same purpose.[18,19,28]. The choice of DVS as crosslinker is due to a recent study[29] were DVS proves to be effective in creating insoluble PEDOT:PSS films fully biocompatible and it is a better support for neuroregeneration than GOPS-cross-linked material.


### 5.2.2. PEDOT:xanthan gum aqueous  dispersion characterization

The chemical oxidation polymerization method to obtain PEDOT aqueous dispersions is very versatile. It allows the synthesis of the dispersion at different PEDOT:xanthan gum ratios  (0.25:0.75, 0.33:0.67, 0.5:0.5, 0.67:0.33). The technique UV−vis-NIR absorbance spectroscopy is used to characterize them and the data is plotted in the Figure 5.2b.  In the four dispersions studied, the two characteristic PEDOT absorption bands are observed. The broad absorption band of PEDOT π−π* centered at ~800nm,[30] and a second polaron band at higher wavelengths centered at 1200 nm. These two absorption bands indicate the presence of doped PEDOT chains as cation and dication forms,[31] and they are related to the conductivity of the material confirming the conducting nature of the PEDOT chains in these PEDOT:xanthan gum dispersions. Although the absorbance of both bands is visible in the four dispersions studied, they are higher in the case PEDOT:xanthan gum (0.5:0.5). This indicates the higher presence of doped chains in this dispersion and this is the motivation to continue the study with this dispersion PEDOT:xanthan gum (0.5:0.5). When drop-casted, the dispersion forms a film which has conductivity of $10^{-2}$ S cm$^{-1}$ measured by four-point probe. Although it might seem to be a low value, it is only one order of magnitude less than pristine PEDOT:PSS conductivity.[32]
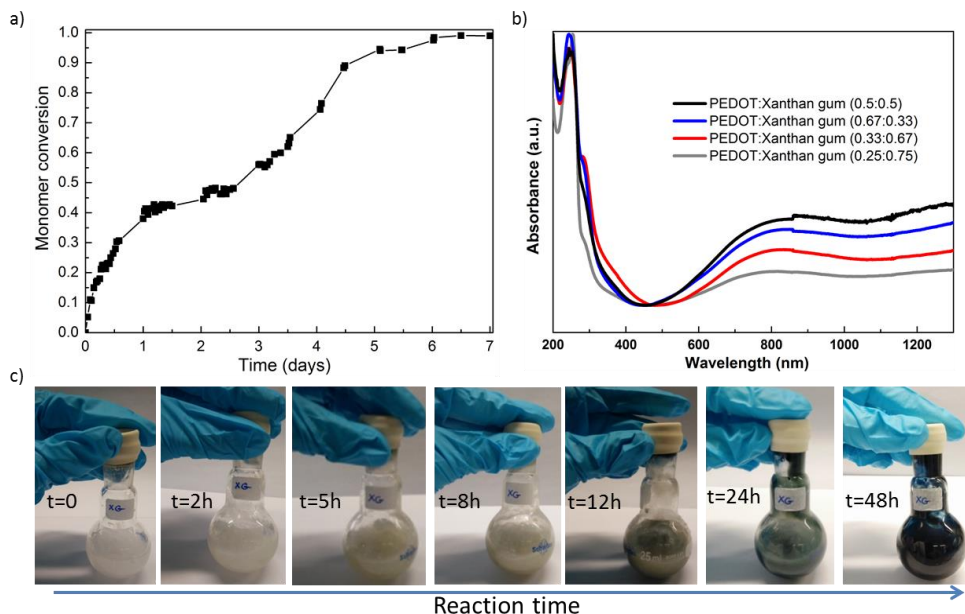
**Figure 5.2**. PEDOT:xanthan gum dispersion characterization. a) PEDOT:xanthan gum reaction kinetics, EDOT monomer conversion over reaction time, b) UV spectra of PEDOT:xanthan gum dispersions at different concentrations (0.25:0.75, 0.33:0.67, 0.5:0.5, 0.67:0.33), (c) PEDOT:xanthan gum (0.5:0.5) color change during the first 48 h reaction time.

The kinetics of this dispersion was studied by High Pressure Liquid Chromatography (HPLC) and it can be observed in Figure 5.2a. After 6 days reaction time, 99% monomer conversion is reached. The colour change during the reaction was followed and it can be found in Figure 5.2c. Initially the colour of the reactants is white given by the solution in MilliQ water of xanthan gum. As the polymerization of EDOT is taking place, the dispersion turns first more yellowish (from 2 to 8 h, 0.2 monomer conversion) to more greyish at 12-24 h (0.4 monomer conversion) to then acquire the bright blue color characteristic of

PEDOT chains which starts to be visible once we pass the 0.4 monomer conversion happening after 48 h reaction time.
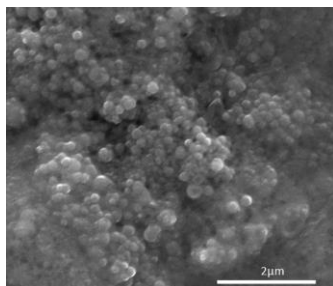


**Figure 5.3.** SEM image of PEDOT:xanthan gum (0.5:0.5) dispersion

SEM images were taken of PEDOT:xanthan gum (0.5:0.5) dispersion to study the morphology of the particles. We found once again that PEDOT:xanthan gum agglomerates in spheres as in the case of PEDOT:guar gum in the Chapter 4.

### 5.2.3. Scaffolds characterization

Porous scaffolds are formed by the freeze-drying technique according to the following schema.
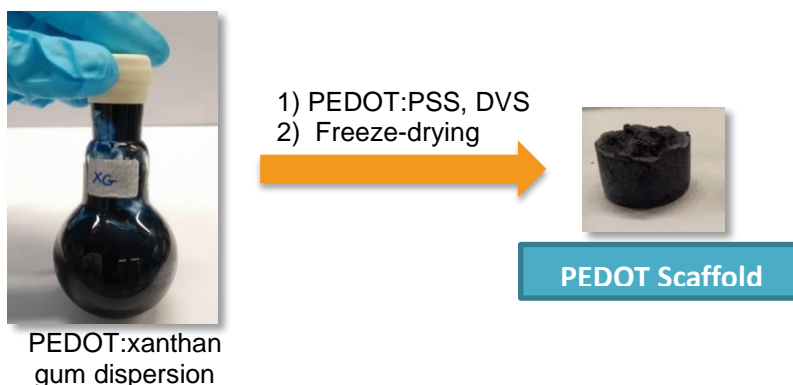


**Figure 5.4**. PEDOT scaffolds synthetic route.

In order to study the versatility and tunability of the porous structure of the scaffolds synthesized by this method, PEDOT:xanthan gum (0.5:0.5) dispersions were synthesized at 3 different solids content by varying the water content (1, 2, and 3 % wt). After the freeze-drying step, SEM images were taken of these different scaffolds (Figure 5.5). In the Figure 5.5a, the 1% wt scaffold shows a void structure based on a network of fibers. In Figure 5.5b, the 2% solids content shows pores with high polydispersity and pore size around ø 50-150 μm. In Figure 5.5c the 3% solids content scaffold shows smaller pores with less polydispersity and pore size around ø 10-30 μm. This experiment shows the tunability of the porosity of these scaffolds which is an advantage of this method. According to the type of cell that will be studied, the porosity can be tuned within the given porosity range by varying the initial solids content of the synthesized PEDOT:xanthan gum dispersion. This factor can be very practical since the optimal porosity varies according to the cell type.[33]

The highly interconnected porous structure of the scaffolds is also clearly visible in these SEM images. This represents a second advantage of this method, as the interconnection of pores facilitates mass-transport and cell migration.
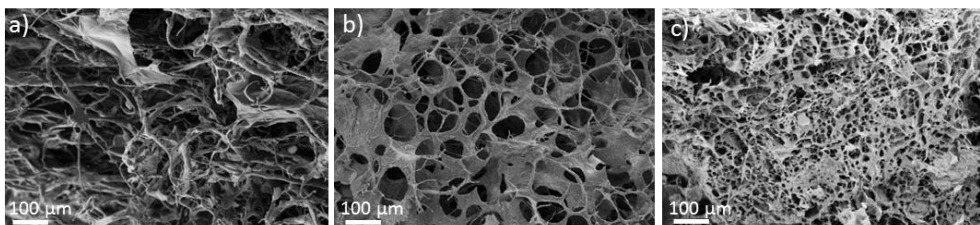


**Figure 5.5.** PEDOT:xanthan gum scaffolds SEM porosity characterization. a) PEDOT:xanthan gum (0.5:0.5) 1 % solids content b) PEDOT:xanthan gum (0.5:0.5) 2 % solids content, and (c) PEDOT: xanthan gum (0.5:0.5) 3 % solids content.

A second study was carried out by SEM to study the effect of PEDOT and xanthan gum at different ratios on the structure and mechanical properties of the scaffold. In this case, the PEDOT scaffolds with 2% solids content was chosen due to the intermediate pore size (50-150 µm ø) of the generated scaffolds, a pore size that facilitates cell nutrient percolation, cell attachment and colonization.[34,35] In Figure 5.6 we can find the SEM images of  PEDOT:xanthan gum (0.25:0.75, 0.33:0.67, 0.5:0.5, and 0.67:0.33). Among them, we observe the effects of a higher content of the PEDOT (Figure 5.6a) where we can see smaller pores and thicker walls connecting these pores. In Figure 5.6e we observe the scaffold with higher polysaccharide content.

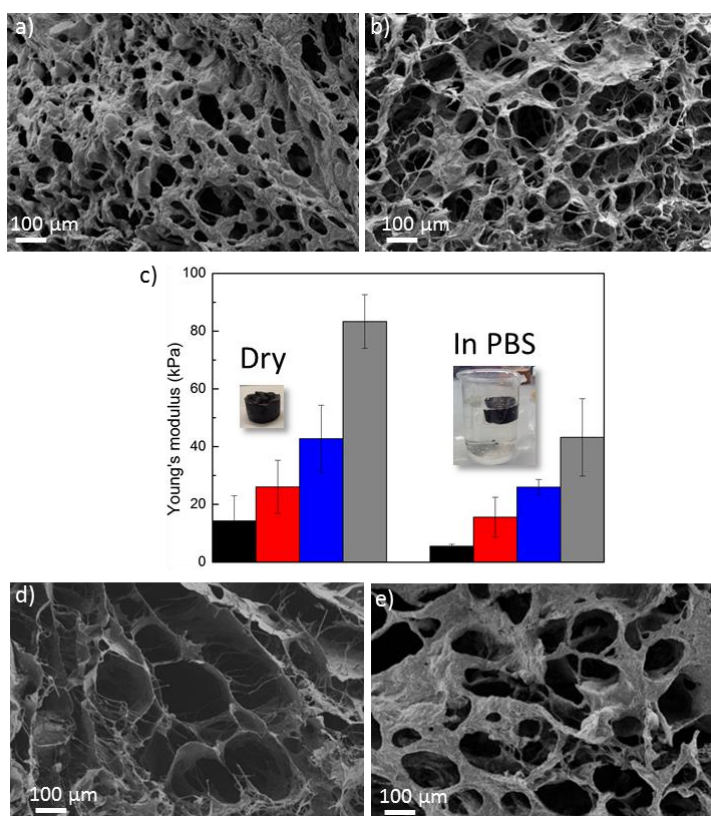**Figure 5.6**. PEDOT:xanthan gum scaffold characterization. (a) PEDOT:xanthan gum (0.67:0.33) (b) PEDOT: xanthan gum (0.5:0.5) (c) Young's modulus of PEDOT:xanthan gum scaffolds dry and in PBS solution at different ratios (0.25:0.75) black, (0.33:0.67) red, (0.5:0.5) blue, and (0.67:0.33) grey, (d) PEDOT: xanthan gum (0.33:0.67), e) PEDOT: xanthan gum (0.25:0.75).

A trend or dramatical differences among scaffolds porosity are not observed by SEM but there is a very clear trend when by compression (a strain-stress study) the Young's modulus of each scaffold is obtained (Figure 5.6c). This test was performed on dry and wet scaffolds after 8 h in PBS buffer. Xanthan gum is a soft polymer making the scaffold more flexible overall. On the contrary, PEDOT chains are stiff, and the higher the content of PEDOT in the scaffold, the higher the Young's modulus of the material which indicates a stiffer material. Once the scaffolds are in PBS solution; the structures hydrate and swell becoming softer but keeping their structure. We observe a reduction in the Young's moduli in all cases to approximately half the value in dry conditions. Similar values were reported for PEDOT:PSS scaffolds (73 kPa dry and 42 kPa in PBS).[28] The young's modulus values of these scaffolds are all <100 kPa which corresponds with the values of our body tissues where Young's modulus is in the range 1-100 kPa depending on the tissue.[36] The polysaccharide content of these scaffolds helps to reduce the mismatch of rigidity between a synthetic scaffold and the ECM. In conclusion, this is another way in which we can show that this synthetic way to obtain PEDOT scaffolds is very versatile as not only porosity but also the stiffness of the scaffolds can be varied varying the initial content of PEDOT and polysaccharide.

### 5.2.4. Scaffolds cell culturing and electrical measurements

Conducting scaffolds are platforms for cell sensing. The cell growth and colonization of the scaffold brings changes in its electrochemical impedance.[37]

This change can be used to track cell growth. In a first experiment, (Figure 5.7) the cell growth and stability of these scaffolds in cell media was assessed. For that, MDCK II eGFP cells were seeded on a sterilized scaffold PEDOT:xanthan gum (0.5:0.5) 2 % wt.  After 7 days of culture at 37°C, 5% $CO_2$, scaffolds maintained their structural integrity and we estimated roughly an ~80% cell coverage by image observation. We were able to observe good cell attachment due to the roughness of the structure and high degree of pore coverage. Thanks to the interconnection of pores within the structure, cells were able to migrate throughout almost the whole scaffold.
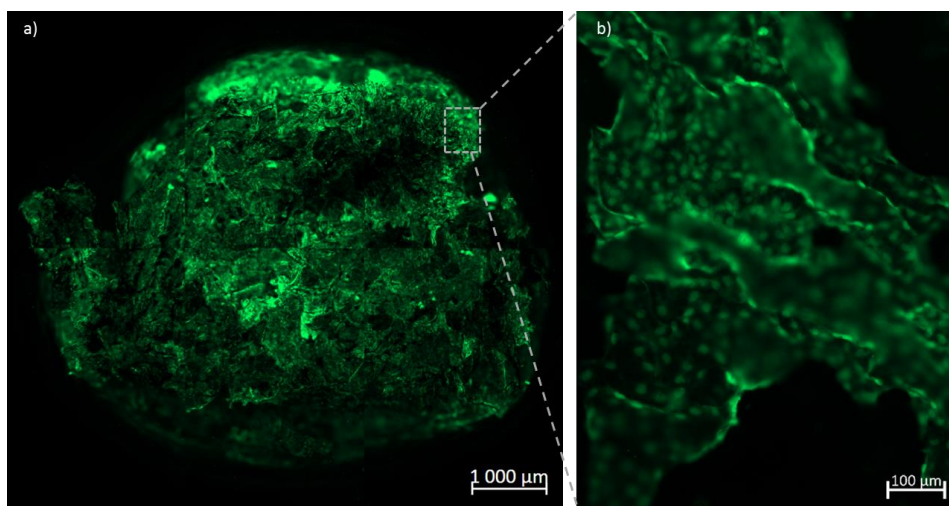


**Figure 5.7**. MDCK II eGFP cell growth on on PEDOT:xanthan gum (0.5:0.5) 2 % solids content scaffold 14 days culture, 37°C, 5% CO2. An estimation of 80% coverage. a) Confocal microscope image of the entire scaffold 14 days after cell seeding cells, b) zoomed image of the scaffold 14 days after cell seeding

Knowing that the PEDOT:xanthan gum scaffolds can efficiently facilitate cell culture, we investigated the electrical properties by means of electrochemical impedance spectroscopy (EIS) and studied their evolution during cell growth as

an in situ tool to monitor cell growth. For this experiment, MDCK II LifeAct cells were seeded on a sterilized scaffold PEDOT:xanthan gum (0.5:0.5) 2 % wt and an electrode based device was fabricated as shown in Figure 5.8c. Specifically, gold electrodes were patterned on top of glass substrates, while a PDMS "well" was placed on top in order to confine the scaffolds inside the electrode area. Figure 5.8d shows the comparative impedance spectra of the scaffolds before and after 7 days of cell growth and Figure 5.8a, b, show the cell growth in the scaffold after 7 days. Significant changes can be observed in the low frequency regime (0.1 to 100 Hz), with a dramatic increase in the impedance value of almost an order of magnitude (From $|Z|=4.5$ kΩ to $|Z_{cell}|=45$ kΩ) in the case of cells containing scaffolds. Similarly, the phase data (Figure 5.8e) displayed a shift in the phase angle maximum toward lower frequencies accompanied by an increase of $22^{o}$ (from $\varphi= 52^{o}$ to $\varphi_{cell}= 74^{o}$). Such changes indicate the presence of an additional capacitance element in the circuit which corresponds to the growth of insulating cell layers inside the scaffold. A less pronounced change can be observed for mid to high frequencies, with a slight increase in the impedance values most likely associated with the presence of cells contributing to the increase of the ohmic resistance at the working electrode-electrolyte interface. The abovementioned findings are consistent with previous EIS studies of 3D cell cultures in PEDOT based conducting scaffolds.[19]
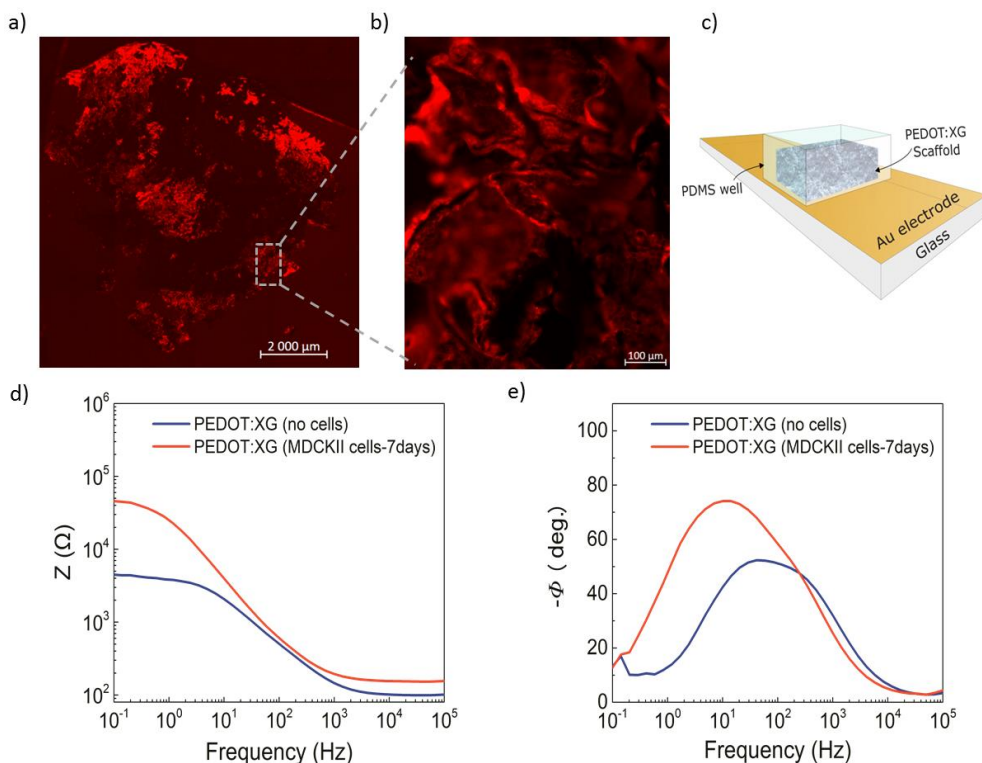
**Figure 5.8.** Cell growth on PEDOT:xanthan gum (0.5:0.5) 2 % solids content scaffold and impedance measurements. a) Confocal microscope image of the entire scaffold 7 days after cell seeding with fluorescence MDCK II LifeAct cells, b) zoomed image of the scaffold 7 days after cell seeding, c) representation of the electrode based device and scaffold on top, d) Impedance measurement of of the scaffold before cell seeding and 7 days after cell seeding, e) phase angle of the impedance of the scaffold before cell seeding and 7 days after cell seeding.

## 5.3. Conclusions

We have developed a new synthetic strategy for preparing conducting PEDOT scaffolds with the ability to host and monitor cells. By freeze drying a

113

homogeneous PEDOT:xanthan gum dispersion, elastic, soft, and flexible conducting scaffolds are obtained. Their mechanical properties and porosity can be tuned with the concentration of the dispersion and the ratio in between conducting polymer content and polysaccharide. Scaffolds pore size ranges between 10 to 150 μm and Young's moduli between 10 to 45 kPa, giving the possibility to optimize pore size and stiffness according to the target cell culture. Xanthan gum was employed in this study because it has already been used for scaffold fabrication with satisfactory results. This study is a proof of concept, other polysaccharides (or mixtures of polysaccharides) can be included in these scaffolds and via the functional groups of the polysaccharides, even protein anchoring is possible. With the same methodology but varying the polysaccharide used, a library of scaffolds can be synthesized broadening the applications towards different cell cultures.

## 5.4. Experimental section

**Dispersion synthesis:** PEDOT:xanthan gum dispersions with 1, 2 and 3 % solids content and at different PEDOT:xanthan gum ratios were synthetized by oxidative polymerization according to the following procedure. In a 25 mL round bottom flask containing 19.6 mL of MilliQ water 0.3 g, 0.27 g, 0.2 g or 0.13 g of xanthan gum (Acros) were dissolved and purged with $N_2$. Afterwards, 0.1 g, 0.13 g, 0.2 g, or 0.27 g of EDOT monomer (Acros), together with the 1.5 eq of ammonium persulfate (($NH_4$)$_2S_2O_8$, Sigma) and a catalytic amount (5 mg) of iron (III) sulfate ($Fe_2(SO_4)_3$, Sigma) were added respectively. Reaction was kept at 0 $^o$C until completion (144 h). The dispersions were purified by dialysis with MilliQ water and regenerated cellulose dialysis membrane (12-14 kD) from Spectrumlabs. Finally, dispersions containing different PEDOT:xanthan gum ratios were obtained varying the initial amount of grams (0.25:0.75, 0.33:0.67, 0.5:0.5, and 0.67:0.33).

**Scaffold synthesis:** 0.5g of PEDOT:PSS (Heraeous PH 1000) per 10 mL dispersion and 0.1 g of DVS (Acros) per 10 mL dispersion were added to each PEDOT:xanthan gum dispersion. Scaffolds were formed by freeze drying this polymeric mixture with a LyoQuest-85 apparatus from Telstar. After freeze drying, scaffolds were heated up at 50 $^{o}$C for 1 h at mild vacuum (0.5 bar) for evaporation of DVS in excess. Scaffolds were freeze dried in cylindrical polydimethylsiloxane (PDMS from Dow coning) molds of two dimensions: 8 mm diameter and 8 mm height for mechanical testing and 3 mm diameter and 2 mm height for impedance measurements and cell culture.

**Dispersion characterization:** UV-Vis-NIR measurements were taken with a UV/Vis/NIR spectrometer PerkinElmer Lambda 950. Employing quartz cuvettes, a 2% v/v solution in MilliQ water of each PEDOT:xanthan gum dispersion was analyzed. Spectra were normalized. The kinetics of the polymerization reaction of PEDOT:xanthan gum (0.5:0.5) 2 %wt. were followed during 7 days by High Pressure Liquid Chromatography (HPLC) using a Hewlett-Packard HPLC series 1100 equipment with a Lichrosphere 100 CN (5 µm) column supplied by Agilent Technologies. The eluent is water:acetonitrile 1:1 0.7 mL min$^{-1}$ at room temperature (r.t.). A reactor sample was taken every 30 min according to the following, 10 µL of reactor sample mixture were put in 5 mL of ACN containing 1 µL of benzyl alcohol as internal standard. 20 µL of this solution are injected into the HPLC. EDOT concentration is calculated by plotting the area of each EDOT peak (5.3 min retention time) in a calibration line. The conductivity of the dispersions was calculated on a four-point probe Veeco/Miller FPP5000 using layer resistivity function.

**Scaffold characterization:** Scaffolds were characterized by SEM and mechanically using and Instron. SEM images were taken with a Zeiss Sigma FESEM equipment. With an Instron apparatus, the compressive modulus of the

dry and hydrated scaffolds (submerged 2 h in standard Dulbecco's PBS solution) were calculated. The Instron had a load cell of 1kN and the compression speed was set at 1 mm min$^{-1.}$ Young's modulus values were calculated from the slope of the linear part of the strain stress curve.

**Scaffold cell culture:** MDCK II cells were kindly provided by Frederic Luton (IPMC, Valbonne). MDCK II LifeAct were prepared for this study in the same manner according to the manufacturer's guidelines (Ibidi, GmbH) and as described previously using pCMVLifeAct-TagRFP.[32] Cells were cultured in DMEM low glucose supplemented with 10% fetal bovine serum, $2*10^{-3}$ M glutamine, 50 U mL$^{-1}$ penicillin, 50 µg mL$^{-1}$ streptomycin. To keep pressure on the fluorescent actin expression, 500 µg mL$^{-1}$ of Geneticin were added to the media. MDCK II eGFP (gift from Frederic Luton) was cultured in the same media as MDCK II LifeAct cells.

Prior any experiment, scaffolds were deep into ethanol 70 % during 1 h for sterility then washed three times 1 h each with sterile water to ensure that all the ethanol was removed. Scaffolds were kept in cell media for 1 h before being dried using sterile absorbers. Scaffolds were deep into 2 mL of $6*10^6$ MDCK II cells in suspension allowing cells penetration by capillarity. After cell seeding, the scaffolds were incubated overnight at 37 °C to allow the cells to adhere, after which 5 mL of fresh media was added to the well and half-changed every two days until scaffolds were ready.

**Fluorescent images:** MDCK II cells were fixed in 4% paraformaldehyde for 10 min at room temperature. The scaffolds were washed extensively with PBS and water before being monitored under epifluorescence/confocal microscope (AxioObserver Z1 LSM 800 ZEISS).

**Scaffold electrical characterization:** scaffolds were characterized by electrochemical impedance spectroscopy (EIS) using an Autolab potentiostat in the frequency range $10^{-1}$-$10^{5}$ Hz. A commercial Ag/AgCl electrode from Metrohm, and a platinum mesh were employed as reference and counter electrode respectively. The cell culture medium was the electrolyte solution.

## 5.5 References

1   J. L. Drury and D. J. Mooney, *Biomaterials*, 2003, **24**, 4337–4351.
2   B. P. Chan and K. W. Leong, *Eur. Spine J.*, 2008, **17**, 467–479.
3   Q. L. Loh and C. Choong, *Tissue Eng. Part B Rev.*, 2013, **19**, 485–502.
4   B. J. Lawrence and S. V. Madihally, *Cell Adhes. Migr.*, 2008, **2**, 9.
5   V. B. Bueno, S. H. Takahashi, L. H. Catalani, S. I. C. de Torresi and D. F. S. Petri, *Mater. Sci. Eng. C*, 2015, **52**, 121–128.
6   L. Ghasemi-Mobarakeh, M. P. Prabhakaran, M. Morshed, M. H. Nasr-Esfahani, H. Baharvand, S. Kiani, S. S. Al-Deyab and S. Ramakrishna, *J. Tissue Eng. Regen. Med.*, 2011, **5**, e17–e35.
7   J. C.-C. Wu, S. Ray, M. Gizdavic-Nikolaidis, B. Uy, S. Swift, J. Jin and R. P. Cooney, *Synth. Met.*, 2014, **198**, 41–50.
8   R. Sarvari, M. Akbari-Alanjaraghi, B. Massoumi, Y. Beygi-Khosrowshahi and S. Agbolaghi, *New J Chem*, 2017, **41**, 6371–6384.
9   M. Marzocchi, I. Gualandi, M. Calienni, I. Zironi, E. Scavetta, G. Castellani and B. Fraboni, *ACS Appl. Mater. Interfaces*, 2015, **7**, 17993–18003.
10  A. Lari, T. Sun and N. Sultana, *J. Nanomater.*, 2016, **2016**, 1–12.
11  Q. Wang, *Smart Materials for Tissue Engineering: Applications*, Royal Society of Chemistry, 2017.
12  R. Balint, N. J. Cassidy and S. H. Cartmell, *Acta Biomater.*, 2014, **10**, 2341–2353.
13  S. Wang, S. Guan, J. Xu, W. Li, D. Ge, C. Sun, T. Liu and X. Ma, *Biomater Sci*, 2017, **5**, 2024–2034.
14  S. Wang, C. Sun, S. Guan, W. Li, J. Xu, D. Ge, M. Zhuang, T. Liu and X. Ma, *J Mater Chem B*, 2017, **5**, 4774–4788.
15  M. H. Bolin, K. Svennersten, X. Wang, I. S. Chronakis, A. Richter-Dahlfors, E. W. H. Jager and M. Berggren, *Sens. Actuators B Chem.*, 2009, **142**, 451–456.
16  N. A. Zubair, N. A. Rahman, H. N. Lim and Y. Sulaiman, *Nanoscale Res. Lett.*, , DOI:10.1186/s11671-017-1888-0.

17 S. M. Richardson-Burns, J. L. Hendricks, B. Foster, L. K. Povlich, D.-H. Kim and D. C. Martin, *Biomaterials*, 2007, **28**, 1539–1552.

18 A. M.-D. Wan, S. Inal, T. Williams, K. Wang, P. Leleux, L. Estevez, E. P. Giannelis, C. Fischbach, G. G. Malliaras and D. Gourdon, *J Mater Chem B*, 2015, **3**, 5040–5048.

19 S. Inal, A. Hama, M. Ferro, C. Pitsalidis, J. Oziat, D. Iandolo, A.-M. Pappa, M. Hadida, M. Huerta, D. Marchat, P. Mailley and R. M. Owens, *Adv. Biosyst.*, 2017, **1**, 1700052.

20 Z. Ma, Z. Mao and C. Gao, *Colloids Surf. B Biointerfaces*, 2007, **60**, 137–157.

21 J. M. Aamodt and D. W. Grainger, *Biomaterials*, 2016, **86**, 68–82.

22 S. Hinderer, S. L. Layland and K. Schenke-Layland, *Adv. Drug Deliv. Rev.*, 2016, **97**, 260–269.

23 D. F. S. Petri, *J. Appl. Polym. Sci.*, 2015, **132**, n/a-n/a.

24 A. Kumar, K. M. Rao and S. S. Han, *Carbohydr. Polym.*, 2018, **180**, 128–144.

25 V. B. Bueno, R. Bentini, L. H. Catalani, L. R. S. Barbosa and D. F. S. Petri, *Mater. Sci. Eng. C*, 2014, **37**, 195–203.

26 D. Mantione, I. del Agua, W. Schaafsma, J. Diez-Garcia, B. Castro, H. Sardon and D. Mecerreyes, *Macromol. Biosci.*, 2016, **16**, 1227–1238.

27 I. del Agua, D. Mantione, N. Casado, A. Sanchez-Sanchez, G. G. Malliaras and D. Mecerreyes, *ACS Macro Lett.*, 2017, **6**, 473–478.

28 A. G. Guex, J. L. Puetzer, A. Armgarth, E. Littmann, E. Stavrinidou, E. P. Giannelis, G. G. Malliaras and M. M. Stevens, *Acta Biomater.*, 2017, **62**, 91–101.

29 D. Mantione, I. del Agua, W. Schaafsma, M. ElMahmoudy, I. Uguz, A. Sanchez-Sanchez, H. Sardon, B. Castro, G. G. Malliaras and D. Mecerreyes, *ACS Appl. Mater. Interfaces*, 2017, **9**, 18254–18262.

30 N. Massonnet, A. Carella, O. Jaudouin, P. Rannou, G. Laval, C. Celle and J.-P. Simonato, *J Mater Chem C*, 2014, **2**, 1278–1283.

31 I. Cruz-Cruz, M. Reyes-Reyes, I. A. Rosales-Gallegos, A. Y. Gorbatchev, J. M. Flores-Camacho and R. López-Sandoval, *J. Phys. Chem. C*, 2015, **119**, 19305–19311.

32 Z. Yu, Y. Xia, D. Du and J. Ouyang, *ACS Appl. Mater. Interfaces*, 2016, **8**, 11629–11638.

33 F. J. O'Brien, *Mater. Today*, 2011, **14**, 88–95.

34 C. M. Murphy, M. G. Haugh and F. J. O'Brien, *Biomaterials*, 2010, **31**, 461–466.

35 C. M. Murphy, F. J. O'Brien, D. G. Little and A. Schindeler, *Eur. Cell. Mater.*, 2013, **26**, 120–132.

36 A. J. Engler, S. Sen, H. L. Sweeney and D. E. Discher, *Cell*, 2006, **126**, 677–689.

37 A. Karimullah, D. R.S. Cumming, M. Riehle and N. Gadegaard, *Sens. Actuators B Chem.*, 2013, **176**, 667–674.

38 M. Ramuz, A. Hama, J. Rivnay, P. Leleux and R. M. Owens, *J Mater Chem B*, 2015, **3**, 5971–5977.

# Chapter 6.
# Conclusions

# Chapter 6. Conclusions

The emerging area of bioelectronics needs a new generation of organic materials with soft mechanical properties and superior ionic/electrical conductivity in order to interface between biology and electronics. This doctoral thesis aimed at synthetizing new polymeric materials with mixed conduction that would result in improvements in certain bioelectronics applications. As a result of this work, new and innovative materials such as cross-linked PEDOT:PSS free standing films and textiles, highly conductive hydrogels, PEDOT iongels, PEDOT:polysaccharide dispersions and porous scaffolds have been synthetized and successfully tested in diverse applications as summarized next.

Conducting polymer electrodes based on poly(3,4-ethylenedioxythiophene) poly(styrene sulfonate) (PEDOT:PSS) present many advantages for biological signal recording over traditional metal electrodes, and they are being steadily evaluated in health monitoring applications. A main requirement for wearable electrodes based on PEDOT:PSS is that selected additives, such as cross-linking agents and adhesion promoters, allow to avoid the redispersion of the polymer or its post-process delamination. For these reasons, in the second chapter of this work, we have presented a novel approach in fabrication of water stable conducting free-standing films and textile electrodes by using divinyl

sulfone (DVS) crosslinker. The stability of the conducting PEDOT:PSS was achieved without reducing its conductivity or stiffening its mechanical properties. PEDOT:PSS:DVS formulation was easily applied to any substrates and used as low surface resistance electrodes. The electrochemical and stretchable properties of these electrodes have been tested in air and in an aqueous environment and they have been successfully employed in recordings of electrophysiological signals such as ECG and EMG. These new electrodes showed great potential to make wearable devices for healthcare applications. Even this novel PEDOT:PSS:DVS composition could be also highly attractive for the development of washable electroactive textiles.

In the third chapter of this work, we presented a new polyethylene glycol hydrogel with very high ionic conductivity and properties which make it ideal for different bioelectronics devices based on PEDOT:PSS. This universal hydrogel was synthesized using cost-effective photopolymerization of poly(ethylene glycol)-dimethacrylate and sodium acrylate. Due to the high water content (83% w/w) and the presence of free small sodium cations, the hydrogel showed high ionic conductivity values at room temperature ($10^{-2}$ S cm$^{-1}$). Due to the soft nature, conformability and adhesive properties of the hydrogel, it was applied on cutaneous electrodes, being successfully employed for electrocardiography recordings. Furthermore, because of its solid nature and the fact that contains highly mobile sodium cations, the hydrogel was also tested as a solid electrolyte in Organic Electrochemical Transistors (OECTs). The OECTs showed excellent transconductance values, fast switching ON and OFF in less than 100 ms and very high stability under high duty cycling tests with only a 3% drop in measured current after 6 h operation time. Overall achieving similar OECT performances than with liquid electrolytes while the devices were protected with a soft-solid layer.

Conducting polymer hydrogels are attracting much interest in biomedical and energy-storage devices due to their unique electrochemical properties including their ability to conduct both electrons and ions. They suffer, however, from poor environmental stability due to water evaporation which causes the loss of mechanical and ion conduction properties. For this reason, in chapter 4 we have shown for the first time an environmentally stable conducting polymer gel where the continuous phase was a non-volatile ionic liquid. The novel conducting iongel was formed by a natural polysaccharide (guar gum), a conductive polymer poly(3,4-ethylenedioxythiophene) (PEDOT) and an ionic liquid (IL) 1-butyl-3-methylimidazolium chloride (BMIMCl). Firstly, an aqueous dispersion of PEDOT:guar gum was synthesized by an oxidative polymerization process of EDOT in the presence of the polysaccharide as stabilizer. The resulting PEDOT:guar gum was isolated as a powder by removing the water via freeze drying process. In the final step, conducting iongels were prepared by the PEDOT:guar gum mixed with the ionic liquid by a heating-cooling process. The rheological properties showed that the material exhibits gel type behavior between 20 and 80 ºC. Interestingly, the conducting polymer iongel presented redox properties as well as high ionic conductivities ($10^{-2}$ S cm$^{-1}$). This material had a unique combination of properties by mixing the electronic conductivity of PEDOT, the ionic conductivity and negligible vapor pressure of the ionic liquid and the support and flexibility given by guar gum.

Last, in the 5th chapter of this work, an original synthetic route for poly(3,4-ethylenedioxythiophene) (PEDOT) porous scaffolds containing polysaccharides was developed and successfully employed for cell monitoring *in vitro*. Conducting porous scaffolds in general, present an advance in cell studies as excellent supports for cell growth combined with electrical cell stimuli. Poly(3,4-ethylenedioxythiophene) xanthan gum (PEDOT:XG) scaffolds were synthetized in this work by the freeze-drying method for cell culture and sensing. We have

shown novel scaffolds which combine the conductivity of PEDOT, and the mechanical support and biocompatibity properties provided by a polysaccharide, xanthan gum. The key difference of these scaffolds among available PEDOT scaffolds was the synthetic strategy followed that allowed to include a homogeneously distributed polysaccharide in the structure. The polymerization of EDOT was carried out in the presence of polysaccharides, which provide intimate contact among the polymers, a key advantage of these systems. The porosity of the scaffolds and mechanical properties are tuned by the formulation of the initial PEDOT:polysaccharide dispersion. Mechanical and electrical properties were assessed by mechanical testing and impedance spectroscopy, respectively. These scaffolds are relatively soft with Young's modulus values in between 15 and 85 kPa when they are dry and in between 5 and 40 KPa when hydrated. They have pore sizes in between ø 10-150 µm. The scaffolds successfully support 3D cell cultures of MDCK II eGFP and MDCK II LifeAct epithelial cells, observing good cell attachment with very high degree of pore coverage (50-80 %) after 7 days cell culture.

All in all, after this 3-years long work facing difficulties and challenges; and enjoying successes, four new materials have been born with unique and improved properties. Some applications have been successfully tested and we believe that many more will come due to the potential of these materials to be employed in bioelectronics. These materials could be employed as such or with small modifications in order to suit the requirements that may arise for certain applications.

# Resumen

El campo de los polímeros conductores se encuentra en auge debido a sus peculiares características que no corresponden con las propiedades que comúnmente se esperan de los polímeros. Aunque los polímeros por naturaleza son no conductores, este tipo de polímeros lo son debido a sus cadenas con dobles enlaces conjugados.
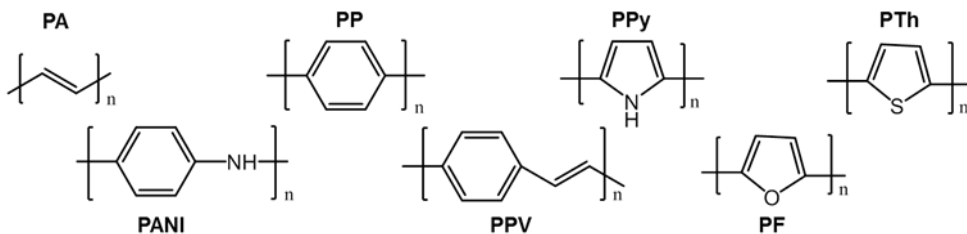


**Figura R.1.** Estructura de diferentes polímeros conductores.

En el campo emergente de la bioelectrónica existe la necesidad de crear una nueva generación de materiales orgánicos con propiedades mecánicas blandas y mejor conductividad iónica y electrónica. Estos nuevos materiales han de ser la interface entre la electrónica y la biología. Los dispositivos electrónicos son capaces de grabar señales y emitir estímulos a nuestros tejidos corporales cuya información se transmite principalmente con flujos de iones aunque también con

señales eléctricas. Entre la electrónica y nuestros tejidos existe una gran diferencia en cuanto a las propiedades físicas que muchas veces limitan las posibilidades del campo. La creación de nuevos materiales puede ayudar a conseguir que los dispositivos electrónicos encuentren nuevas aplicaciones y que sean capaces de grabar y estimular señales más complejas de adquirir dentro de nuestro organismo como son las señales eléctricas de las neuronas en nuestro cerebro. Para ello, estos nuevos materiales han de ser blandos, con conductividad electrónica e iónica, biocompatibles y capaces de interaccionar con los tejidos de forma que estimule su crecimiento de manera muy similar a la natural.

## 1. El polímero conductor más común, PEDOT:PSS

Polímeros conductores hay muchos pero el que tiene especial importancia el Poli(3,4-etilendioxitiofeno) (PEDOT), comúnmente dopado con PSS: Poli(3,4-etilendioxitiofeno)-poli(estireno sulfonato) (PEDOT:PSS).
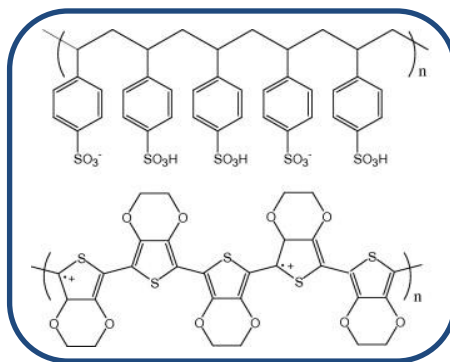


**Figura R.2.** Estructura de PEDOT:PSS.

El éxito de esta combinación de polímeros reside en su disponibilidad como dispersión acuosa que permite que sea aplicada y procesada usando numerosas técnicas que se usan tanto en el laboratorio a pequeña escala como en la

industria a escala mucho mayor. Algunos ejemplos de estas técnicas son: spin-coating, drop-casting, inyección de tinta, doctor blade, etc. No solo eso, también debido a su gran conductividad tanto electrónica como iónica, su biocompatibilidad y sus otras características como la estabilidad, el electrocromismo y la transparencia, hacen que PEDOT sea el polímero conductor más usado en la industria con numerosísimas aplicaciones en energía, como en paneles solares y baterías pero también como sensores de gas y en el campo de la ingeniería biomédica sirven como electrodos, bioactuadores, suministro de medicinas, como interface neuronal y como tejidos artificiales.

Las cadenas de PEDOT por si solas no son conductoras. Necesitan ser tratadas para que lo sean. Este tratamiento se conoce como dopado y se hace con oxidantes que crean huecos electrón en la estructura creado cargas deslocalizadas. Las cargas crean deformaciones en la red cristalina del polímero y la carga y la deformación juntas reciben el nombre de polarón. Cuando los polarones se mueven a través de las cadenas, hay conducción electrónica. La función del dopante es introducir cargas positivas en las cadenas de PEDOT y a su vez contrarrestarlas con sus cargas negativas. PSS es el dopante más común de PEDOT pero no el único. Hay numerosas átomos, moléculas, e incluso polímeros que pueden doparlo. Dopantes de PEDOT pueden ser iones monoatómicos como cloruros, poliatómicos como sulfato y también aniones orgánicos como tosilato o el polímero PSS. El dopante elegido afecta a la oxidación de las cadenas de PEDOT y por lo tanto a su nivel de dopado afectando también a sus propiedades electrónicas y a las propiedades del complejo de PEDOT en su conjunto.

## 2. PEDOT dopado con biopolímeros

Biopolímeros como proteínas y polisacáridos pueden ejercer el papel de dopantes y estabilizantes de las cadenas de PEDOT en dispersión debido a sus

diversos grupos funcionales. Una estrategia para mejorar la biocompatibilidad y reducir la citotoxicidad de los polímeros conductores como PEDOT es el uso de biopolímeros como dopantes. Incorporar biopolímeros puede expandir el uso de PEDOT para ciertas aplicaciones en biología. Aunque PEDOT:PSS es un material apropiado para el cultivo de células, el objetivo es proporcionar un material que estimule y mejore las condiciones para el crecimiento celular. Inganäs et al. fueron los primeros que sintetizaron PEDOT con biopolímeros. Usaron la técnica de electropolimerización del monómero EDOT en presencia de diversas biopolímeros como heparina, ácido hialurónico, goma guar, celulosa, goma xantana, y pectina. Demostrando su no toxicidad y usándolos como interface para electrodos para registros de células. Estos trabajos han servido de inspiración para la síntesis de dispersiones en agua de PEDOT:biopolímeros por polimerización química. Método más apropiado para su síntesis a mayor escala y para poderlo procesar y depositar usando las técnicas que se usan en la industria.

## 2. El trabajo de la tesis doctoral

Esta tesis doctoral tiene como objetivo la síntesis de nuevos materiales poliméricos con conductividad iónica y electrónica que supongan una mejora en ciertas aplicaciones bioelectrónicas. Como resultado de este trabajo, nuevos e innovadores materiales han sido sintetizados y caracterizados y algunas aplicaciones han sido estudiadas con resultados muy satisfactorios.
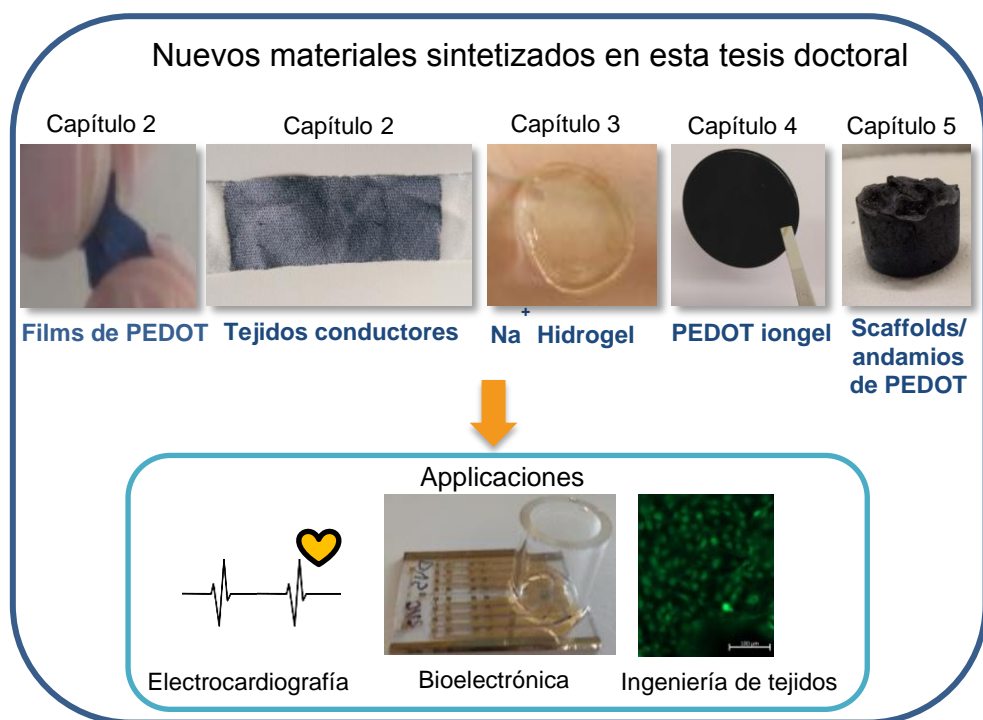
**Figura R.3**. Trabajo de tesis.

El trabajo realizado en esta tesis doctoral se ha centrado en tres aspectos:

**1.** El estudio de un nuevo reticulante de PEDOT:PSS llamado divinilsulfona (DVS) para la fabricación de electrodos de PEDOT:PSS como films y también sobre textil. De esta manera hemos creado tejidos inteligentes capaces de medir constantes vitales como la actividad del corazón (electrocardiografía, ECG) y la de los músculos del brazo (electromiografía, EMG) al estar en contacto con la piel. Al añadir DVS al PEDOT:PSS se consigue estabilizar el material sin reducir su conductividad y sin endurecerlo. Incluyendo DVS en PEDOT:PSS, se forma un film muy conductor y elástico de manera muy sencilla que se adapta a la piel y se puede usar como electrodo para ECG. Esta misma formulación se puede

depositar sobre fibras de poliéster. De esta manera se consiguen electrodos textiles de PEDOT con mejores propiedades a los ya existentes. Estos son más conductores y preservan mejor la conductividad al ser estirados.

**2.** La mejora de electrodos de PEDOT para electrofisiología con la síntesis de un nuevo hidrogel con capacidad de conducción iónica, comportamiento de sólido y propiedades adhesivas que hacen más practico su uso. El hidrogel se sintetiza por fotopolimerización de polietilenglicol dimetacrilato y acrilato de sodio. Este hidrogel hace de interface entre los electrodos de PEDOT:PSS y la piel. Así se consigue mejorar los registros de ECG al reducir la impedancia del contacto entre el electrodo y la piel. Además, con estos mismos hidrogeles de polietileglicol (PEG) que contienen iones de sodio y gran capacidad de retención de agua, hemos sido capaces de operar transistores tipo OECT con muy buenos resultados. El hidrogel usado como electrolito gel es capaz de dopar y de-dopar un film de PEDOT:PSS a gran velocidad de una manera reversible gracias a su gran conducción iónica.

**3.** La fabricación de nuevos materiales de PEDOT partiendo de la síntesis de dispersiones en las que PEDOT está estabilizado con polisacáridos como la goma xantana y la goma guar en vez del con PSS. Partiendo de estas dispersiones que han sido realizadas en este trabajo por primera vez, hemos sido capaces de crear 2 materiales. Los geles iónicos de PEDOT, que son únicos ya que nunca antes se había fabricado un gel iónico que a su vez contuviese PEDOT. La fabricación de este material consiste en dos pasos. Primero el agua se retira por liofilización y el sólido restante se disuelve el líquido iónico a >80$^{o}$C. Al enfriarse, la mezcla gelifica formándose el gel iónico de PEDOT. Este material presenta propiedades redox y una gran conductividad iónica ($10^{-2}$ S cm$^{-1}$) gracias a que contiene el líquido iónico 1-butyl-3-methylimidazolium chloride (BMIMCl) en su estructura. El estudio reológico de

130

este material muestra su comportamiento de sólido entre 20 y 80 $^o$C. Este material presenta propiedades únicas que surgen de la combinación de materiales del que está hecho. Presenta conductividad electrónica dada por el PEDOT, conductividad iónica por el líquido iónico y la elasticidad impartida por el polisacárido goma guar. En general, este material supera a los hidrogeles de PEDOT que ya existen ya que no se secan. Estos materiales son más estables y no pierden ni sus propiedades mecánicas ni su conductividad.

El segundo material que se ha fabricado a partir de la dispersión de PEDOT:polisacárido son los andamios porosos de PEDOT que sirven como soporte para el cultivo de células *in vitro*. La técnica usada es la liofilización, que permite quitar el agua creando una estructura porosa. Gracias al contenido de polisacárido y a sus poros interconectados, las células presentan una especial afinidad por estos andamios. Se ha demostrado que tanto la porosidad como las propiedades mecánicas de estos materiales se pueden modificar muy fácilmente dependiendo de la aplicación para la que se los quiera usar. Variando el contenido de PEDOT y de polisacárido los poros pueden tener mayor o menor diámetro y el andamio en su conjunto ser más blando o más duro.

# List of acronyms

| | |
|---|---|
| **4PP** | Four point probe |
| **ACN** | Acetonitrile |
| **AMIMCI** | 1-allyl-3-methylimidazolium |
| **BMIMCI** | 1-Butyl-3-methylimidazolium chloride |
| **CE** | Counter electrode |
| **CP** | Conducting polymer |
| **CV** | Cyclic voltammetry |
| **DBSA** | Dodecylbenzenesulfonic acid |
| **DMSO** | Dimethyl sulfoxide |
| **DNA** | Deoxyribonucleic acid |
| **DVS** | Divinyl sulfone |
| **ECG** | Electrocardiography |
| **EDOT** | 3,4-ethylenedioxythiophene |
| **EEC** | Electroencephalography |
| **EG** | Ethylene glycol |

| | |
|---|---|
| **EMG** | Electromyography |
| **EMIMMP** | 1-ethyl-3-methylimidazolium methylphosphonate |
| **G'** | Elastic modulus |
| **G''** | Viscous modulus |
| **GAG** | Glycosaminoglycan |
| **GOPS** | (3-Glycidyloxypropyl)trimethoxysilane |
| **HPLC** | High-pressure liquid chromatography |
| **IL** | Ionic liquid |
| **L-929** | Mouse fibroblast cell line |
| **LiTFSi** | Lithium bis(trifluoromethanesulfonyl)imide |
| **MDCK** | Madin Darby Canine Kidney cell line |
| **MeTHF** | 2-Methyltetrahydrofuran |
| **NMR** | Nuclear magnetic resonance |
| **OECT** | Organic electrochemical transistor |
| **OFETs** | Organic field-effect transistor |
| **OEIP** | Organic electronic ion pump |
| **PA** | Polyacetylene |
| **PANI** | Polyaniline |
| **PBS** | Phosphate buffer saline |
| **PC12** | Cell line derived from a pheochromocytoma of the rat adrenal medulla |
| **PDMS** | Polydimethylsiloxane |

| | |
|---|---|
| **PEDOT:PSS** | Poly(3,4-ethylenedioxythiophene):poly(styrenesulfonate) |
| **PEG** | Polyethylene glycol |
| **PEO** | Poly(ethylene oxide) |
| **PF** | Polyfuran |
| **PPy** | Polypyrrole |
| **PPV** | Poly(p-phenylene-vinylene) |
| **PTh** | Polythiophene |
| **PVA** | Poly(vinyl alcohol) |
| **RE** | Reference electrode |
| **RT** | Room temperature |
| **SEM** | Scanning electron microscope |
| **TEM** | Transmission electron microscope |
| **THF** | Tetrahydrofuran |
| **UV-Vis** | Ultraviolet–visible |
| **VPP** | Vapor phase polimerization |
| **WE** | Working electrode |

# Collaboration and funding

This PhD thesis work has been carried out in between the POLYMAT labs in the University of the Basque Country in San Sebastian, Spain under the supervision of Prof. David Mecerreyes and Dr. Ana Sanchez-Sanchez and the BEL lab at the Ecole des Mines de Saint Etienne in Gardanne, France under the supervision of Prof. George G. Malliaras.

# Curriculum Vitae

Isabel del Agua Lopez

idelagualopez@gmail.com
isabel.delagua@ehu.es

## Education

2014-January 2018 **PhD student** in Applied chemistry and polymeric materials, University of the Basque Country, San Sebastian (Spain). *Conducting polymer materials for bioelectronics applications.*

> Secondment at the Bioelectronics group, Ecole des Mines de St. Etienne, supervisor: George G. Malliaras, Gardanne, (France) from April 2016 to September 2017

2011-2013 **MSc in Environmental Technology and Engineering.** UNESCO-IHE Delft (The Netherlands), ICT-Prague (Czech Republic), Ghent University (Belgium)

> MSc thesis: Study of pumpkin processing wastewater by anaerobic digestion. Department of Biological and Environmental Engineering at Cornell University (US) (7 months)

2006-2011 **BSc in Chemistry** (Licenciatura de Quimicas), University of Valladolid (Spain). Final two academic years (2009-2011) as part of the Erasmus programme at Ghent University (Belgium)

## Experience

July-August 2012 **Internship** at the company Kompetenzzentrum Wasser Berlin (Germany).

## Languages and skills

Spanish (native), English (C2), Dutch (B2), French (A1)

Holder of a category B driver license

Mastery of Microsoft Office programs (Word, Excel, PowerPoint)

Knowledge of Origin and MATLAB

# Courses and schools

| | |
|---|---|
| 2017 | Polymers for bioelectronics applications and soft skills (UPV/EHU, Spain) |
| 2016 | Ionic Liquids and Polymers, Lyon (France) |
| 2015 | Bio-compatibility of neural systems on organic materials and biopolymer in vitro and in vivo and Soft Skills training (UPV/EHU, Spain) |
| 2015 | Spectroscopy tools and Transparency in Animal Research (IIT, Milan, Italy) |
| 2014 | Optogenetics and Neural Interfaces (IIT, Geneva, Italy) |
| 2014 | Emulsion Polymerization Processes (UPV/EHU, Spain) |
| 2013 | Advance Course on Nanotechnology (Gent University, Belgium) |
| 2012 | Nutrient Recycling in Agricultural Systems (Gent University, Belgium) |

# Awards, Grants, and Honors

| | |
|---|---|
| 2017 | Best oral presentation (E-MRS), Strasbourg (France) |
| 2016 | Doctoral Grant, EU (Marie Curie Fellow, Orgbio Project, ITN, FP7) |
| 2014 | Doctoral Grant, EU (Marie Curie Fellow, OLIMPIA Project, ITN, FP7) |
| 2011 | MSc graduated with Greatest Distinction |

# Publications

1. Ana Sanchez-Sanchez, **Isabel del Agua,** George G. Malliaras, David Mecerreyes. Book chapter "Smart Polymers and Their Applications". Editorial Elsevier (Submitted).

2. **Isabel del Agua,** Vincenzo F. Curto, Gerwin Dijk, Magali Ferro, Simone Fabiano, David Mecerreyes, George G. Malliaras. A Comparison Study of DVS and GOPS as PEDOT:PSS Crosslinkers (In preparation).

3. **Isabel del Agua,** Sara Marina**,** Ana Sanchez-Sanchez, David Mecerreyes Polímeros Conductores y su Aplicación en Bioelectrónica. (In preparation for Plásticos modernos)

4. **Isabel del Agua,** Daniele Mantione, Usein Ismailov, Ana Sanchez-Sanchez, Nora Aramburu, George G. Malliaras, David Mecerreyes and Esma Ismailova. DVS-crosslinked PEDOT:PSS Free-standing and Textile Electrodes Towards Wearable Health Monitoring DVS (Submitted to Adv. Materials Technologies).

5. **Isabel del Agua,** Luca Porcarelli, Vincenzo F. Curto, Ana Sanchez-Sanchez, Esma Ismailova, David Mecerreyes, and G. G. Malliaras. A $Na^+$ hydrogel for applications in organic

electrochemical transistors (Submitted).

6. **Isabel del Agua**, Daniele Mantione, Sara Marina, C. Pitsalidis, M. Ferro, Ana Sanchez-Sanchez, R.M. Owens, George Malliaras, David Mecerreyes. Conducting Polymer Scaffolds based on PEDOT and Xanthan Gum for live-cell Monitoring (Submitted).

7. Daniele Mantione,[1] **Isabel del Agua**,[1] Ana Sanchez-Sanchez, David Mecerreyes. Conductive polydioxythiophene (PEDOT) type materials for bioelectronics. Polymers 2017, 9, 354.

8. **Isabel del Agua**, Daniele Mantione, Nerea Casado, Ana Sanchez-Sanchez, George G. Malliaras, David Mecerreyes. Conducting Polymer Iongels Based on PEDOT and Guar Gum. ACS Marco Letter 2017, 6, 473.

9. Daniele Mantione,[1] **Isabel del Agua**,[1] Wandert Schaafsma, Ilke Uguz, Mohammed ElMahmoudy, Ana Sanchez-Sanchez, Haritz Sardon, Begoña Castro, George G. Malliaras David Mecerreyes. Low-Temperature Cross-Linking of PEDOT:PSS Films Using Divinylsulfone. ACS Appl. Mater. Interfaces 2017, 9, 18254.

10. Daniele Mantione, **Isabel del Agua**, Wandert Schaafsma, Javier Diez, Begona Castro, Haritz Sardon, David Mecerreyes. Poly(3,4-ethylenedioxythiophene):GlycosAminGlycan (PEDOT:GAG) aqueous Dispersions: Towards Electrically Conductive Bioactive Materials for Neural Interfaces. Macro. Biosci 2016, 16, 1227.

11. **Isabel del Agua**, J. G. Usack, L. T. Angenent. Comparison of semi-batch vs. continuously fed anaerobic bioreactors for the treatment of a high-strength, solids-rich pumpkin processing wastewater. Environ Technol. 2015, 15, 1974.

[1] These authors contributed equally

## Conferences

| | |
|---|---|
| 2017 | Oral presentation *Conducting PEDOT: Polysaccharide Scaffolds for Tissue Engineering.* Seminario Jóvenes investigadores en polímeros, Madrid (Spain) |
| 2017 | Oral presentation *Flexible PEDOT:PSS:DVS-coated textiles for wearable electronics*. E-MRS, Strasbourg (France) |
| 2016 | Oral presentation *Synthesis of PEDOT:GUAR dispersions as versatile materials for bioelectronics.* Bioel, Kirchbourg (Austria) |
| 2015 | French-Spanish Congress for Young Researchers in Polymers (JIP- JEPO), San Sebastian (Spain) |
| 2012 | Microbial Electrochemistry and Technology, Ghent (Belgium) |